

~~NRA-OI/569~~

NRA-Anglian/48

DRAFT

2781

Anglian Region OI Project OI/569

WAVE ATTENUATION  
OVER SALTMARSH SURFACES

Department of Geography  
University of Cambridge  
August 1994

Anglian Region OI Annual Interim Report OI/569

## WAVE ATTENUATION OVER SALTMARSH SURFACES

Annual Interim Report for Anglian Region OI Project OI/569: literature review and outline of field technology.

T Spencer

Research Contractor:  
Cambridge University

National Rivers Authority (Anglian Region)  
Kingfisher House  
Goldhay Way  
Orton Goldhay  
Peterborough  
PE2 5ZR

Anglian Region OI Annual Interim Report OI/569



**Commissioning Organisation**

National Rivers Authority (Anglian Region)  
Kingfisher House  
Goldhay Way  
Orton Goldhay  
Peterborough  
PE2 5ZR

Tel: 0733 371811

Fax: 0733 231840

© National Rivers Authority 1994

All rights reserved. No part of this document may be produced, stored in a retrieval system, or transmitted, in any form or by any means, electronic, mechanical, photocopying, recording or otherwise without the prior permission of the National Rivers Authority.

**Dissemination Status**

Internal: Limited Release

External: Restricted

**Research Contractor**

This document was produced under Anglian Region OI Project OI/569 by:

Department of Geography  
University of Cambridge  
Downing Place  
Cambridge  
CB2 3EN

Tel: 0223 333399

Fax: 0223 333392

**NRA Project Leader**

The NRA's Project Leader for Anglian Region OI Project OI/569 was:

DJ Leggett - NRA (Anglian Region)

**Additional Copies**

Further copies of this document may be obtained from Regional R&D Coordinators or the R&D Section of NRA (Anglian Region)

Anglian Region OI Annual Interim Report OI/569/

# MEMORANDUM



**To:** Quality Review Panel  
**From:** Daniel Leggett, Coastal Processes Engineer  
**Our Ref:** DJL/KJM/C6.5  
**Your Ref:**  
**Date:** 2 August, 1994

---

## WAVE ATTENUATION OVER SALTMARSHES OI Project OI/569

Please find enclosed a copy of Anglian Region OI Project OI/569, Wave Attenuation over Saltmarsh Surfaces.

Please can any comments be passed to Daniel Leggett by 23 August 1994.

**DANIEL LEGGETT**  
Coastal Processes Engineer

Encs:

Distribution:

M Smalls  
S Jeavons  
M Dixon  
C Redmond

## CONTENTS

	Page
LIST OF FIGURES AND TABLES	ii
1. INTRODUCTION	1
2. LITERATURE REVIEW	1
2.1. The role of saltmarshes in coastal defence management	5
2.2. The effect of future sea-level change	9
2.3. Changing meteorological conditions and wave climate in the North Sea	13
2.4. Properties of water waves	16
2.5. Generation of waves in deep water	24
2.6. Wave transformations and generation in shallow coastal water	33
2.7. Breaking waves	42
3. PROJECT OBJECTIVES AND FIELD METHODS	45
3.1 Main aims	45
3.2 Field site	45
3.3 Data collection	51
i. archival data and possible sources	51
ii. field data (methods and technology)	53
3.4. Data processing and analysis	58
3.5. Preliminary data	60
4. APPENDICES	62
5. REFERENCES	71

## LIST OF FIGURES AND TABLES

- Table 1: Semi-empirical deep-water forecasting equations (source: CERC, 1984).
- Table 2: Comparison of wave predictions by various methods (source: Komar, 1976).
- Table 3: Time limits available for logging different numbers of variables at different frequencies (for 21X Campbell Scientific Logger).
- Table 4: Weights of sediment collected during two individual tidal cycles at Stiffkey.
- Fig. 1: The relationship between mud-flat morphology and sediment variation as found in the Wash, eastern England (source: Pethick, 1986).
- Fig. 2: Typical cross-marsh zonation, showing the range of physical factors influencing vegetation. (Idealized salt marsh vegetation associations for Europe and North America are also given). (source: Carter, 1988)
- Fig. 3: General distribution of salt marshes around the coastline of Great Britain (source: Burd, 1989).
- Fig. 4: Brampton's model results showing wave height reduction over coastal salt marshes (source: Brampton, 1992).
- Fig. 5: 'Best guess' of climate-induced global sea-level rise ('business-as-usual-scenario') (source: Wigley and Raper, 1992).
- Fig. 6: Map of estimated current rates of crustal movement in Great Britain ( $\text{mm yr}^{-1}$ ) (source: Shennan, 1989).
- Fig. 7: North Atlantic mean wave height trends (data from the early 1950s to the late 1980s)(source: Bacon and Carter, 1991)
- Fig. 8: Annual total of 'deep cyclones' (with core pressures  $<950$  hPa) from 1930-1991 (bold line = applied gaussian (6 year) filter) (source: Schinke, 1991).
- Fig. 9: Schematic illustration of the main wave characteristics (source: CERC, 1984).
- Fig. 10: Schematic representation of the relative energy contained in water waves and the resulting classification of ocean waves (source: Kinsman, 1965).
- Fig. 11: Water particle motions for deep and shallow water waves (source: CERC, 1984).
- Fig. 12: The applicability of different wave theories as a function of  $H/h$  and  $h/L$  (where  $H$  = wave height,  $h$  = water depth, and  $L$  = wave length) (source: Komar, 1976).
- Fig. 13: Various contributions to the energy budget of wind waves (source: Carter, 1988).
- Fig. 14: Fetch graph showing the relationship between fetch distance, wind speed, and significant wave height established by Sverdrup and Munk (source: Horikawa, 1978).

- Fig. 15: The growth of wave spectra from high to low frequencies and the corresponding co-cumulative power spectrum (source: Kinsman, 1965).
- Fig. 16: Wave spectra and 'cut-off frequencies' for different wind speeds, fetch, duration (source: Pierson, Neuman and James, 1955).
- Fig. 17: Spectral width parameters for ideal wave height and frequency distributions (source: Carter, 1988).
- Fig. 18: Wave shoaling transformations ( $H$ ,  $C$ ,  $L$  = wave height, celerity, and length respectively (where the subscript  $o$  indicates deep water values), and  $d$  = water depth) (source: Pethick, 1986).
- Fig. 19: The relationship between wave approach angle ( $\alpha$ ), water depth ( $d$ ), and wave crest length ( $s$ ). Wave rays are normal to the wave crests. (see equation 22 and text).
- Fig. 20: Location of deep water spectrum on a hypothetical refraction function (source: Kinsman, 1965).
- Fig. 21: Deep water and refracted shallow water spectra as calculated for the hypothetical example in figure 21 (source: Kinsman, 1965).
- Fig. 22:
- a. Generation of wind waves over a constant depth bottom for unlimited wind duration. After Bretschneider (source: Horikawa, 1978).
  - b. Generation of wind waves over a bottom of constant slope for unlimited wind duration, and  $f/m = 5.28$ . After Bretschneider (source: Horikawa, 1978).
- Fig. 23: Examples of forecasting curves for shallow-water waves (source: CERC, 1984).
- Fig. 24: Breaker type classification on three laboratory beaches (source: Galvin, 1968).
- Fig. 25: Breaker height index versus deep water wave steepness (see equation 30) (source: CERC, 1984).
- Fig. 26: The marshes between Stiffkey and Warham (source: Bayliss-Smith *et al.*, 1979).
- Fig. 27: Sketch of the Stiffkey marsh field site produced from air photographs.
- Fig. 28: The 'low' marsh at Stiffkey, fronting the shingle ridge.
- Fig. 29: The 'high' marsh at Stiffkey, between the mainland and the shingle ridge.
- Fig. 30: Return periods of annual maximum tidal stage at Wells Harbour (source: T. Bayliss-Smith, unpublished)
- Fig. 31: The structure, data collection scheme, and data processing of the proposed project.
- Fig. 32: One of the wave recording stations on the 'low' marsh during fieldwork in February 1994.

- Fig. 33: The basic design for the dexion towers used to protect the data loggers from tidal inundation and waves.
- Fig. 34: Accretion plate (20x20 cm) before insertion underneath the marsh surface at Stiffkey 'low' marsh.
- Fig. 35: Logger readings (in mV) compared with hydrostatic pressure (in Pa) calculated from observed water heights in Stone Meal Creek, Stiffkey.
- Fig. 36: Time series of water pressure for both locations (at the seaward and landward edge of the 'low' marsh) for a tide on the 27/2/94.
- Fig. 37: Time series of water pressure for both locations (at the seaward and landward edge of the 'low' marsh) for a tide on the 28/2/94.
- Fig. 38: Tidal stage recorded on Stiffkey 'low' marsh during the morning tide of the 17/12/93 (unfortunately, recording stopped before tidal stage had returned to zero).
- Fig. 39: Time series residuals (after removal of the tidal trend in the series).
- Fig. 40: Example of a water pressure time series residuals and the corresponding Fourier spectrum (produced using 'Mathematica' software). 'Pressure' given in unconverted logger readings (mV) (for conversion into water pressure (in Pascal) see figure 36).
- Fig. 41: Fourier spectra for the marsh edge station (a) and the station at the back (b) of the 'lower' marsh for a 5-minute 'burst' of pressure readings on the 27/2/94.
- Fig. 42: Fourier spectra for the marsh edge station (a) and the station at the back (b) of the 'lower' marsh for a 7-minute 'burst' of pressure readings on the 28/2/94.



## **I. INTRODUCTION**

The aim of this study is to determine the effect of an open coast salt marsh on nearshore wave height and energy variations. The project will provide input into studies on the significance of coastal marshes as natural coastal defences and on the possible artificial rehabilitation of saltmarshes currently undergoing degradation.

The Anglian Region OI Interim Report (OI/569/1/A) outlined the main project objectives, site selection criteria, initial project activities and direction of research. This report follows on from the first report (OI/569/1/A) and includes a literature review on the role of salt marshes in coastal defence management, the effect of changes in sea-level and sea-state on marsh development and coastal defence issues (Sections 2.1 to 2.3). An introduction to the physics (generation and transformation) of wind waves is given in Sections 2.4 to 2.7). Section 3 describes the project objectives, field methods and techniques, and preliminary data collected in February 1994 in more detail.

## **2. LITERATURE REVIEW**

Salt marshes are common coastal features and conditions suitable for marsh development are found along estuaries, shallow coasts or behind offshore bars or islands along the shorelines of most continents. Such marshes form high in the intertidal zone (the surface elevation of mature north Norfolk marshes dominated by tidal inputs of inorganic sediments in conditions of stable sea-level is typically around 60 to 80 cm below Highest Astronomical Tide (HAT) (Pethick, 1981)). Fine sediment (progressively decreasing in average grain size towards the land) deposition (figure 1) and the exposure of the surface during seasonal neap tide low water periods provides an opportunity for plant colonisation (figure 2). Open coast marshes are particularly important in modifying the coastal wave climate during high water. They are also particularly vulnerable to changes in relative sea-level as the development and survival of marsh vegetation is related to the timing, duration, and frequency of submergence.

Marshes support a varied community of halophytic plants (figure 2) and scientific interest in salt marshes has long focussed on marsh evolution, flora and species zonation (see for example Steers, 1983; Steers, 1946; Chapman, 1974; Zedler, 1977; Adam, 1981). More recently, marsh initiation and growth in relation to past and present sea-level variations (DeLaune, et al., 1978; Pethick, 1980, 1981; Allen, 1990; Reed, 1990; Allen, 1991; French, 1993) as well as spatial variation in marsh surface accretion (Letzsch and Frey, 1980; Stumpf, 1983; French and Spencer, 1993) has become the focus of many studies. Other studies have focused particularly

on marsh creek hydrodynamics, suspended sediment balance and its relation to marsh morphological development (Bayliss-Smith *et al.*, 1979; Healey *et al.*, 1981; Reed *et al.*, 1985; Reed, 1987; French and Clifford, 1992; French and Stoddart, 1992). All of these studies have focused primarily on input/output measurements and tidal, seasonal, or annual water, sediment, or nutrient balances. Although these studies have contributed important information on the long-term evolution and maintenance of these wetland systems, there is now a need to better understand the **internal** linkages between marsh hydrology, sedimentation, vegetation, nutrient cycling, and wave conditions close to high water. Knowledge of present wave conditions and tidal regimes is essential for an understanding of these linkages (such as for example the link between overmarsh flows and sediment transport), but little research has been carried out on wave conditions over coastal salt marshes during tidal inundation.

Furthermore, as a result of recent predictions of sea-level rise in response to climatic change, coastal engineers have begun to review traditional approaches involving 'hard' coastal defence (the building of sea-walls, groynes, revetments, etc.) . 'Soft' options (i.e. the conservation or creation of coastal landforms - such as salt marshes - which reduce wave energy during storm conditions) or 'managed retreat' of traditional sea defences are now being considered as a cost-effective alternative to the building, replacement, maintenance, and adaptation of old structures to accommodate a possible increase in flooding which may result from sea-level rise. Although some authors (e.g. Wayne, 1976; and Brampton, 1992) have addressed the question of wave height reduction over salt marsh surfaces, detailed studies on the importance of marshes as natural sea defences are still lacking.

Knowledge relating to wave attenuation over salt marsh surfaces is likely to increase in importance as a result of the following two possible consequences of climatic change:

First, a future accelerated relative sea-level rise may lead to increased inundation depths and altered vegetation cover, sediment and nutrient budgets of the marsh surface. If relative sea-level rise exceeds marsh accretion in the long or the short term, increased marsh water depths at high (spring) tides may lead to reduced wave attenuation leaving the adjacent mainland exposed to more severe wave conditions.

Second, a possible future increase in the frequency of deep cyclones over the North Sea as a result of ocean-atmosphere interactions (Rye, 1976), an increase in prevailing westerly winds, or changes in sea-level pressure oscillations (Neu, 1984) may lead to more frequently occurring storm surges and a higher energy wave environment along the coast (Schinke, 1992; Schmidt and von Storch, 1993) (see Section 2.3.).

In the UK, salt marshes cover just under 2000 km of the coastline (Burd, 1989) and 15,883 ha along Britain's North Sea coast (Fowler, 1991) (see figure 3). A substantial proportion (around 38%) of the European salt marshes are foreland (open coast) marshes (Dijkema, 1987) and therefore directly exposed to waves generated offshore. As such, these marshes are of importance in modifying the coastal wave climate during high water. They therefore play an important role in coastal defence issues. Their position high in the tidal frame and their dependence on tidal range, wave climate, and sediment supply, however, also make these coastal features very susceptible to changes in relative sea-level and/or changes in meteorological conditions and wave climate, both of which may result from climatic warming.

The role of salt marshes in coastal defence management and the effect of rising sea-level and changing meteorological and wave conditions are discussed in turn below. This discussion is followed by a review of the literature on wave characteristics, wave generation, propagation, and shallow water transformations which forms the theoretical background to the core part of the fieldwork for this project: the measurement of wave characteristics across a salt marsh surface.

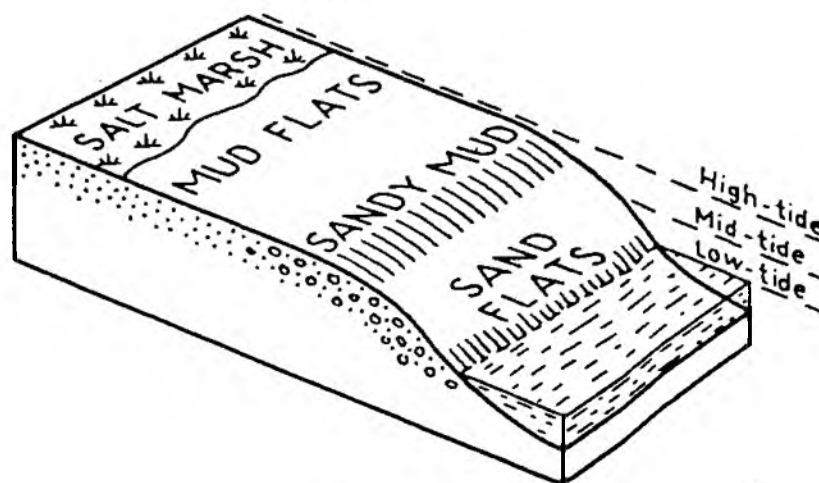


Fig. 1: The relationship between mud-flat morphology and sediment variation as found in the Wash, eastern England (source: Pethick, 1986).

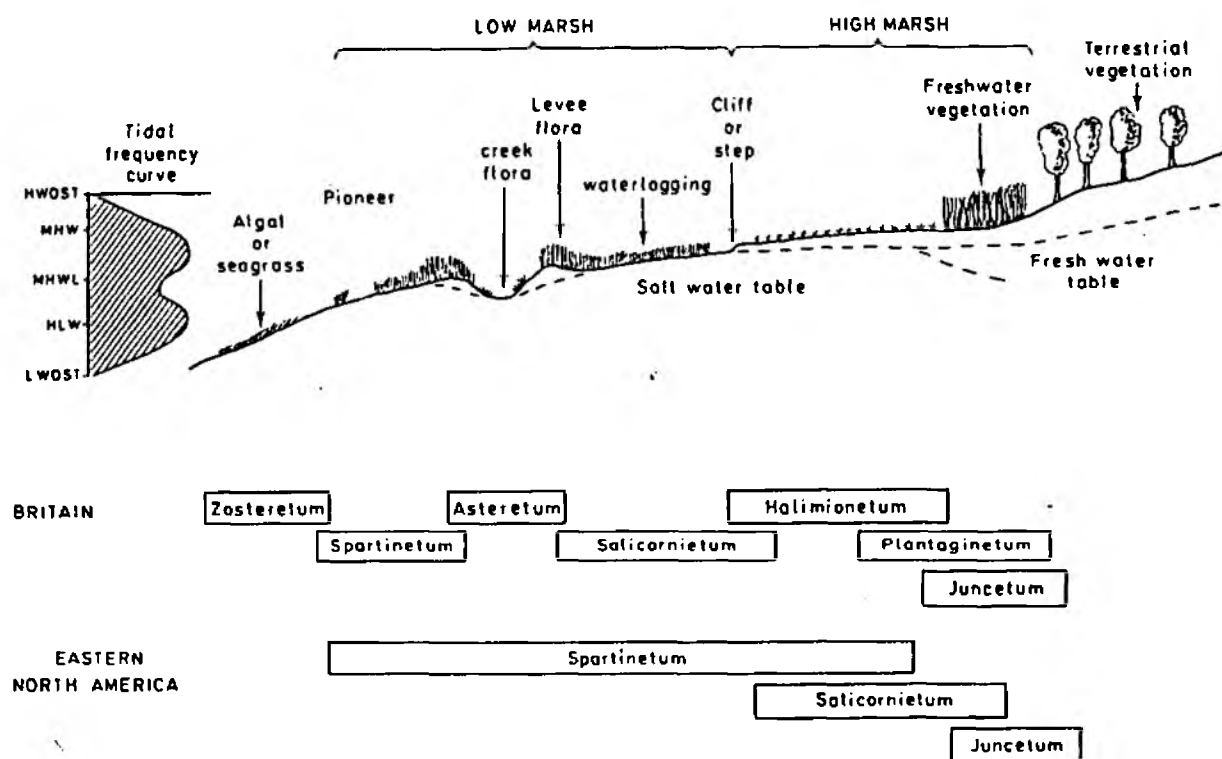


Fig. 2: Typical cross-marsh zonation, showing the range of physical factors influencing vegetation. (Idealized salt marsh vegetation associations for Europe and North America are also given). (source: Carter, 1988)

## **2.1. The role of salt marshes in coastal defence management**

As a result of estimates of future sea-level rise and recent North Sea storm surges, sea defence (the protection of low-lying areas from tidal flooding) has become of great social and economic importance in the UK. Severe coastal floods such as those of 1953 and 1978 have led to a considerable amount of coastal defences in the form of groynes, seawalls, or revetments. In 1976, for example, structures of this sort had been extended to cover 67% of the coastline of East Anglia. In 1991 the NRA states that around 804 km of sea defences exist to protect 426 km of the Anglian coastline, one fifth of which is below flood risk level (NRA, 1991a).

In the light of the continuing importance of sea defences, it is surprising, that very little comprehensive studies of the UK coastal zone have been carried out. The last comprehensive study of the entire UK coastal zone was carried out by the Royal Commission on Coastal Erosion and Afforestation from 1906-1911. It was not until the severe surge of 1953 that coastal defence was addressed again as an issue of general importance, but from 1953 until the 1990s little change took place in the approach which Authorities took towards coastal defence. Clayton (1990, p.282) notes that (more than 30 years after the 1953 North Sea surge) 'for the height of sea defences the guidelines laid down by the Waverley Committee (1953) following the storm surge of that year are still being followed'.

Past approaches towards sea defence and coastal protection have been characterized by the attempt to directly reduce the impact of waves on the shore locally through fixed, engineered structures. In doing so, the lack of knowledge on coastal sediment transport and tidal currents has frequently led to changes in sedimentation, beach lowering in front of structures and the undermining and ultimate destruction of such defences by the sea itself. Already in 1941, B. Keay noted that 'the efforts of man to prevent erosion are sometimes the cause of its increase, either at the site of his works or elsewhere along the coast' (quoted in Barrett, 1992, p.11) - this problem, however, is now more widely acknowledged and alternative approaches to coastal defence are being considered (see below). In addition to the building cost of 'hard engineering' structures, their maintenance is very expensive (Clayton, 1976). According to the NRA's 'Sea Defence Survey' (NRA, no date (b)), about £30 million is spent each year on capital works for sea defences with a further £30 million spent on tidal defences in estuaries in England and Wales. £200 million is needed to secure the defences of Norfolk, Suffolk, and Essex in the next 10 years (NRA, no date ((b))). In addition to sea defence structures, structures as part of local coast protection schemes (set up to protect the coast from erosion and prevent land being lost to the sea) have often been undermined through basal scouring resulting in subsequent cliff retreat at rates similar to those that occurred before the structure was built. This



Fig. 3: General distribution of salt marshes around the coastline of Great Britain (source: Burd, 1989).

was for example the case at Lowestoft Ness, the easternmost point of England, at which sea walls had to be replaced repeatedly while cliff retreat continued at a rate of  $1\text{ m yr}^{-1}$  (Clayton, 1990). In many cases, local schemes of coastal protection are also likely to have reduced an important source of sediment supply to accreting coastal areas elsewhere. The protection of rapidly eroding Quaternary cliffs in East Anglia, for example, may be partly responsible for the reduction in accretion rates on the coastal marshes of north Norfolk (Clayton, 1990). A subsequent reduction in the height or width of accreting environments will not only reduce the extent of important ecological habitats but is likely to decrease the protection of the adjacent coastline from direct wave action.

One of the reasons for the failure of past coastal management schemes is that coastal defence has for a long time been dealt with by the responsible Authorities on a parochial basis with very little regard to the impact of their actions on neighbouring territory. In the late 1980s, however, a more comprehensive coastal management approach including the entire coastline was adopted by the newly established National Rivers Authority (NRA, 1991a). This move towards an appreciation of wider coastal issues and large scale coastal processes is also reflected in the formation of 18 voluntary coastal groups acting as coordinating bodies and funding coastal research in England and Wales (Barrett, 1992).

Traditionally, conservationist interests have focused on the preservation of marsh biodiversity and marshes as important wildlife habitats. This interest led to 80% of the UK salt marshes being designated SSSI (Sites of Special Scientific Interest) in 1981 (Burd, 1989) and 847 km of coastline being obtained by the National Trust (Carter, 1988). Recently, improved knowledge on coastal hydrodynamic and sedimentary processes (e.g. the longshore drift off the East Anglian coast) has increased the awareness of the potential importance of wave energy dissipation over salt marshes as a very cost effective natural coastal defence. It is now apparent that 'in the past too much reliance has been placed on engineered structures with insufficient account taken of the essential role of the natural coastline itself, the beaches, dunes and saltmarshes' (Clayton, 1990, p.284).

Recent engineering studies (such as Brampton, 1992) suggest a movement towards a wider approach of coastal engineering which integrates the effect of natural features on the wave environment. The traditional 'hard engineering' approach is now being challenged by a more recent 'soft engineering' approach which recognises the importance of natural coastal processes. From the flood defence point of view, marshes could be particularly important in breaking waves and in partially absorbing energy during severe storm events. In this context, 'managed retreat' (i.e. moving coastal defences further inland to allow the landward migration of

marshes in response to higher relative sea-levels) and the restoration of old - or the creation of new - protective marshes may become a new, alternative, cost effective option for coastal defence management. Figure 4 illustrates the results of the modelling approach adopted by Brampton (1992) which suggests a significant reduction of wave height over a distance of about 20 meters from the salt marsh edge towards the coast. A study on the northeast coast of Florida had already suggested in the late 1970s, that wave height and energy can be reduced by as much as 71% and 92% respectively over a 20 metre transect across a *Spartina alterniflora* marsh (Wayne, 1976). Wave energy on salt marsh coasts has also been studied in relation to sediment transport (Pethick, 1992). The problem when considering coastal marshes as a flood defence component is that no detailed empirical field studies have been conducted to verify Brampton's (1992) model and Wayne's (1976) initial findings and that there are no guidelines regarding the management of existing - or the creation of new - salt marshes (e.g. the degree to which - and by what means - plant colonisation and/or sedimentation should or should not be encouraged).

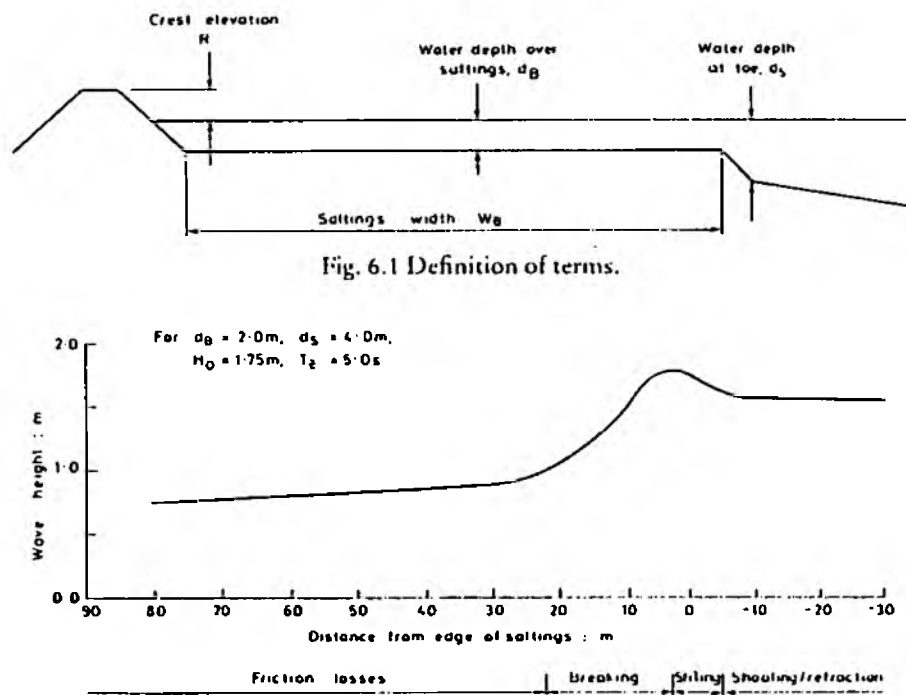


Fig. 4: Brampton's model results showing wave height reduction over coastal salt marshes (source: Brampton, 1992).



## 2.2. The effect of future sea-level change

The importance of coastal wetlands as natural sea defences (as discussed above) will depend to a large extent on their evolution through time. An understanding of the processes influencing marsh initiation and growth is therefore necessary if the management and/or creation of marshes is considered as a 'soft' engineering option. The initiation and maintenance of salt marshes is the result of a very delicate balance between surface elevation, relative sea-level, tidal range, wave climate, and sediment supply.

Suspended sediment may be supplied from offshore or from eroding cliff faces located further along the coast (as in the case of the Quaternary cliffs of East Anglia which provide a source of sediment for the north Norfolk marshes), although the relative importance of offshore sediment for marsh accretion is not well documented. As sediment supply to each marsh system depends largely on cliff erosion elsewhere along the coast it also varies as a result of changing relative sea-level (Pethick, 1993) and cliff protection schemes (see above) (Clayton, 1990; Titus, 1986).

Whether such material deposits on the intertidal flat depends, however, on the surface elevation relative to the tidal prism and on the duration of the period of low current velocities around high water. Marshes, therefore, develop preferentially in low wave energy environments of estuaries (for example in Cardigan Bay in Wales (Shi, 1993)) and behind offshore barrier islands or spits (as in the case of most of the Norfolk marshes). Open coast marshes occur when fronted by extensive tidal flats (such as in the case of the Stiffkey marshes (Norfolk) or the Dengie Peninsula (Essex)). Changes in tidal range and sea-level both affect the relative marsh surface elevation and duration of marsh inundation. In the case of the Dutch Wadden Sea, for example, the closing of the Zuiderzee in 1932 increased the tidal range by 10 to 60 cm which was followed by rapid accretion until the 1950s when the marsh surface elevation had increased sufficiently relative to HAT (Highest Astronomical Tide) for sedimentation to decrease (deJonge *et al.*, 1993). In addition to tidal range it is the marsh surface elevation relative to the tidal prism which ultimately determines tidal inundation duration, plant growth and marsh surface accretion (providing sediment supply is sufficient). This relative elevation will change in response to local isostatic and/or tectonic land movement and eustatic sea-level change. Relative sea-levels in the southern North Sea have fluctuated considerably during the Holocene. About 8425±170 BP, for example, relative sea level was at least 37 m lower than at present at the Norfolk coast (Jardine, 1979; Jelgersma, 1979).

As a result of the high spatial variability of isostatic and/or tectonic land movement, global estimates of past, present or future sea-level rise are of little value for reconstructing the history or predicting the future of a particular coastline. Furthermore, the absence of a vertically stable reference datum means that 'the determination of a single sea-level curve of global applicability is an illusory task' (Pirazzoli, 1993, p.141). Gornitz and Lebedeff (1987) for example used 130 tide gauge records from around the world of a minimum length of 20 years, corrected for recent earth movements and derived a mean rate of sea-level rise of  $1.2 \pm 0.3 \text{ mm yr}^{-1}$ . In contrast, Peltier and Tushingham (1989) who used 81 stations of 50 years length (1920 to 1970) derived a sea-level rise of  $2.4 \pm 0.9 \text{ mm yr}^{-1}$ . In addition, global sea-level estimates have a geographical bias towards the northern hemisphere (and Europe in particular) where most tide gauge stations are located. According to Gröger and Plag (1993) who discuss the Permanent Service for Mean Sea Level (PSMSL) global record, tide gauge records covering 30 years or more are highly clustered in the Northern Hemisphere with none located in Africa or Antarctica and only three in Australia. Limiting the analysis of sea-level trends to those stations between  $55^{\circ}\text{N}$  and  $55^{\circ}\text{S}$  (with 20-year records) - i.e. eliminating the uplifting areas of the Northern Hemisphere - increased the global median by more than 45% and illustrates the impossibility of determining a 'global' sea-level trend from very limited existing data sets. It is, however, worth noting that all available estimates of global (average) sea-level rise from tide gauge records are positive for the past 100 years and that the recently predicted global sea-level rise in response to climatic warming over the next 110 years (4.8 cm by the year 2100 as 'best estimate' (see figure 5)) is likely to be four times faster than it was over the past century (Wigley and Raper, 1992). Although most records suggest that recent eustatic sea-level rise in Europe has been less than  $1.26 \text{ mm yr}^{-1}$  (Pirazzoli, 1993), with regard to the future evolution of salt marshes, the sea-level rise estimates justify concern (Barkham *et al.*, 1992).

More particular studies in Europe have shown that the average sea-level rise over the last 100 years ranges from  $0.4$  to  $0.6 \text{ mm yr}^{-1}$  (Pirazzoli, 1989; Woodworth, 1990), although local average rates for the last century have been as high as  $3\text{-}5 \text{ mm yr}^{-1}$  on the Essex coast (NRA, 1991c). Slightly lower rates of relative sea-level rise ( $1.5 \text{ mm yr}^{-1}$  during the past 2800 years) have been reported for the north Norfolk coast (Pethick, 1992). The regional rate of crustal subsidence of this area (suggested to be  $-1$  to  $-2 \text{ mm yr}^{-1}$  by Shennan (1989) (see figure 6)) contributes significantly to the present total relative sea-level rise of ca  $2 \text{ mm yr}^{-1}$  (French and Spencer, 1993).

In order to determine whether a particular marsh is 'keeping pace' with such rates of sea-level rise, or whether inundation depths and therefore wave dynamics are likely to change, marsh surface accretion rates need to be assessed. Numerous studies have assessed salt marsh age and

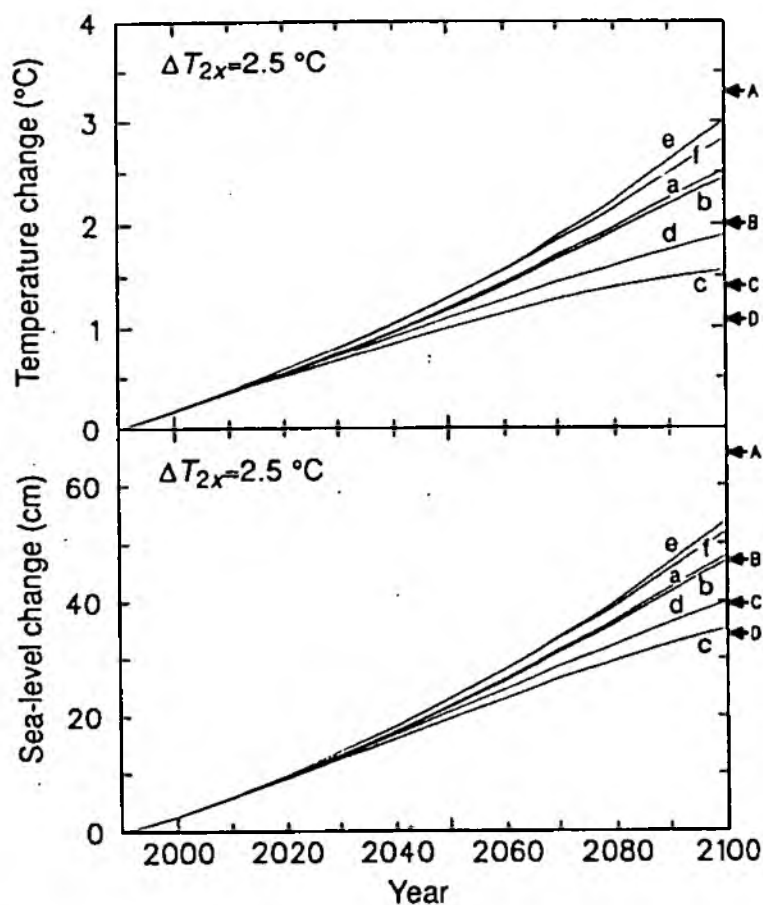


Fig. 5: 'Best guess' of climate-induced global sea-level rise ('business-as-usual-scenario') (source: Wigley and Raper, 1992).

accretion rates in relation to local relative sea-level change by using direct and indirect methods such as historical information on marsh initiation (Allen, 1991; Anderson *et al.*, 1992; Pethick, 1980 (maps, air photographs)), artificial marker horizons (e.g. sand (Steers (ed.), 1960; French and Spencer, 1993) or white clay (Bauman, *et al.*, 1984)), or natural marker horizons (e.g. core peat strata (Stumpf, 1983), storm deposits (Clymo, 1967),  $^{137}\text{C}$  dating (Delaune, *et al.*, 1978)). Most studies of salt marsh accretion in northwest Europe suggest rates of 1 to 25 mm annual vertical accretion (French, in press), but accretion measurements should be interpreted with great care. Autocompaction and the high temporal variability of sedimentation may lead to overestimation of long-term trends from short-term (e.g. annual) measurements. French and Spencer (1993), for example, have shown that the spatial pattern of very short-term vertical accretion (over a single tide) is considerably different from the spatial pattern measured on an annual time-scale.

Although rates of vertical accretion of northwest European salt marshes seem to keep pace with local relative sea-level rise, serious marsh erosion has been observed in several locations. Allen and Pye (1992), for example, observed wave eroded marsh cliffs at Stiffkey, Norfolk (the field location for the project proposed in this report). More detailed studies have been carried out on

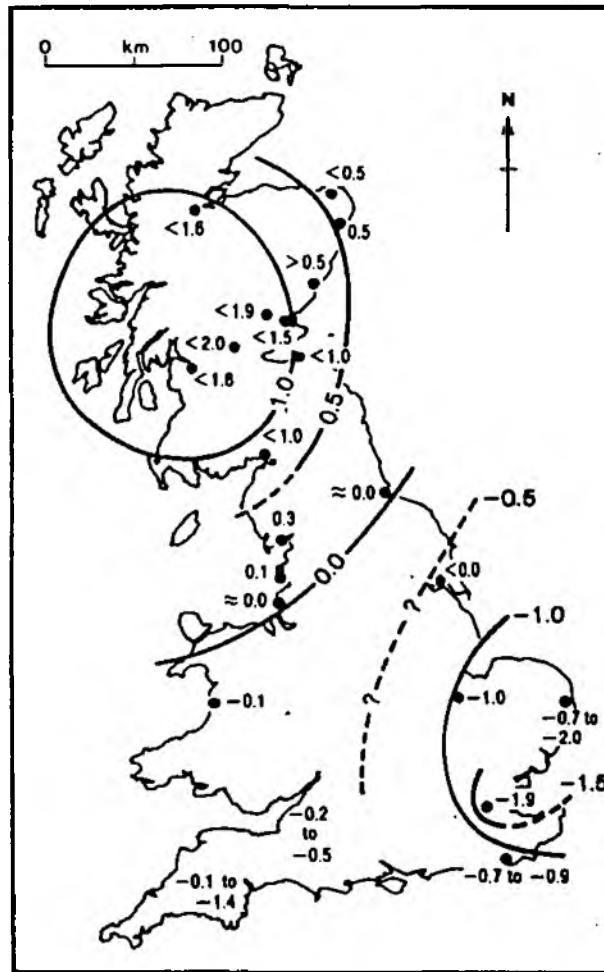


Fig. 6: Map of estimated current rates of crustal movement in Great Britain ( $\text{mm yr}^{-1}$ ) (source: Shennan, 1989).

the Essex coast where a 10% loss of salt marsh area between 1960-1981 has been suggested by Dijkema (1987). The enlargement of pans and creeks within the marsh has also been reported from the Tollesbury marshes in Essex (Allen and Pye, 1992).

Earlier periods of sea-level rise during the Pleistocene are likely to have resulted in the landward migration of salt marshes (Dijkema, 1984) in response to the landward migration of mean sea-level. Today, the protection of much of the coast by sea walls on the landward edge of open coast marshes (e.g. 480 km seawall in Essex) prevents the landward migration of marshes and results in a net loss of area. Such a horizontal and/or vertical loss of salt marsh is likely to reduce their effect in damping wave energy during high water and especially during storm surges. More detailed information on marsh surface accretion/erosion, possible future rates of relative sea-level change, and wave damping by the marsh surface is needed to assess future coastline evolution. Such information should form an integral part of future shoreline management.

### 2.3. Changing meteorological conditions and wave climate in the North Sea

The future importance of coastal marshes as natural sea defences does not only depend on relative sea-level rise but also on possible changes in the wave regime of the adjacent ocean. It is reasonable to assume that possible climatic changes may also influence oceanographic parameters other than sea-level due to the close interaction of the ocean and the atmospheric boundary layer. An increase in latitudinal pressure differences caused by differential warming of the atmosphere could for example lead to more severe wind conditions over the oceans and an increase in wave heights. With regard to the North Sea, several studies (e.g. Rye, 1976; and Bacon and Carter, 1991) suggest that changing local meteorological conditions over the past 4 to 5 decades have led to an increase in wave heights and storm surge frequency. Although these studies are often based on observations at only a few locations covering very limited time periods, the possibility of a future change in the North Sea wave climate should not be ignored as it would have important repercussions for sea defence management in general and the importance of 'soft' engineering options in particular.

One of the first authors to address the question of changing wave climate in the North Sea was Rye (1976). Instrumentally recorded wave data for the North Sea, however, only dates back as far as 1969 when the first wave data collection programmes were initiated at two locations (off the Norwegian coast and in the central North Sea). The lack of instrumental data forced Rye to consider visually estimated wave heights and supporting meteorological evidence. From this dataset, it appears that visually observed wave heights increased significantly during the period 1959 to 73 and 1950 to 69 at the rescue ship 'Famita' in the central North Sea (57°N) and at the weathership off the Norwegian coast (66°N), respectively. According to Rye, the observations from the rescue ship 'Famita' indicate an increase in the 100-year extreme wave height of 1 m  $\text{yr}^{-1}$ , or 3 to 4 % per year. This agrees with a trend observed for 5-year running means of wind speed and wave height for 9 weather ships located in the North Atlantic. In addition to the wave data, Rye found a significant increase in the atmospheric pressure drop rates (i.e. the number of pressure drop rates larger than 10mb within a 6 hour time interval) from observations made at the light house Ferder, Skagerak.

In contrast to Rye, more recent studies have been able to draw upon at least a few years of instrumental wave records. A review of visual and instrumental data on wave climate available for the North Atlantic and the North Sea shows an increase in mean wave heights for all records except one (Bacon and Carter, 1991) (see figure 7).

On average, this increase in mean wave heights amounts to approximately 2% per year - a trend which is in agreement with Carter and Draper's (1988) observations of a significant increase in

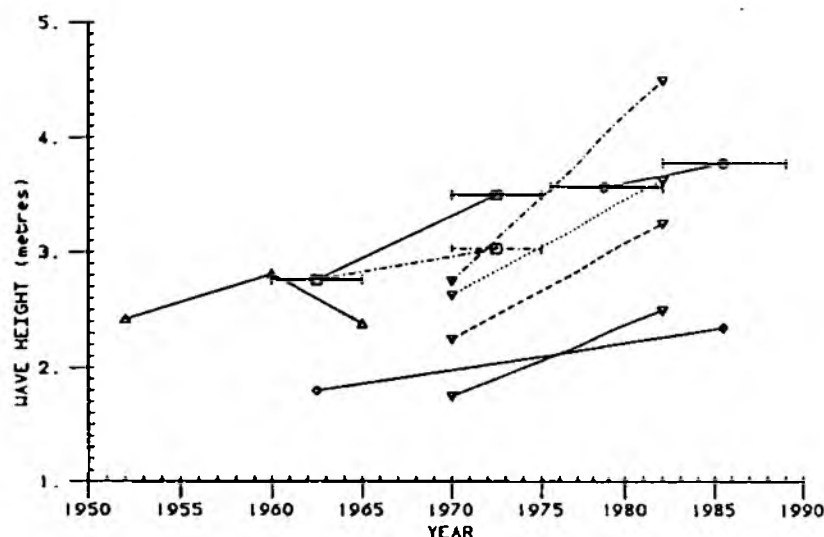


Figure 5. North Atlantic mean wave height trends showing data from the early 1950s up to the end of 1989. Error bars indicate periods over which data have been averaged over time. ( $\Delta$ — $\Delta$ , all nine OWSs (Rodewald, 1972);  $\nabla$ — $\nabla$ , BIO grid box C4 (Neu, 1984);  $\square$ — $\square$ , BIO grid box D7 (Neu, 1984);  $\diamond$ — $\diamond$ , BIO grid box E10 (Neu, 1984);  $\circ$ — $\circ$ , BIO grid box E14 (Neu, 1984);  $\square$ — $\square$ , OWS India (Draper, 1986);  $\diamond$ — $\diamond$ , OWS Juliett (Draper, 1986);  $\circ$ — $\circ$ , Seven Stones LV (present paper);  $\circ$ — $\circ$ , OWS Lima (present paper))

Fig. 7: North Atlantic mean wave height trends (data from the early 1950s to the late 1980s)(source: Bacon and Carter, 1991)

wave heights off Land's End. Neu (1984) also found an overall upward trend in 'significant wave heights' (i.e. the mean of the highest one-third of waves) in the North Atlantic from 1970 to 82. His analysis, however, was based on synoptic charts of wave height derived from visual and instrumental data so that slight inaccuracies might have been introduced through the incompatibility of the data sets. In terms of wave energy, his calculations suggest that wave energy in the central North Atlantic was 2.5 to 3.0 times higher in 1982 than in 1970.

Records of the North Sea itself only show an increase in wave heights from the 1960s to the late 1970s, after which heights do not follow any consistent trend (Bacon and Carter, 1991). With regard to the meteorological conditions in the European North Atlantic, an analysis of historical weather maps has revealed a substantial increase in the number of severe storms (extreme low pressure systems with a core pressure of  $\leq 950$  hPa) from the 1930s to the 1980s (Schinke, 1992) (see figure 8). From an analysis of daily pressure fields for the North Sea (1881 to 1989), the NRA (1991a) concludes that there exists no long-term periodicity in annual North Sea gale occurrences, but that the last 20 years have been characterised by a steady increase in the total number and intensity of gales. As the North Sea is a partially enclosed sea and fetch-limited in all directions except the north, it is likely, that local meteorological

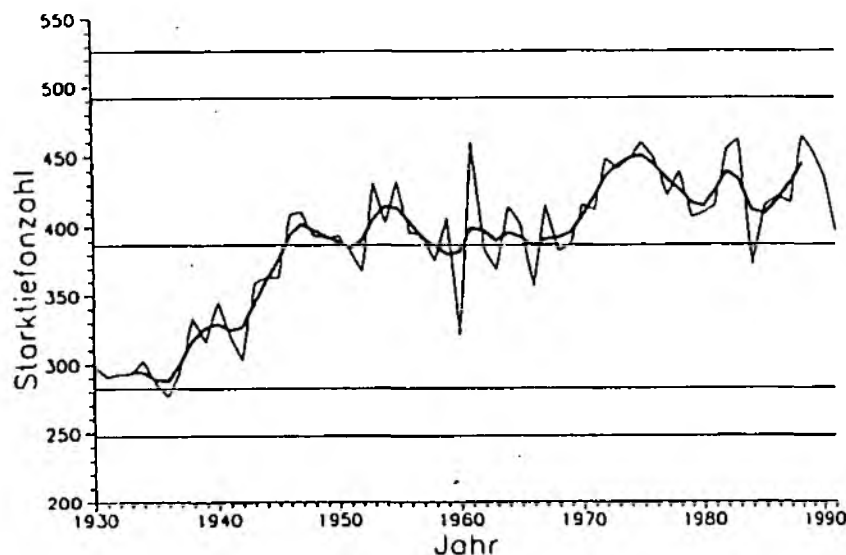


Fig. 8: Annual total of 'deep cyclones' (with core pressures <950 hPa) from 1930-1991 (bold line = applied gaussian (6 year) filter) (source: Schinke, 1991).

conditions have a more dominant effect on its wave climate than in the open ocean. The high frequency of deep cyclones in the late 1970s identified by Schinke does, however, agree with the observations of increased wave heights in the late 1970s in the North Sea. This might be explained by the fact, that low pressure systems located in the north-east Atlantic at the transition zone between the relatively shallow continental shelf and the much deeper Atlantic Ocean are likely to generate strongly convergent mass transport and a resulting change in water level which propagates into the North Sea as an 'external' surge (Heaps, 1983). In this way, an increased occurrence of deep cyclones in the north-east Atlantic is likely to result in an increased surge frequency in the North Sea.

The interpretation of ocean wave records is as controversial an issue as that of tide gauge records. Schmidt and von Storch (1993, p.791) rightly point out, that it is 'not possible to tell whether the extremes had become worse or if reporting systems have improved'. The evidence from meteorological analyses in addition to the wave records, however, supports many of the observations and suggests, that an increase in North Sea storm surges and wave heights is likely to exacerbate the effect of a possible sea-level rise on the coastline.

## 2.4. Properties of water waves

Water waves can be described by using a limited set of wave characteristics (such as wave height, length, and period) (see figure 9). The relationships between these wave parameters and the basic theories of wave motion and propagation will briefly be considered in this Section. An understanding of these basic physical properties of water waves and of the mathematical equations used to describe these properties is crucial to the interpretation of the wave records.

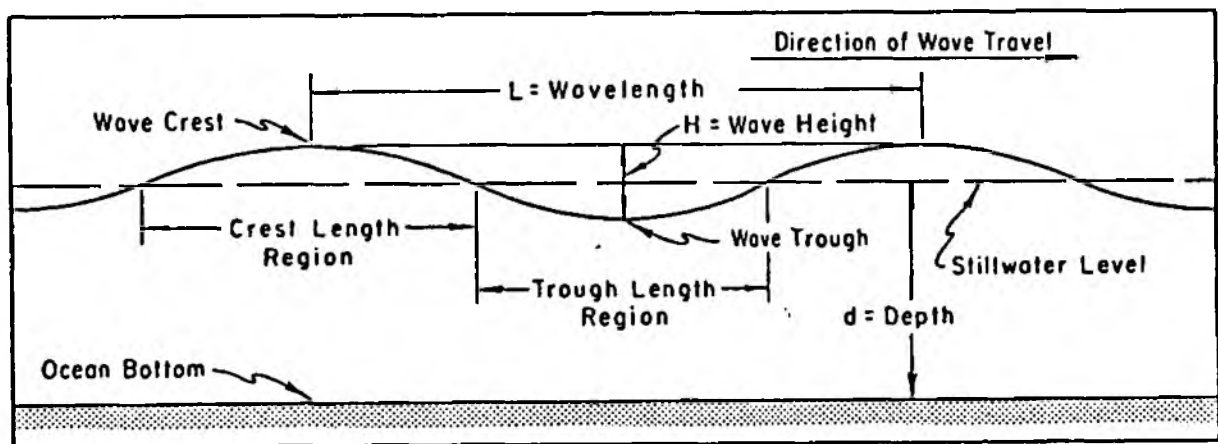


Fig. 9: Schematic illustration of the main wave characteristics (source: CERC, 1984).

In their simplest form, waves can be described by a sinusoidal curve with a distinct height ( $H$ ) length ( $L$ ) period ( $T$ ) (the time for a wave to travel a distance of one wavelength), or frequency ( $f=1/T$ ). Classification schemes for water waves are usually based on their period or frequency. According to this classification (see figure 10) ocean waves fall mainly into the category of 'gravity waves' which have periods from 1 to 30 seconds. For these waves, gravity is the main force returning the fluid to its equilibrium position. Gravity waves also contain a very large percentage of the total energy of the complete frequency spectrum and are therefore of particular importance with respect to coastal geomorphological and engineering issues.

The complexity of the ocean surface and of its change in time and space is the most fundamental problem in oceanographic or coastal research. In order to assess and compare the state of the sea at different locations or at different times it is necessary to simplify this complexity through establishing models of the sea surface. Such models can be divided into two main categories: First, deterministic models introduce a set of mathematical assumptions about the nature of waves which greatly simplify computations. As a result, relatively accurate predictions of individual wave characteristics (such as the pressure beneath a wave, wave energy, etc.) are



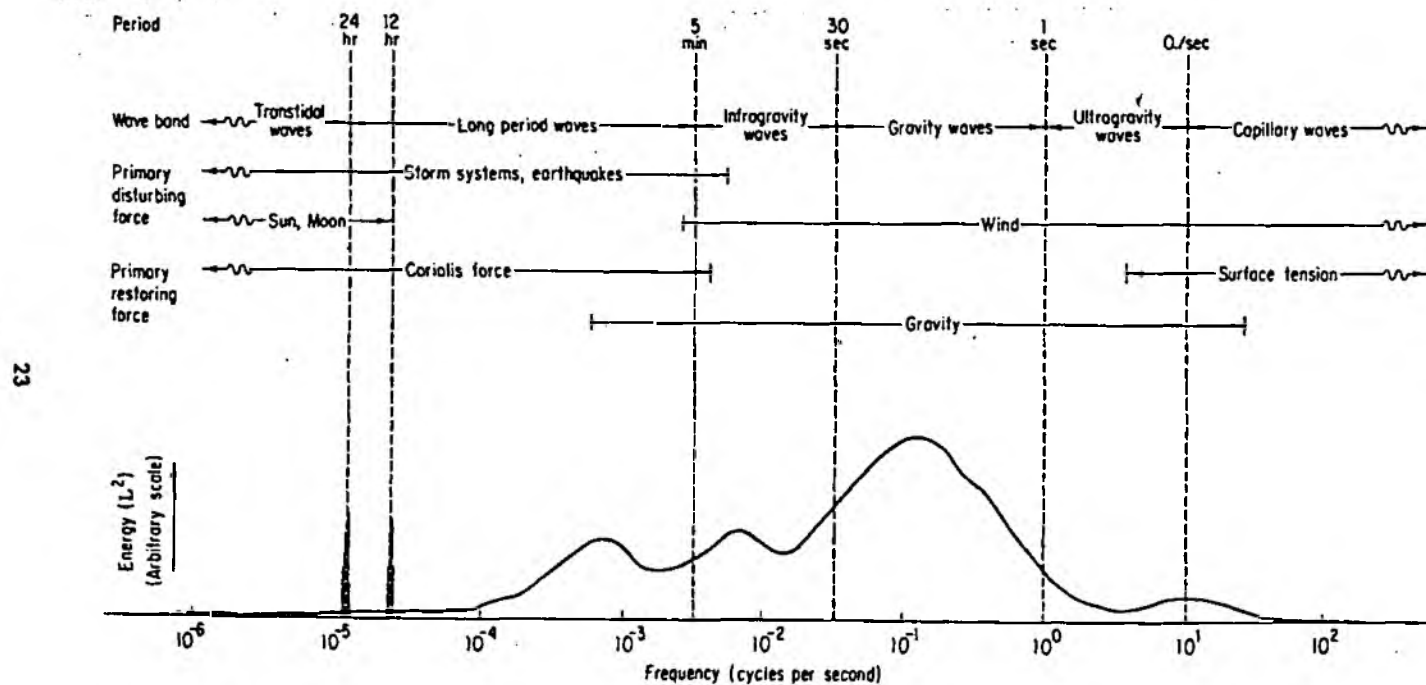


Fig. 10: Schematic representation of the relative energy contained in water waves and the resulting classification of ocean waves (source: Kinsman, 1965).

possible, although these models are very poor descriptors of the actual form of the sea surface due to the mathematical simplifications made. Second, stochastic models describe the sea surface form relatively well, but do not provide an accurate method for the prediction of wave characteristics.

The following discussion focuses on the deterministic description of water waves, as this project is concerned with the change of wave characteristics (such as subsurface pressure, wave height, wave energy) which are best estimated using analytical models. Stochastic models, however, are useful tools for wave spectra prediction and will be discussed in Section 2.5.

The first comprehensive deterministic wave theory was developed by Airy in the mid nineteenth century. This linear wave theory provides a relatively simple mathematical description of water waves based on the assumption that wave forms over deep water and outside the area of generation approximate sinusoidal curves with infinitesimal amplitude and that water particle orbits beneath the surface are closed circles (see figure 11). Furthermore, the water motion is assumed to be irrotational (i.e. individual particles will retain their original orientation throughout the movement), the fluid is assumed to be inviscid, incompressible and homogeneous (i.e. the effect of viscosity can be ignored and water density remains constant), the effect of the coriolis force and of surface tension is neglected, the pressure at the free surface is assumed to be uniform and constant, and the bed is assumed to be horizontal, fixed, and impermeable.

Although Airy wave theory describes deep water waves relatively well, it is an inaccurate description of shallow water waves which have distorted wave forms and elongated, open particle orbits (figure 11). In order to deal with such shallow water wave transformations, higher order theories such as Stokes' finite-amplitude theory and solitary wave theory have been developed (figure 12). Stokes' theory includes wave forms with an asymmetrical distribution around still water level (SWL), i.e. steeper crests and longer troughs than simple sine waves. Solitary wave theory has been developed to describe wave forms in shallow water which are assumed to have finite amplitudes but infinite lengths. The disadvantage of Stokes' and solitary wave theory, however, is their computational complexity, which makes them inapplicable for most practical purposes (CERC, 1984). Furthermore, Stokes' and solitary wave theory themselves only have limited applicability (see figure 12).

For the purpose of this project, preliminary calculations will be based on linear (Airy) wave theory, as the mathematical solutions of the higher order theories do not usually lead to single valued solutions. Furthermore, adjustments of linear wave theory calculations can be made to

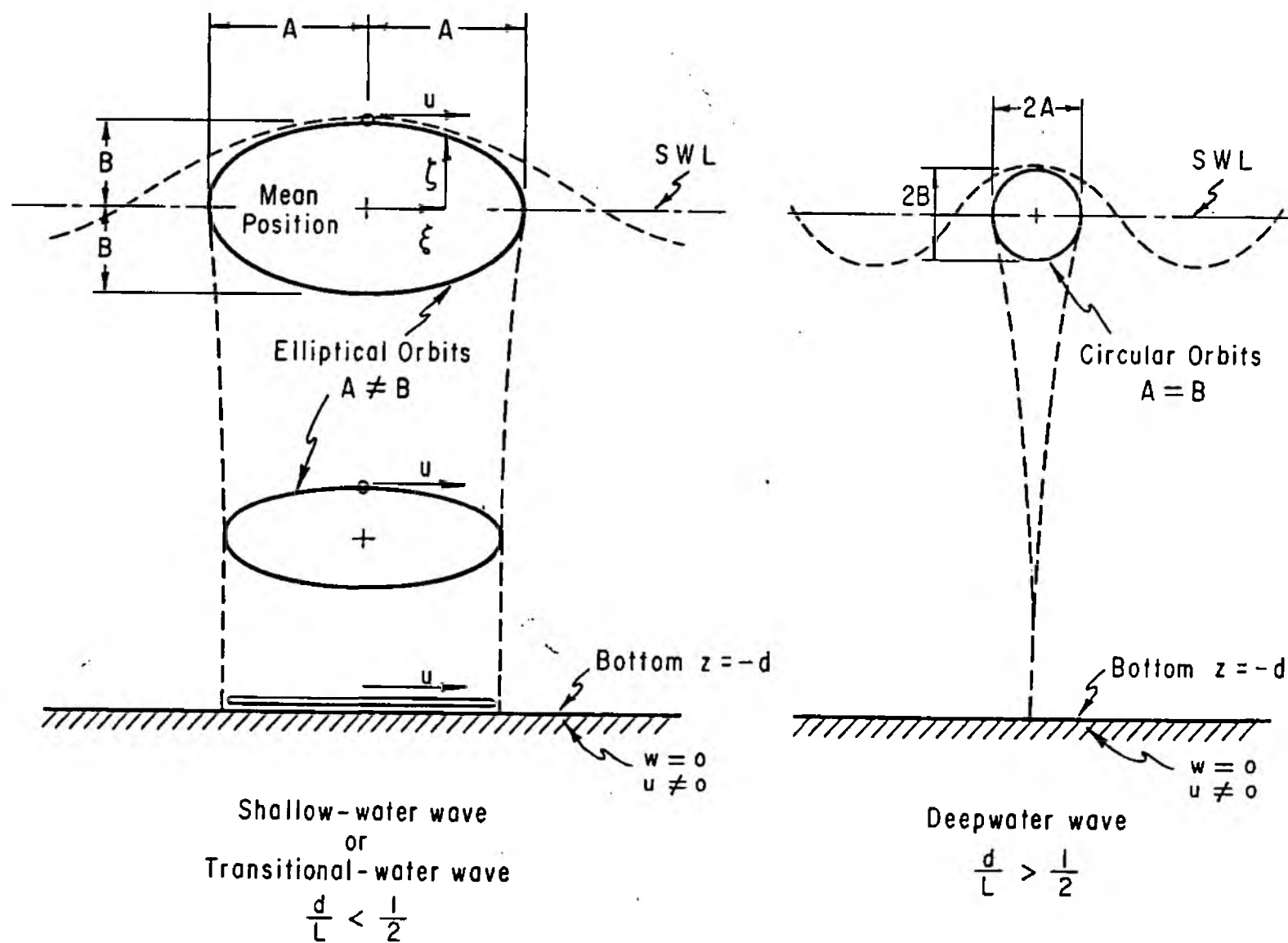


Fig. 11: Water particle motions for deep and shallow water waves (source: CERC, 1984).

account for non-linear processes in shallow water (Lee and Wang, 1984). Linear wave theory remains the most practical approach for the analysis of wave (pressure) records (CERC, 1984).

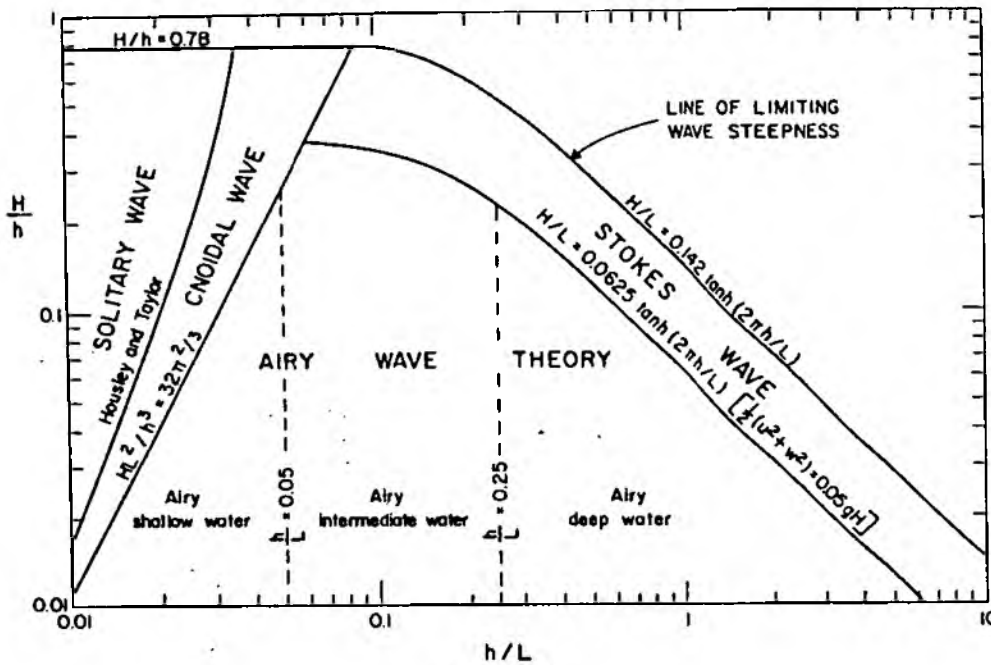


Fig. 12: The applicability of different wave theories as a function of  $H/h$  and  $h/L$  (where  $H$  = wave height,  $h$  = water depth, and  $L$  = wave length) (source: Komar, 1976).

**Basic wave parameters.** Taking a sinusoidal curve as the nearest approximation to the wave form, the surface displacement relative to SWL (Still Water Level) ( $h$ ) can be described as a function of the location ( $x$ ) and time ( $t$ ):

$$h = a \cos\left(\frac{2\pi x}{L} - \frac{2\pi t}{T}\right) = \frac{H}{2} \cos\left(\frac{2\pi x}{L} - \frac{2\pi t}{T}\right) \quad (1)$$

where  $L$  = wave length,  $T$  = wave period,  $H$  = wave height,  $2\pi/L = k$  (wave number), and  $2\pi/T = \omega$  (angular wave frequency).

Wave speed ( $c$  = celerity) can be approximated by

$$c = \frac{gT}{2\pi} \tanh\left(\frac{2\pi d}{L}\right) \quad (2)$$

and wave length by

$$L \cdot \frac{gT^2}{2\pi} \sqrt{\tanh\left(\frac{4\pi^2 d}{T^2 g}\right)} \quad (3)$$

which is an approximation sufficiently accurate for most calculations (as it gives a maximum error of 5% when  $2\pi/L = 1$ , i.e.  $d/L = 0.16$ ) (CERC, 1984).

The above equations can be approximated by simpler equations if the ratio of water depth to wave length ( $d/L$ ) satisfies certain conditions. If  $d/L > 0.5$  (usually defined as 'deep water'), the  $\tanh\left(\frac{2\pi d}{L}\right)$  approximates unity and

$$c_o = \frac{gT}{2\pi} = 1.56 T \text{ m/s}$$

$$L_o = \frac{gT^2}{2\pi} = 1.56 T^2 \text{ m} \quad (4)$$

where the subscript 'o' indicates deep water conditions. If  $0.5 > d/L > 0.04$ , however, the error introduced when using this approximation (4) is high (ca 9% for  $d/L = 0.25$ ) and the original equations (2) and (3) should be used. In very shallow water where  $d/L < 0.04$  the  $\tanh(x)$  approximates  $x$ , so that wave speed depends only on water depth:

$$c_s = \sqrt{gd} \quad (5)$$

where subscript 's' indicates shallow water conditions.

**Water pressure beneath waves.** Records of water pressure fluctuations at a certain distance below SWL are frequently used to obtain information on wave height, period, length, etc. According to linear wave theory (Kinsman, 1965) the total pressure under a wave is given as

$$[\text{total pressure}] = [\text{hydrostatic pressure}] + [\text{pressure due to wave form}] + [\text{pressure due to local kinetic energy of water motion}]$$

Pressure fluctuation due to local kinetic energy of water motion can usually be neglected as it is very small compared to pressure fluctuation due to the wave form. Therefore:

$$P = rg \frac{\cosh \left[ \frac{2\pi(z+d)}{L} \right]}{\cosh \left( \frac{2\pi d}{L} \right)} \frac{H}{2} \cos \left( \frac{2\pi x}{L} - \frac{2\pi t}{T} \right) - rgz + p_a \quad (6)$$

where  $P$  = total pressure,  $p_a$  = atmospheric pressure,  $r$  = water density,  $z$  = vertical distance between SWL and the point under the wave where the pressure is recorded, and  $d$  = water depth (at SWL). From equation (1),

$$P = rgh \frac{\cosh \left[ \frac{2\pi(z+d)}{L} \right]}{\cosh \left( \frac{2\pi d}{L} \right)} - rgz + p_a$$

and

$$K_z = \frac{\cosh \left[ \frac{2\pi(z+d)}{L} \right]}{\cosh \left( \frac{2\pi d}{L} \right)} \quad (7)$$

where  $K_z$  is the 'pressure response factor'. When the pressure is at a maximum,  $A = H/2$ , and  $p_a$  has been accounted for, equation (6) can be written as

$$A = \frac{N(p+rgz)}{rgK_z} \quad (8)$$

where  $N$  is a correction factor which decreases with decreasing period ( $N=1$  if linear wave theory applies and  $N < 1.0$  for short period waves) (CERC, 1984). Draper (1957) calibrated pressure readings against actual water level fluctuations derived from a capacitance-wire wave recorder and found the following relationship between bottom pressure and wave amplitude:

$$A = P \left[ 0.16 + \cosh \left( \frac{2\pi d}{L} \right) \right] \quad (9)$$

with an estimated error range of +2.9% to -3.9% (where  $A = H/2$ ,  $P$  = bottom pressure,  $d$  = water depth, and  $L$  = wave length).

Using equation (9), wave height  $H$  can be calculated from the maxima observed in water pressure records. It is this method which will be used in this project to convert pressure readings taken on the Stiffkey marsh to wave heights (see Section 3).

**Wave energy.** Another variable of particular interest with respect to coastal defence and coastal geomorphology is wave energy. In order to assess wave attenuation, wave energy needs to be determined at several locations along the path of wave propagation. The total energy of a wave is the sum of its kinetic and potential energy. Using linear wave theory, the total average wave energy per unit surface area,  $E$ , (i.e. the 'specific energy' or 'energy density' (CERC, 1984)) can be calculated once wave height  $H$  is known:

$$E = \frac{1}{8} \rho g H^2 \quad (10)$$

and the average energy flux (per unit wave crest) transmitted across a vertical plane at an angle,  $f$ , to the direction of wave propagation (the wave 'power') can be calculated from

$$P = E c n \sin f = E c_g \sin f \quad (11)$$

with

$$n = 0.5 \left[ 1 + \frac{\frac{4\pi d}{L}}{\sinh\left(\frac{4\pi d}{L}\right)} \right]$$

where  $c$  = wave speed and  $c_g$  = wave group velocity, with  $n = 0.5$  in deep water and  $n = 1$  in shallow water.

The above equations illustrate the mathematical simplicity of the linear (Airy) wave theory. As mentioned above, however, this theory has only very limited applicability for the study of shallow water waves. Longuet-Higgins (1975) and Cokelet (1977) for example found that for waves of finite amplitude, wave velocity and fluxes of energy and mass obtain maximum values for waves which have not yet obtained their maximum height. In addition to the limiting assumptions made by linear wave theory, the measurement of bottom pressure is itself limited by the attenuation of wave motion with depth. In coastal areas knowledge of tidal variations in SWL is therefore essential for the calculation of wave heights from pressure records. Furthermore, it is crucial that pressure records obtained under field conditions are calibrated against actual wave height observations from wave staffs or - as suggested in Section 3 - video techniques. Draper (1957), however, has shown that - once calibrated in the field - pressure records can give a very accurate estimate of wave spectra.

## **2.5. Generation of waves in deep water**

In addition to the theoretical knowledge of the relationships between the basic wave parameters discussed in the previous section, an understanding of the processes which lead to the measured wave characteristics is necessary if useful inferences about wave damping or about the effect of different meteorological conditions are to be made. This section provides a brief review of the main theories of wave generation and wave transformation and their theoretical and practical limitations with respect to this project.

Waves observed at a coastal site (such as the Stiffkey marshes) are the result of both offshore and shallow-water processes. Long-period swell waves created by distant North Sea storms are transformed as they pass through shallow coastal areas. In addition, local coastal winds may generate waves immediately offshore which then interfere with the swell waves, resulting in complex coastal wave spectra. The formation of waves through the action of wind can be divided into three main stages: First, the formation of initially very small capillary waves; second, the growth of those infinitesimal waves to form a wave field in deep water; and third, the transformation of the generated wave field over time and with increasing distance from the generating area. With respect to wave forecasting or the interpretation of coastal wave records the latter two stages are most important. The formation of capillary waves on an initially smooth water surface will therefore only be discussed briefly below.

It was not until the 1950s, that Phillips presented his theory on wind wave generation from an initially smooth water surface. According to this theory, pressure fluctuations in the wind field cause the initially infinitesimal surface fluctuations (see for example Bretschneider, 1966).

Once these infinitesimal waves are present on the surface, they grow as a result of instabilities at the water-air interface caused by the wind. In addition, the waves themselves change the wind pressure pattern: pressure differences between the leeward side (low pressure) and the windward side (high pressure) of the waves cause the wave to move in the direction of the wind. According to Jeffrey, the lowest windspeed required for this process to operate is  $1 \text{ ms}^{-1}$  (see Horikawa, 1978, for a more detailed discussion of this process).

Research on ocean wave development and especially ocean wave forecasting became strategically important during the second World War. This was the time when Sverdrup and Munk developed their semi-empirical forecasting method for statistical wave parameters (see below). Their theory of wave growth emphasised the importance of the energy balance of



waves which results from the energy transfer from the wind to the waves and the energy loss of the waves due to viscosity and turbulence.

Once the waves have been created through the action of wind on the water surface, the duration for which they persist depends on the headwind they encounter and the smoothness of the wave shapes (with steeper waves causing more resistance and dying out faster than smoother wave shapes). Wave height and its development through time and over distance will depend on wind force (speed), the duration for which the wind persists and the distance over which the wind blows (fetch). The various contributions to the energy budget for wind waves are presented in diagrammatic form in figure 13. Wave forecasting methods are therefore based on the development of equations which allow the calculation of wave height(s) as a function of wind speed, duration and fetch.

The currently most advanced forecasting methods require extensive computations (see CERC, 1984) and are not suited for practical wave spectra predictions which are required in this project. Here, the simpler wave forecasting techniques which provide estimates of the wave spectra accurate enough for the purpose of this project are discussed.

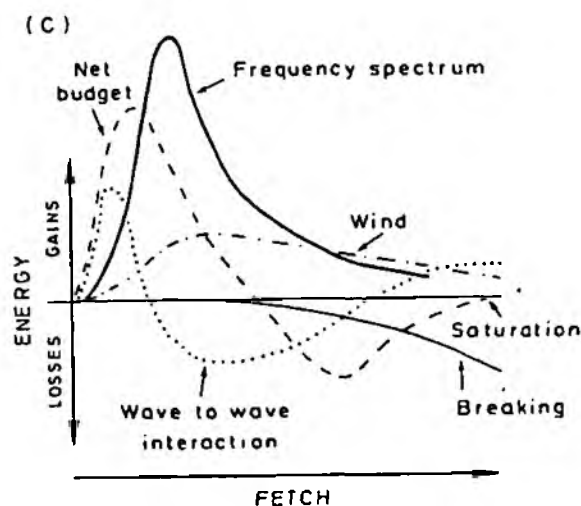


Fig. 13: Various contributions to the energy budget of wind waves (source: Carter, 1988).

Sverdrup and Munk, for example, established a fetch graph on the basis of two equations which express the relationship between the significant wave height ( $H_{1/3}$ ), the significant wave period ( $T_{1/3}$ ), the mean wind velocity ( $U$ ) and the fetch ( $F$ ):

$$\frac{gH_{1/3}}{U^2} = 0.3 \left\{ 1 - \frac{1}{(1 + 0.004(\frac{gF}{U^2})^{0.5})^2} \right\}$$

$$\frac{gT_{1/3}}{2\pi U} = 1.37 \left\{ 1 - \frac{1}{(1 + 0.008(\frac{gF}{U^2})^{1/3})^5} \right\} \quad (12)$$

In addition, the minimum required wind duration (i.e. the time required to progress with the group velocity  $c_g$  from the point  $x=0$  to the point  $x=F$ ) is defined as:

$$t_{\min} = \int_0^F \frac{dx}{c_g}$$

It can be calculated from:

$$\frac{gt_{\min}}{U} = \int_0^F \frac{d(\frac{gx}{U^2})}{\frac{gT_{1/3}}{4\pi U}} \quad (13)$$

for which a first approximation was introduced by Bretschneider:

$$T_{1/3} = 0.5 \sqrt[4]{U^2 F}$$

$$H_{1/3} = 0.0555 \sqrt{U^2 F}$$

$$\frac{F_{\min}}{t_{\min}} = 0.57 \sqrt[4]{U^2 F} = 1.14$$

and all variables can be expressed in a wave forecasting chart such as that in figure 14. As Sverdrup and Munk's theory was further developed by Bretschneider it is usually referred to as the 'SMB' method.

The SMB method has its limitations in that it is based entirely on the assumptions of linear (Airy) wave theory (i.e. on small amplitude waves and closed circular particle orbits). It also assumes a fixed fetch and a fixed wind speed for the duration ( $t$ ). When the wind speed changes at a certain time, another procedure has to be followed to calculate the resulting  $H_{1/3}$  on the assumption that  $H^2 T^2$  is constant and no wave energy is dissipated (Horikawa, 1978). Furthermore, the basis for their energy transfer calculations is a statistically defined wave

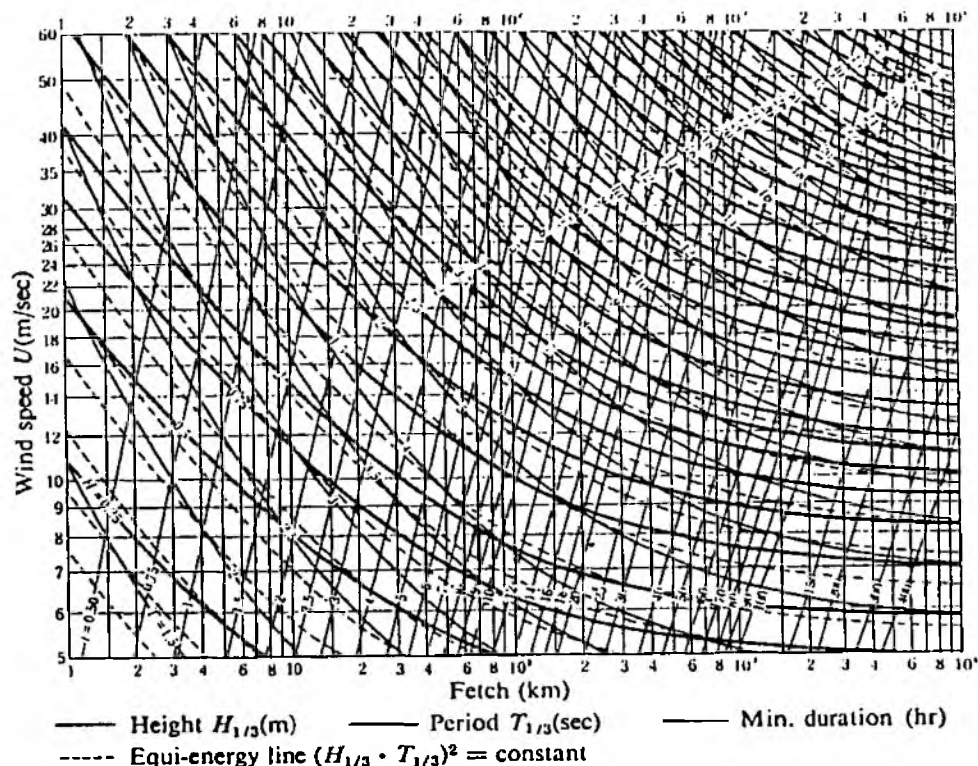


Fig. 14: Fetch graph showing the relationship between fetch distance, wind speed, and significant wave height established by Sverdrup and Munk (source: Horikawa, 1978).

with the 'significant' wave height (i.e. the mean height of the highest one-third of waves present in the sea). As this is a purely statistical variable, it is a gross simplification and of little use for the prediction of individual processes leading to wave growth. Kinsman (1965, p.303) strongly criticises Sverdrup and Munk's theory on the grounds that "... the selection of a single average height and period, which is then to be propagated as though it were a pure sine wave, is carrying the simplification too far. Essential features of the sea surface are lost or falsified. You might as well face the problem squarely: *Significant waves are statistical artifacts*. They have no crest whose identity could be maintained. They are not to be found in the sea. They exist in your mind."

Since the 1960s, however, the use of the 'significant' wave height as a statistic variable has become commonplace (e.g. CERC, 1984) and it has become apparent, that reasonably accurate estimates of wave conditions are only possible if the highly dynamic nature of the sea and the wave generating processes is treated statistically.

Although Wilson established a graphical method to overcome the problem of wave prediction from a moving storm, a more powerful forecasting method to predict the whole wave spectrum (the 'PNJ' method) was developed in the 1950s by Pierson, Neumann and James (Pierson *et al.*, 1955).

From wave observations, Neumann deduced that there exists a critical lower wave frequency ( $s_1$ ) (determined by wind velocity ( $U$ ) and fetch ( $F$ ) or wind velocity ( $U$ ) and duration ( $t$ )). Below this critical frequency, the energy density of the wave spectrum is zero or negligible. Beyond this critical frequency, the energy spectrum is assumed to be equal to the Neumann spectrum, given as:

$$[A(s)]^2 = C \frac{\pi}{2} s^{-6} \exp[-2g^2 s^{-2} U^{-2}] \quad (\text{for } s \geq s_1) \quad (14)$$

where ( $s$ ) is the radian frequency ( $2\pi/T$ ),  $g$  is the gravitational acceleration,  $U$  the wind speed, and  $C$  is a dimensionless number. The idea behind this formula is that the energy spectrum of ocean waves evolves from the high-frequency band to the low-frequency band through time and with increasing distance (fetch). Figure 15 illustrates this relationship schematically.

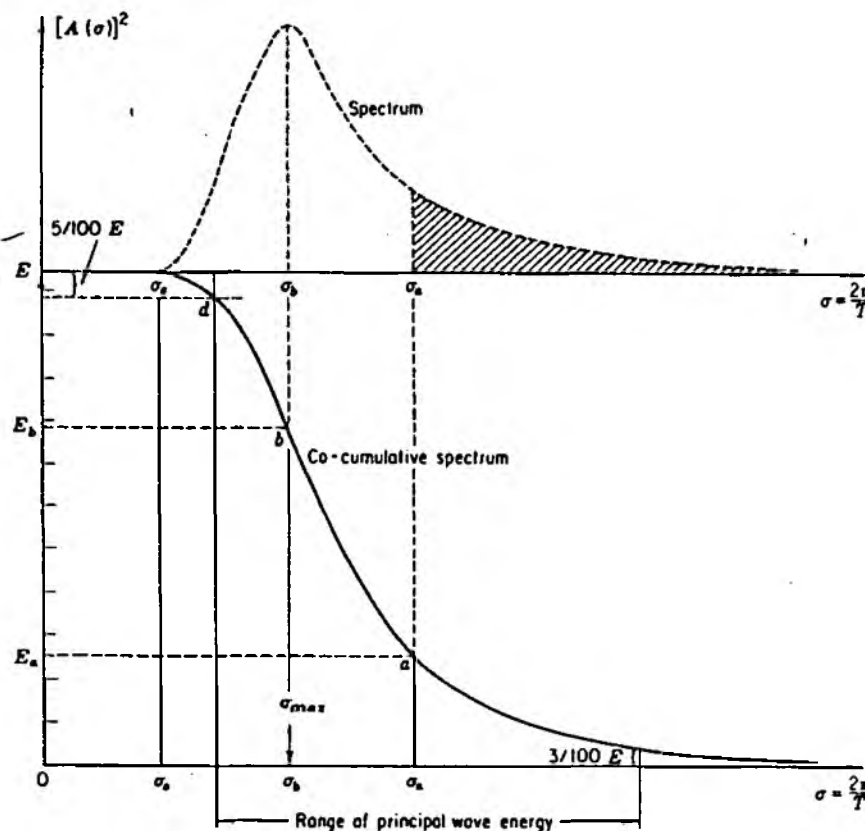


Fig. 15: The growth of wave spectra from high to low frequencies and the corresponding co-cumulative power spectrum (source: Kinsman, 1965).

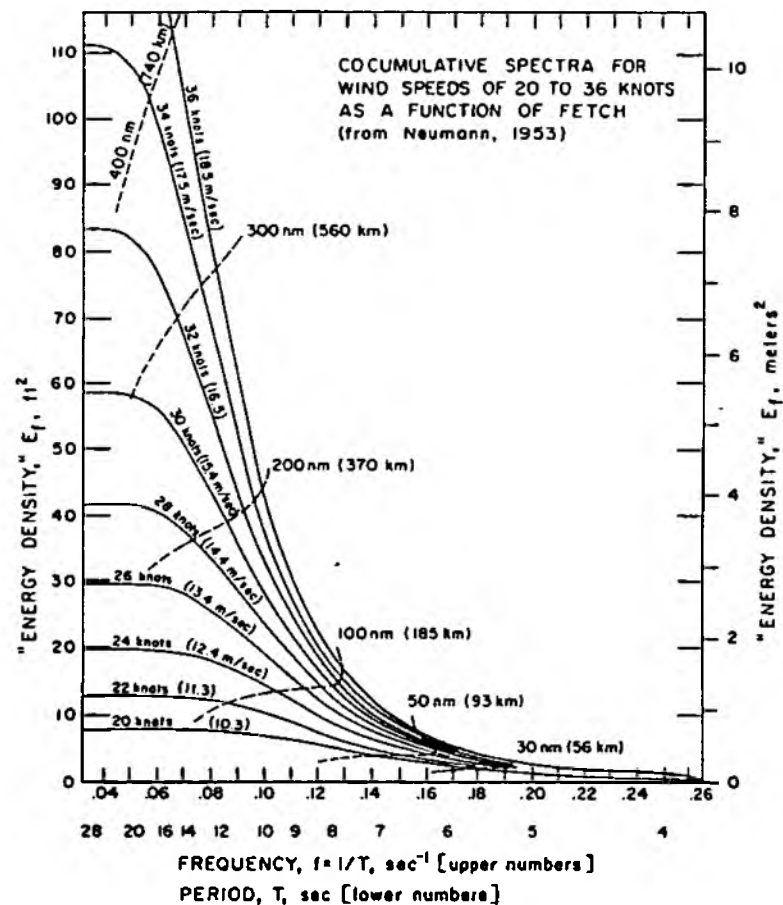


Fig. 16: Wave spectra and 'cut-off frequencies' for different wind speeds, fetch, duration (source: Pierson, Neuman and James, 1955).

Once the energy transferred to the waves equals the energy lost through viscosity and turbulence, i.e. the waves have grown to an equilibrium state, one speaks of a 'fully aroused sea' (FAS). The spectra of waves in conditions of different wind velocities and fetch can be derived from figure 16. Integration of such spectra from high to low frequencies results in the co-cumulative power spectrum (CCS) (see figure 15) from which one derives the total energy present in the wave spectrum:

$$E[s;U] = C \frac{\pi}{2} s^5 \exp[-2g^2 s^{-2} U^{-2}] ds \quad (15)$$

For a partially developed sea, only part of this energy will be contained in the resulting wave spectrum. Taking the values  $U$ ,  $F$ , and  $t$  as given, it is possible to read off the 'cut off'

frequency ( $s_1$ ), the total energy  $E$ , and the range of frequencies present in that partially developed sea (see figure 16). For a 32 Knot ( $16.4 \text{ ms}^{-1}$ ) wind blowing over a distance of 200 nautical miles (370 km) for 20 hours, for example, one derives (from the intersection of the 32 Knot line with the 200 NM line and from the intersection of the 32 Knot line with the 20 hour line) that  $E(U,t) > E(U,F)$ . In this case, the partially developed sea is referred to as fetch limited. Due to the relatively small size of the North Sea, it is expected, that most of the spectra measured on the Norfolk coast will be fetch-limited. Northerly winds, however, are associated with considerable fetch at the Norfolk coast (see Huthnance, 1991).

One main disadvantage of the frequency energy spectrum from equation (14) is its one-dimensionality. It does not include any information on the direction of wave travel. On the basis of very limited observational data, Pierson, Neumann and James (1955) formulated an estimate of a directional (two-dimensional) spectrum:

$$[A(s,q)] = \begin{cases} C s^{-6} \exp[-2g^2 s^{-2} U^{-2}] \cos^2 q & 0 \leq q \leq \pi \\ 0 & \text{otherwise} \end{cases} \quad (16)$$

where ( $q$ ) is the angle relative to the wind direction at which the waves travel. Empirical data has largely confirmed Neumann's spectrum, but more detailed analysis of wave records and meteorological conditions (e.g. by Pierson and Moskowitz (1964) and Hasselmann *et al.* (1973)) has led to the replacement of  $s^{-6}$  by  $s^{-5}$  (see table 1 for a comparison of wave predictions by various methods).

All of these spectra are based on the assumption that the formation of ocean waves is a stationary Gaussian process: They assume that the conditions of wave formation remain constant for a given period of time( $t$ ) although it is to be expected, that even within a generating area, any closely suitable spectrum will be varying with space and time. It is important to note that observations suggest that the distribution of wave heights approximates a Gaussian distribution only during swell conditions, whereas wave heights during sea conditions approximate to a Rayleigh distribution (Longuet-Higgins, 1952; Cartwright and Longuet-Higgins, 1956). Carter (1988) has summarised these conditions in a diagram (figure 17) showing the distribution curves of wave heights for different values of ( $z$ ), where:

$$z = (1 - (\frac{N_z}{N_c})^2) \quad (17)$$

and  $N_C$  = the number of wave crests in the record,  $N_Z$  = the number of still water level up-crossings of the water surface.

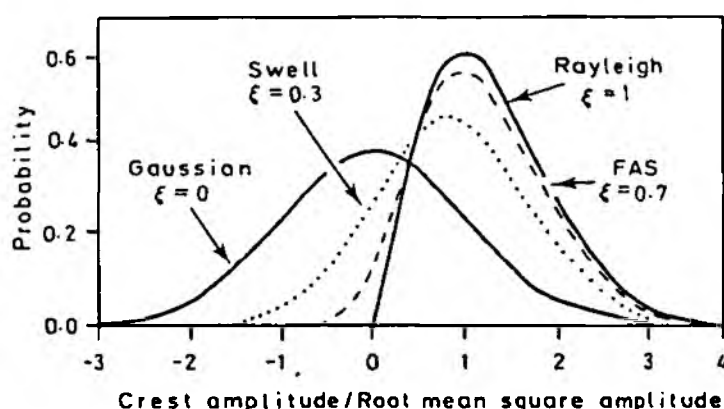


Fig. 17: Spectral width parameters for ideal wave height and frequency distributions (source: Carter, 1988).

As a result of the above statistical assumptions, these wave forecasting methods are not able to provide anything more than a rather crude and simplified estimate of wave spectra at a particular location in deep water. The dynamic and multivariate nature of the processes involved in wave generation and propagation and the lack of detailed meteorological and wave data for the open sea, however, do not leave any other option but to tackle the problem of wave forecasting and hindcasting statistically.

For the purpose of this project, estimates of deep sea wave spectra from the equations in table 1 and estimates of spectrally based significant wave heights derived from the semi-empirically established equations given in the Shore Protection Manual (CERC, 1984) (see table 2) will be sufficient to give an indication of the offshore wave climate during periods of wave recording over the tidal flat and the salt marsh surface (see Section 3.1).

Dimensionless	Metric Units	
	$H(m), T(s), U_A(m/s), F(m), t(s)$	$H(m), T(s), U_A(m/s), F(km), t(hr)$
<b><u>FETCH LIMITED, <math>(F, U)</math></u></b>		
$\frac{H_m}{U_A^2} = 1.6 \times 10^{-3} \left( \frac{F}{U_A^2} \right)^{1/2} \quad (3-33)$	$H_m = 5.112 \times 10^{-4} U_A F^{1/2} \quad (3-33a)$	$H_m = 1.616 \times 10^{-2} U_A F^{1/2} \quad (3-33b)$
$\frac{RT_m}{U_A} = 2.837 \times 10^{-1} \left( \frac{F}{U_A^2} \right)^{1/3} \quad (3-34)$	$T_m = 6.238 \times 10^{-2} (U_A F)^{1/3} \quad (3-34a)$	$T_m = 6.238 \times 10^{-1} (U_A F)^{1/3} \quad (3-34b)$
$\frac{RT_m}{U_A} = 6.88 \times 10^{-1} \left( \frac{F}{U_A^2} \right)^{2/3} \quad (3-35)$	$t = 3.215 \times 10^1 \left( \frac{F}{U_A^2} \right)^{1/3} \quad (3-35a)$	$t = 8.93 \times 10^{-1} \left( \frac{F}{U_A^2} \right)^{1/3} \quad (3-35b)$
<b><u>FULLY DEVELOPED</u></b>		
$\frac{H_m}{U_A^2} = 2.433 \times 10^{-1} \quad (3-36)$	$H_m = 2.482 \times 10^{-2} U_A^2 \quad (3-36a)$	$H_m = 2.482 \times 10^{-2} U_A^2 \quad (3-36b)$
$\frac{RT_m}{U_A} = 8.134 \quad (3-37)$	$T_m = 8.30 \times 10^{-1} U_A \quad (3-37a)$	$T_m = 8.30 \times 10^{-1} U_A \quad (3-37b)$
$\frac{RT_m}{U_A} = 7.15 \times 10^4 \quad (3-38)$	$t = 7.296 \times 10^3 U_A \quad (3-38a)$	$t = 2.027 U_A \quad (3-38b)$
<b><u>NOTATIONS</u></b>	$g = 9.8 \text{ m/s}^2$ $g = 9.8 \text{ m/s}^2$ 1 kilometer = 1000 m 1 hour = 3600 s	

Table 1: Semi-empirical deep-water forecasting equations (source: CERC, 1984)

WIND SPEED (m/sec)	FETCH DISTANCE (km)	SIGNIFICANT WAVE HEIGHT (m)				SIGNIFICANT WAVE PERIOD (sec)			
		S-M-B	P-N-J	Liu	Darbyshire*	S-M-B	P-N-J	Liu	Darbyshire
10	200	2.1	2.4	2.1	1.2-1.4	7	8	7	7
10	1,000	2.7	2.4	3.4	1.2-1.5	11	8	10	7
20	200	5.2	4.3	5.8	4.3-5.2	10	8.5	10	10
20	1,000	8.9	11	9.2	4.6-5.6	15	16	15	11
30	200	8.2	7.9	11	9.7-12	12	10	12	15
30	1,000	15	15	17	11-13	19	15	18	16

\*Darbyshire and Draper (1963) give  $H_{max}$ . The theoretical  $H_{max}$  from Longuet-Higgins (1952) depends on the wave period and on the length of the record (Table 3-1). Thus a range of possible  $H$  values are given for the Darbyshire approach.

Table 2: Comparison of wave predictions by various methods (source: Komar, 1976).



## 2.6. Wave transformations and generation in shallow coastal water

If the PNJ method is to be used successfully for the forecasting or hindcasting of coastal wave spectra processes such as refraction, diffraction, and wave damping have to be considered. Processes of wave transformation in shallow water can be divided into linear and non-linear mechanisms. Linear mechanisms include wave refraction, diffraction, shoaling and transformations due to percolation, bottom motion and scattering of waves by bottom irregularities. Non-linear mechanisms include bottom friction and non-linear wave-wave interactions which redistribute the wave energy within the wave spectrum.

Each of these mechanisms is discussed briefly in turn, although most emphasis is placed on shoaling and refraction, which are likely to be dominant in areas with gently sloping shore profiles (such as on the north Norfolk coast) (Shermin, *et al.*, 1980). Shoaling refers to the change in wave height, length and velocity when waves enter shallow water. From small amplitude wave theory (see Section 2.4):

$$\frac{L}{L_d} = \frac{c}{c_d} = \tanh \frac{2\pi h}{L}$$

which can also be written as:

$$\frac{h}{L_d} = \frac{h}{L} \tanh \frac{2\pi h}{L} \quad (18)$$

(where  $h$  = water depth,  $L_d$ ,  $L$  = wave length in deep and shallow water respectively,  $c$ ,  $c_d$  = wave velocity in shallow and deep water respectively), i.e. the wave length  $L$  at water depth  $h$  is determined by the water depth and the deep water wave length.

If one assumes that the total energy of the waves between two adjacent orthogonals (i.e. lines drawn perpendicular to the wave crests) is conserved as they approach the shore, the following is true:

$$\frac{H}{H_0} = \sqrt{\frac{c_0}{2nc_0}} = K_s \quad (19)$$

where  $H$ ,  $H_0$  = wave height in shallow and deep water respectively,  $c$ ,  $c_0$  = wave speed in shallow and deep water respectively, and  $c_g = cn$  = group velocity (see equation 11).

$K_s$  is named the shoaling coefficient and indicates the change in wave height due to decreasing water depth.  $K_r$  is the refraction coefficient and indicates the change in distance between two

wave rays as the wave crests approach the shore. Important wave shoaling transformations are summarised in figure 18.

As the group velocity becomes equal to the wave speed when waves approach shallow water ( $L/h > 20$ ) the wave crests align themselves parallel to the depth contours. This process is called refraction and is explained in its simplest form in figure 19 in which

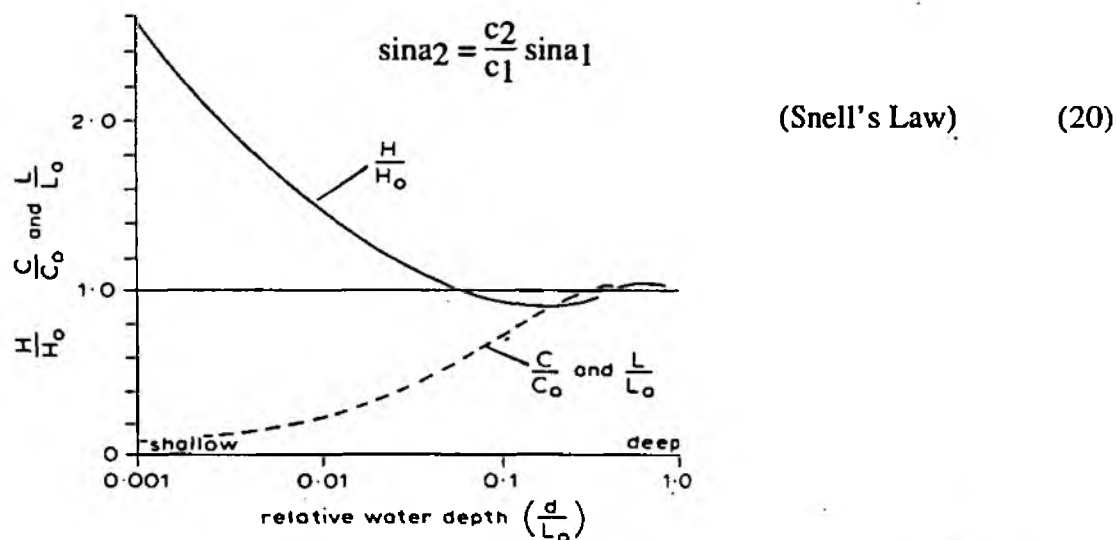


Fig. 18: Wave shoaling transformations ( $H, C, L$  = wave height, celerity, and length respectively (where the subscript 0 indicates deep water values), and  $d$  = water depth) (source: Pethick, 1986).

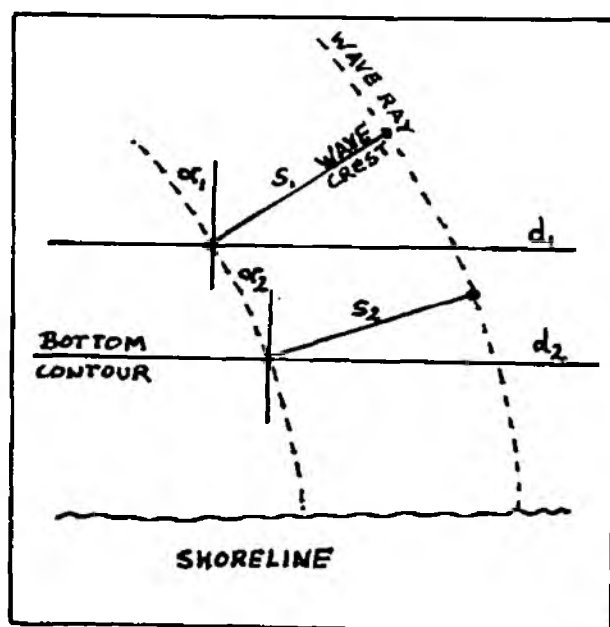


Fig. 19: The relationship between wave approach angle ( $\alpha$ ), water depth ( $d$ ), and wave crest length ( $s$ ). Wave rays are normal to the wave crests. (see equation 22 and text).

Refraction diagrams can be constructed by drawing the orthogonals to the wave crests. If the angle of wave approach ( $\alpha$ )  $< 80^\circ$ , one can construct contours for  $L_0/2$  and then calculate wave speeds  $c$  for the different water depths. By calculating the ratio of  $c_1/c_2$  of wave speeds at adjacent depth contours, one can construct the wave orthogonals using a refraction template (CERC, 1984). For incident angles ( $\alpha$ )  $> 80^\circ$  the procedure is slightly more complex and contour intervals need to be subdivided to calculate wave orthogonals (Horikawa, 1978). The interpretation of such wave refraction diagrams is based on the relationship between wave speed in shallow and deep water as predicted by linear (Airy) wave theory. One therefore assumes that waves are long-crested, of constant period and small amplitude.

Refraction diagrams constructed on the basis of the above formulae are strictly only valid for small waves moving over gentle slopes. Strict accuracy cannot be expected for slopes steeper than 1:10 (CERC, 1984). Furthermore, construction techniques for refraction diagrams based on Snell's Law assume that the direction of wave advance is strictly orthogonal to the wave crest and that the speed of a wave with a given period at a particular location depends only on the depth at that location. The effects of currents, winds, and wave reflections from beaches or underwater topography are not considered in refraction diagrams. The situation gets extremely complicated, when waves of different frequency approach a shallow coastal area with complex bottom features from different directions. Complex coastal wave spectra result which are very different from the deep sea wave spectra off the coast and the graphic methods of constructing wave rays can only lead to an approximation of the coastal spectral energy density function. A useful hypothetical example of such an approach to the forecasting and hindcasting of coastal wave spectra is given by Kinsman (1965) (figure 20 to figure 21). Figure 20 shows the isolines for the values of the refraction function ( $K$ ) which is the function which has to be applied to the deep sea spectra to transform it into shallow water spectra, i.e.

$$[A(s,a)]^2 = [A_d(s_d,a_d)]^2 [K(s_d,a_d)]^2 \quad (21)$$

$K$  depends on the incident wave frequency  $f$  and the direction of wave approach. The function is approximated graphically according to the method described above (Kinsman, 1965; Horikawa, 1978). The deep sea wave spectra recorded in the fields marked in figure 20 is transformed to give the refracted frequency spectrum shown in the bottom half of figure 21 (other examples are given in the Shore Protection Manual (CERC, 1984)).

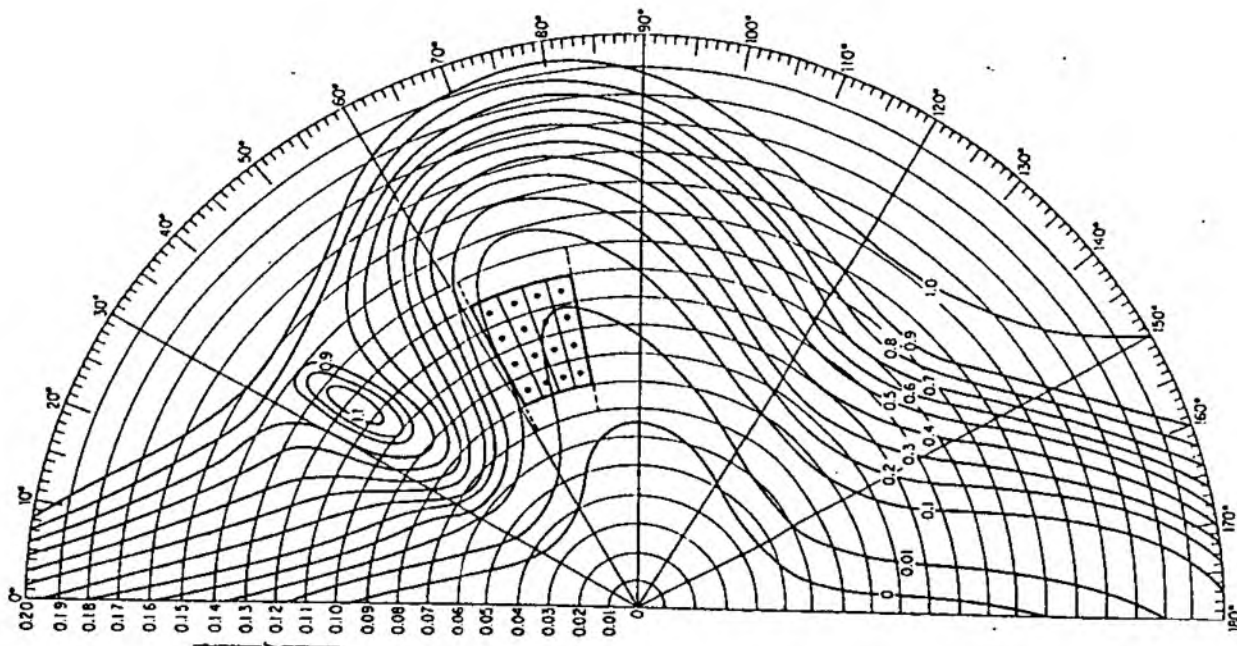


Fig. 20: Location of deep water spectrum on a hypothetical refraction function (source: Kinsman, 1965).

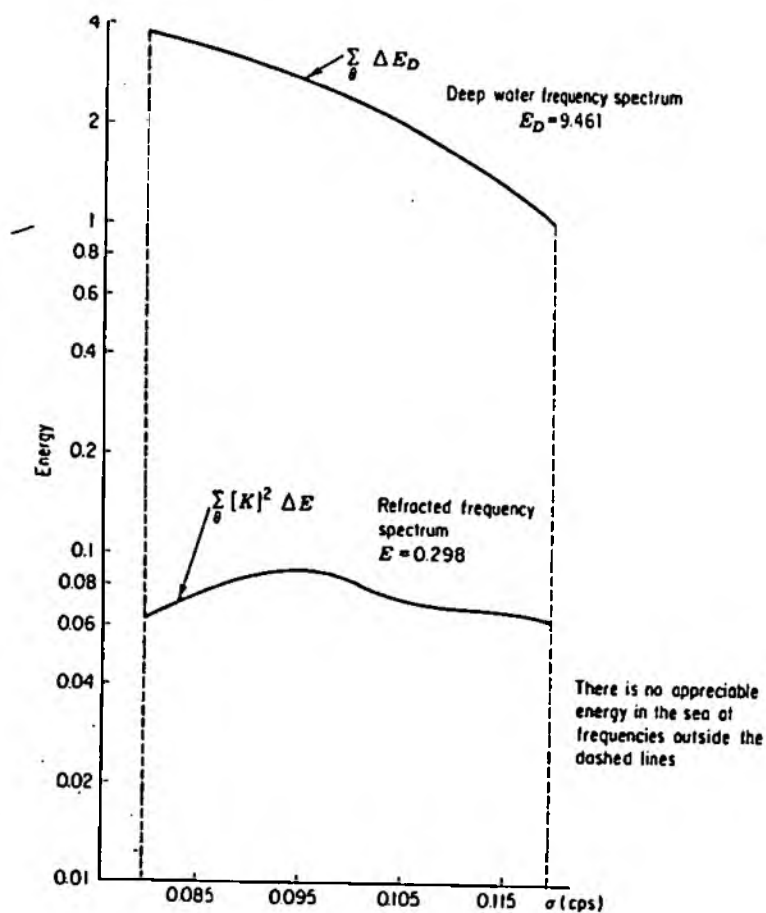


Fig. 21: Deep water and refracted shallow water spectra as calculated for the hypothetical example in figure 21 (source: Kinsman, 1965).

For the purpose of shallow water wave spectra predictions at the Stiffkey marsh field site, the method of constructing wave refraction diagrams as described in the Shore Protect Manual (CERC, 1984) will be used (see Section 3).

The changes of waves approaching shallow water are not solely due to shoaling, refraction, and reflection. Linear mechanisms such as percolation, bottom motion, and the scattering of waves by bottom irregularities and non-linear wave-wave interaction and bottom friction all dissipate wave energy. Shemdin *et al* (1980), for example, studied the relative importance of each of these mechanisms with respect to the data collected in the JONSWAP (Joint North Sea Wave Project) project. With respect to percolation, it was found, that it was an effective mechanism of wave attenuation in coarse sand (diameter > 0.5 mm) but that the effect of bottom friction dominates in finer sand (diameter < 0.4 mm). If sand ripples are present, friction may even dominate over percolation in coarse sand:

Energy dissipation caused by percolation is given by Shemdin *et al.* (1980) as:

$$\frac{\partial E}{\partial t} = -Ek \sqrt{ab} \frac{\tanh \sqrt{a/b} kd}{\cosh^2 kh} \quad (22)$$

where  $h$  = water depth,  $a$ ,  $b$  = horizontal and vertical permeability coefficients, respectively, and  $k$  is the wave number.

Assuming an isotropic sand ( $a=b$ ) and a deep sand layer ( $d > 0.3$  wave length) this equation becomes:

$$\frac{\partial E}{\partial t} = -\frac{Eka}{\cosh^2 kh} \quad (23)$$

or, as Horikawa (1978) used it:

$$D = \frac{\pi k g H^2}{4L \cosh^2(2\pi h/L)} \quad (24)$$

where  $k$  is the coefficient of permeability.

Bottom motion becomes important as a mechanism of energy dissipation when one deals with highly mobile sediments, such as mud or decomposed organic matter. Waves over mudflats bordering salt marshes may therefore be affected by bottom motion.

According to Shemdin *et al.* (1980) the energy dissipation owing to bottom motion for a finite-depth mud layer is

$$\frac{\partial E}{\partial t} = -2k_i c_g E \quad (25)$$

where

$$k_i = k_r + ik_i = \frac{w^2}{g} \frac{1 + \tanh(kh) \Omega}{\tanh(kh) + \Omega}$$

and  $\Omega$  = complex function of mud and water properties.

Scattering of waves by irregularities in bottom topography is dependent on the shape, size, and frequency of those irregularities and no generalisations are possible. It is also very difficult to distinguish wave scattering from the effect of bottom friction. Bottom friction depends not only on the mean diameter of the sediment, but also on sand ripple characteristics which influence the orbital velocities just outside the bottom boundary layer. These variables are included in the equation of the bottom shear stress, ( $t_0$ ):

$$t_0 = C_f \rho u_0^2 \quad (26)$$

where  $C_f$  is a friction coefficient, ( $\rho$ ) the water density and  $u_0$  the horizontal velocity component of a fluid particle near the bottom.

Horikawa (1987) describes the theory formulated by Bretschneider and Reid, who defined a coefficient  $K_f$  which expresses the change in wave height,  $H$ , due to surface friction:

$$K_f = \frac{H_2}{H_1} \cdot \left[ 1 + \frac{64\pi^3}{3} \frac{f H_1 \Delta x}{g^2 h^2} \left( \frac{h}{T^2} \right)^2 \frac{K_s^2}{\sinh^3(2\pi h/L)} \right]^{-1} \quad (27)$$

where  $H_1$  and  $H_2$  are the wave heights in two consecutive sections,  $\Delta x$  apart,  $K_s$  is the shoaling coefficient, and  $h$  the water depth. The analysis of the JONSWAP spectra by Shemdin *et al.* (1980) showed that friction can be the dominant form of wave energy transformation, overruling the effect of refraction and shoaling.

In very shallow water, however, non-linear wave-wave interactions are also likely to affect wave energy spectra. According to Shemdin *et al.*'s (1980) analysis of the JONSWAP data, the importance of non-linear wave-wave energy transfer increases dramatically for  $k_p h \leq 0.5$  (where  $k_p$  = peak wave number,  $h$  = water depth) but is important wherever  $k_p h \leq 1.0$ .

So far, deep water wave generation, propagation and shallow water wave transformations have been discussed as two classes of processes which determine coastal (shallow water) wave spectra. In addition to those two processes, locally wind generated shallow water waves also influence coastal wave spectra. Especially in regions with very gentle sloping beach profiles or offshore sandbars (such as on the north Norfolk coast) waves from distant storms are likely to become unstable and break a considerable distance offshore (see Section 2.7). In this case, shallow water waves will be to a large extent locally reformed wind waves. As waves in shallow water cannot grow beyond a certain limit determined by the water depth (see above) the deep-sea wave forecasting relationships discussed above are not applicable for shallow water wave generation, unless the shallow water wave height transformations over the appropriate length of fetch are accounted for. Attempts have been made by Bretschneider (see Horikawa (1978) and CERC (1984)) to establish a practical prediction method for waves in shallow water of constant depth and in shallow water over a sloping bottom (see figure 22 (a,b) and 23).

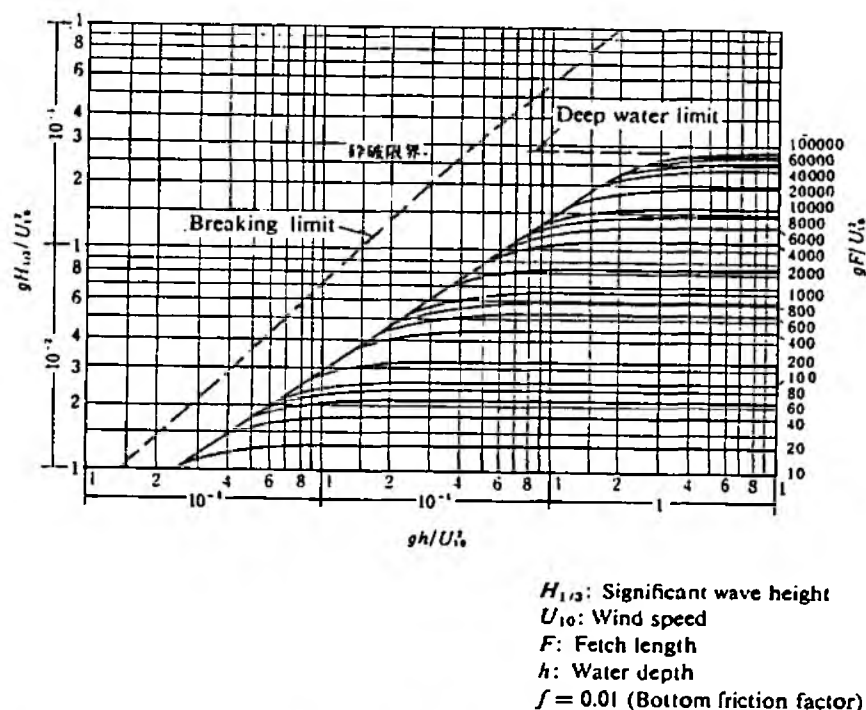
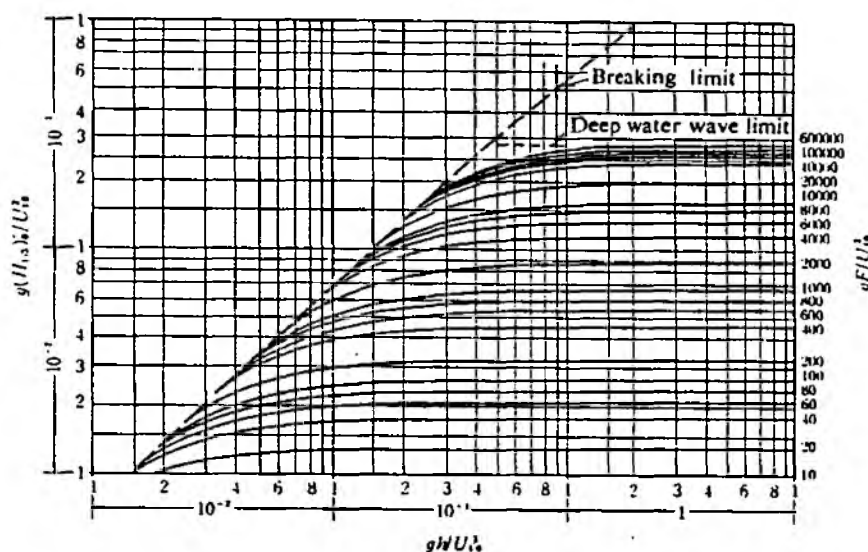


Fig. 22:

a. Generation of wind waves over a constant depth bottom for unlimited wind duration. After Bretschneider (source: Horikawa, 1978).

Exact analytical solutions to the problem of locally generated shallow water waves contributing to coastal spectra are highly complex and inapplicable with respect to the practical purpose of this project as this study will focus on conditions of extreme water elevations and meteorological conditions under which wave spectra are likely to be dominated by waves generated offshore. Practical prediction methods based on Bretschneider's ideas will therefore be used to derive an estimate of the importance of locally generated waves under the different observed tidal and meteorological conditions (see Section 3).

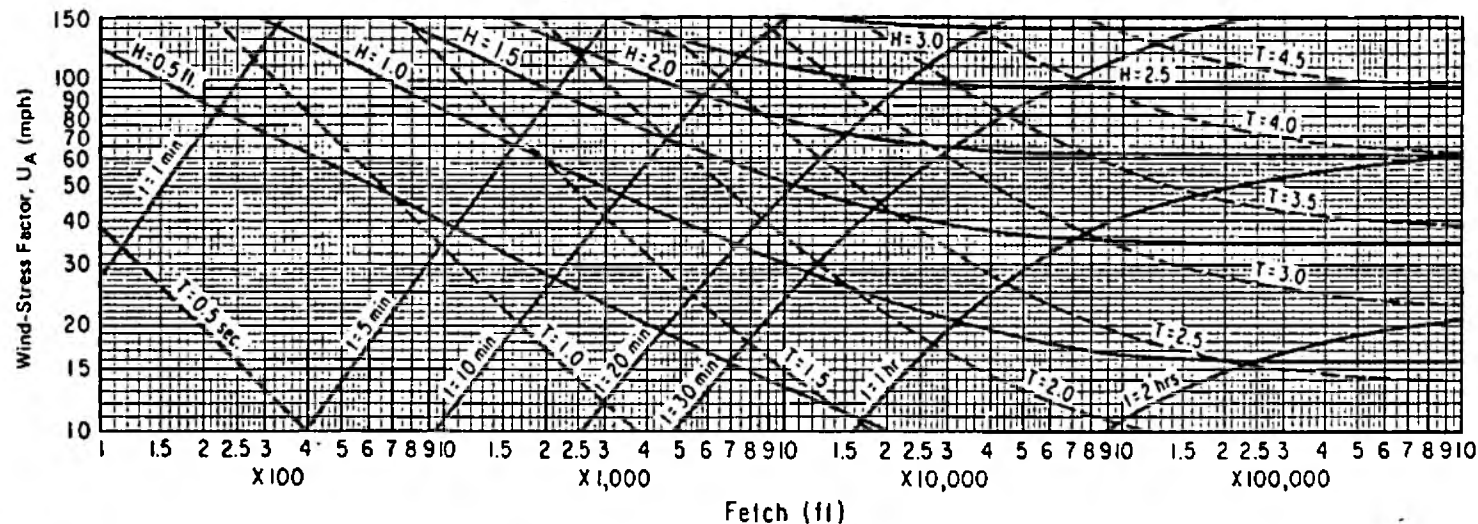


$(H_{1/3})_0$ : Equivalent deep water wave height  
 $U_{10}$ : Wind speed  $F$ : Fetch length  
 $h$ : Depth of water at end of fetch  
 $m$ : Bottom slope  
 $f$ : Bottom friction factor  
 $K_s$ : Shoaling coefficient  
 $H_{1/3} = K_s(H_{1/3})_0$ :  
 Significant wave height

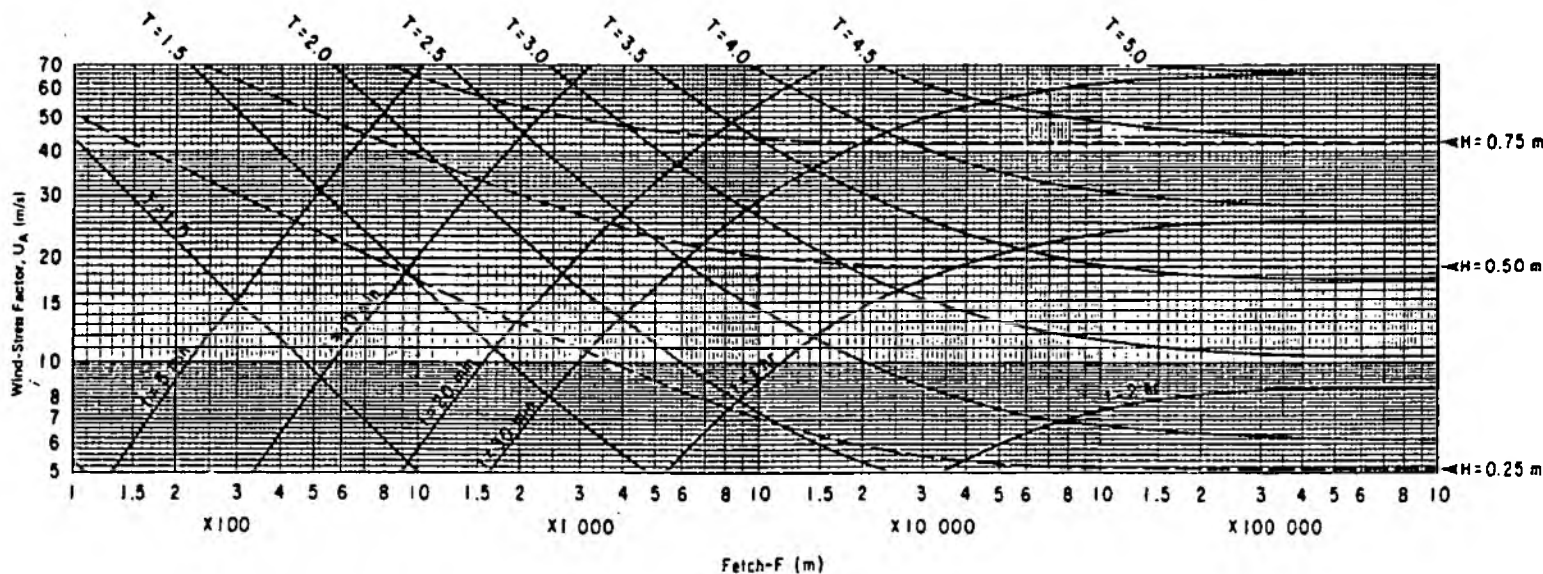
b. Generation of wind waves over a bottom of constant slope for unlimited wind duration, and  $f/m = 5.28$ . After Bretschneider (source: Horikawa, 1978).



Note: Waves in a water depth of 5 feet with wave periods less than 1.4 secs. are considered to be deepwater waves, i.e.,  $d/T > 2.56$ .



Note: Waves in a water depth of 1.5 meters with wave periods less than 1.4 seconds are considered to be deepwater waves, i.e.,  $d/T > 0.78$ .



Forecasting curves for shallow-water waves; constant depths = 5 feet (upper graph) and 1.5 meters (lower graph).

Fig. 23: Examples of forecasting curves for shallow-water waves (source: CERC, 1984).

## 2.7. Breaking waves

As mentioned above, wave height increases as waves progress into shallow water. The result is an increase in wave steepness ( $H/L$ ) which eventually leads to an instability of the wave form and the breaking of the wave. Knowledge on the breaking of waves approaching the shore is of importance for coastal wave spectra forecasting or hindcasting. If the breaking point of ocean waves is located seaward of the wave recording station, the wave spectra obtained are likely to reflect locally generated wind waves rather than ocean swell.

According to Stokes' wave theory, the sharpest wave crest angle possible is  $120^\circ$  when the particle speed at the very crest is equal to or greater than the wave speed and breaking therefore occurs as a result. The maximum wave steepness would then be  $H/L = 1/7 = 0.142$ . Stokes' estimate of this limiting wave steepness only applies to deep water conditions. Once the wave approaches shallow water, its length, height and speed change (see above) and the relative water depth will determine the point at which the waves become unstable.

Breaking waves are usually classed into three categories, illustrated in figure 24, which result from different bottom profiles and their effect on wave energy dissipation. These classes, however, only represent three stages in a continuum of breaking wave forms. The transition from one breaker type to another is a gradual process.

Figure 25 is a graphic representation of the relationship between the 'breaker height index' ( $H_b/H_o'$ , where  $H_b$  = breaker height,  $H_o'$  = unrefracted deep water wave height) and 'deep water steepness' ( $H_o'/gT^2$ ). The curves in figure 25 are given by

$$\frac{d_b}{H_b} = \frac{1}{b - (aH_b/gT^2)} \quad (28)$$

where  $b$  and  $a$  can be approximated by

$$a = 43.75 (1 - \exp[-19m])$$

$$b = \frac{1.56}{(1 + \exp[-19.5m])}$$

and  $m$  = beach slope.

As with most of the other mathematical approximations to water waves mentioned in this section, this method will only give an **estimate** of the location on the beach profile at which waves break. Such an estimate is useful, however, for the interpretation of coastal wave records such as those which will be obtained as part of this project (see Section 3).

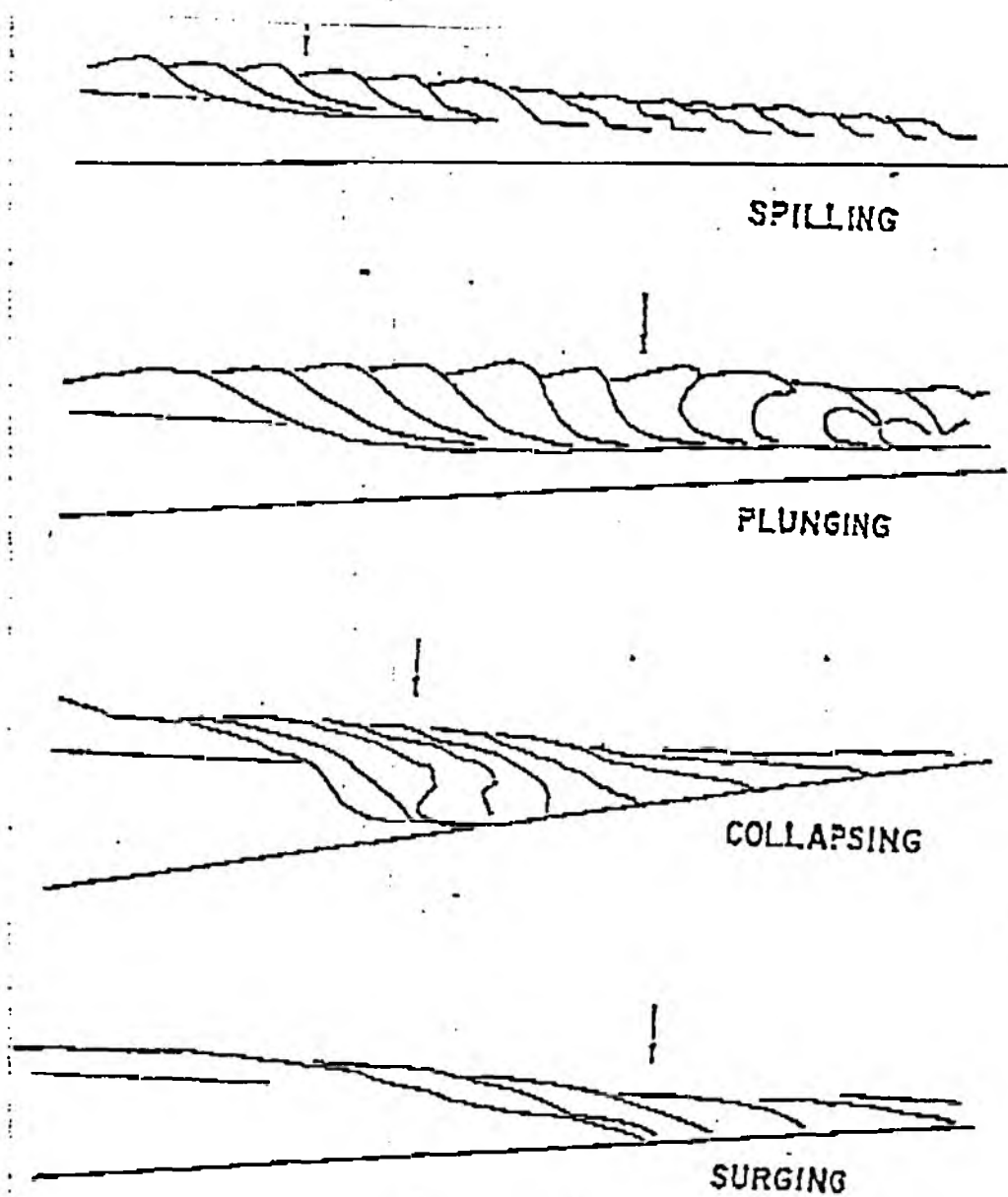


Fig. 24: Breaker type classification on three laboratory beaches (source: Galvin, 1968).

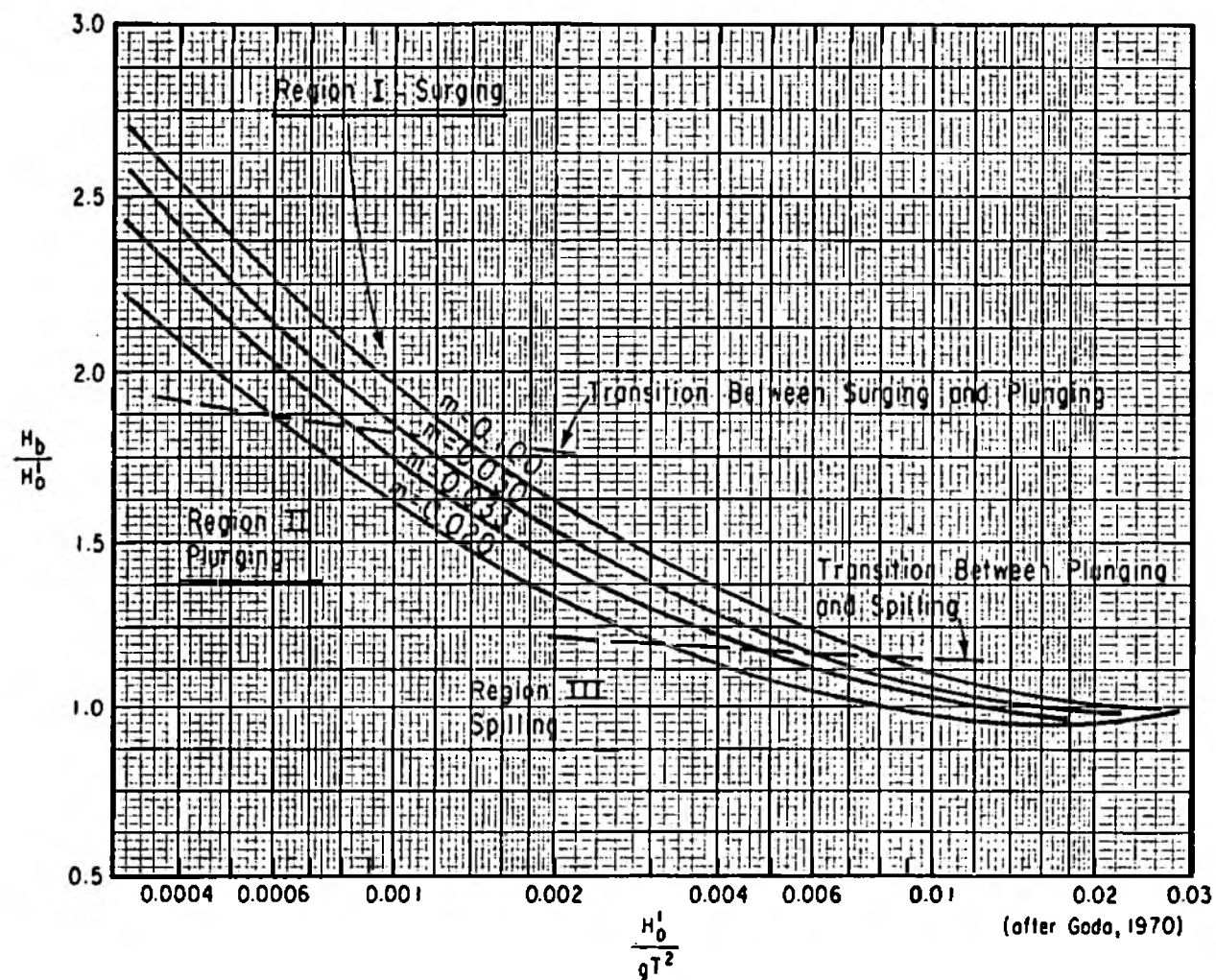


Fig. 25: Breaker height index versus deep water wave steepness (see equation 30)  
(source: CERC,1984).

### 3. THE PROJECT

#### 3.1. Main aims

The main aim of the project is to derive a quantitative estimate of wave attenuation over the salt marsh surface during different tidal inundation depths and meteorological conditions (see also Interim Report OI/569/1/A). Such information is of scientific interest in that it is linked to marsh sedimentation and hydrology and is of importance with respect to coastal defence. Although Brampton (1992) has addressed the question of energy dissipation across a salt marsh surface from an engineers' point of view, his treatment of the subject is restricted to theoretical considerations and limited hardware modelling. Wayne's (1976) study of wave energy dissipation on the coast of Florida indicates some reduction in wave energy across a salt marsh surface, but these findings have not been followed up in further studies. In addition to wave height and energy changes over the tidal flat and salt marsh surface, this study investigates a set of additional influences on wave parameters and the link between wave and tidal conditions and sedimentation patterns. Research will focus in particular on:

- i. the relative importance of offshore and coastal meteorological conditions and bathymetry in determining coastal wave spectra,
- ii. the possible link between wave and tidal conditions and marsh surface flow and sedimentation patterns, and
- iii. the influence of seasonal changes in marsh surface vegetation on wave height attenuation

Results will be used to develop theoretical and empirical relations for wave energy dissipation and sedimentation patterns on marshes of varying width and inundation frequencies. As such, the project will provide input into studies concerned with the artificial rehabilitation of salt marshes currently undergoing degradation and loss of area. The project will also provide useful information on hydrological processes influencing marsh surface sedimentation.

#### 3.2. Field site

The north Norfolk coast has been chosen as the field area, as local subsidence (ca  $1\text{ mm yr}^{-1}$ ) and relatively high storm frequency in the North Sea (see for example Suthons, 1963; Heaps, 1983; Schinke, 1992; and Schmidt and vonStorch, 1993) are likely to exacerbate the areas' response to future accelerated sea-level rise (at present, eustatic sea-level rise is about  $1\text{ mm yr}^{-1}$ ). Past North Sea storm surges (for example those of 1953 and 1978 (see Steers, 1953; Steers *et al.*, 1979; and NRA, no date (a)) have caused many deaths and considerable damage

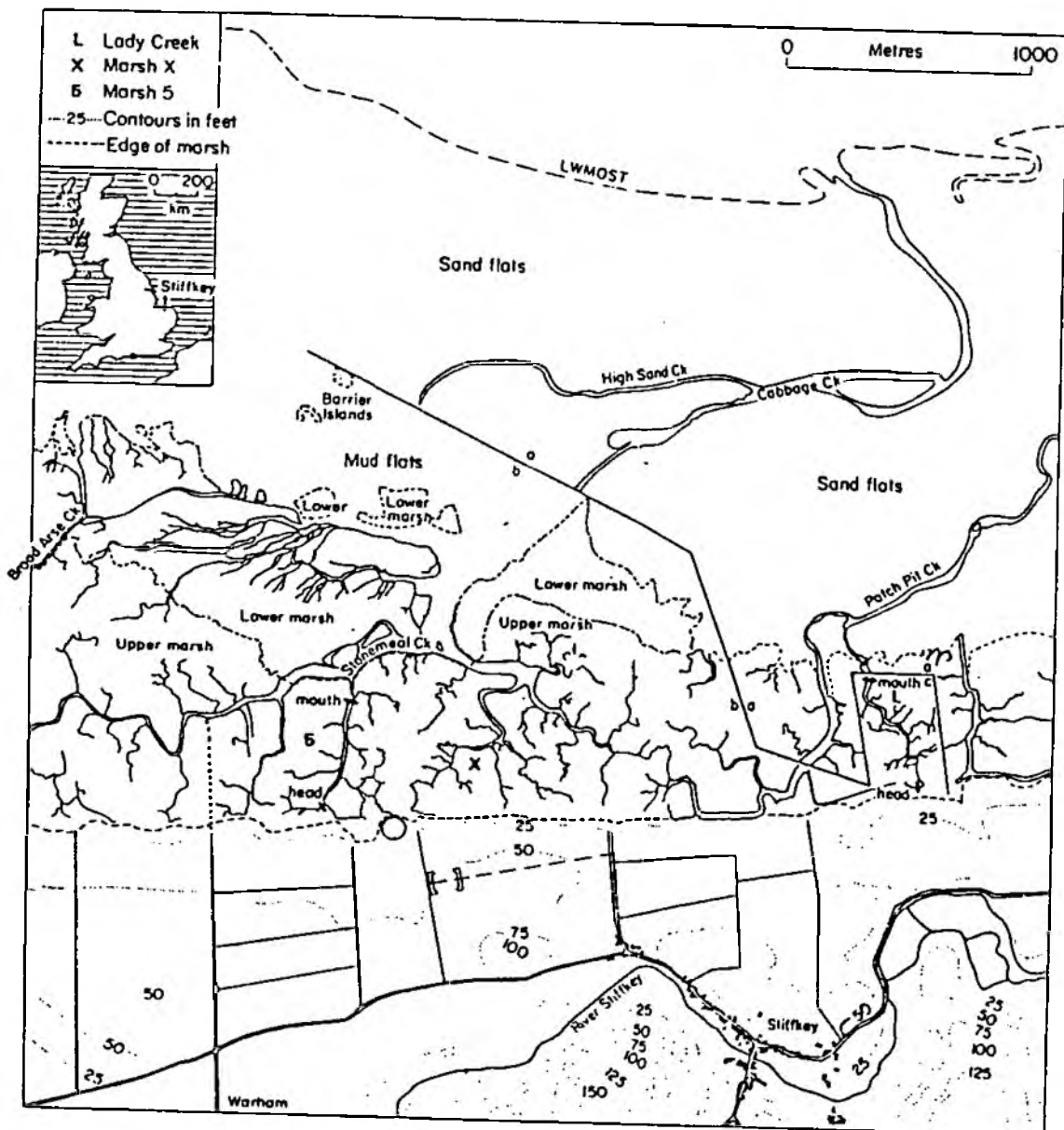


Fig. 26: The marshes between Stiffkey and Warham (source: Bayliss-Smith *et al.*, 1979).



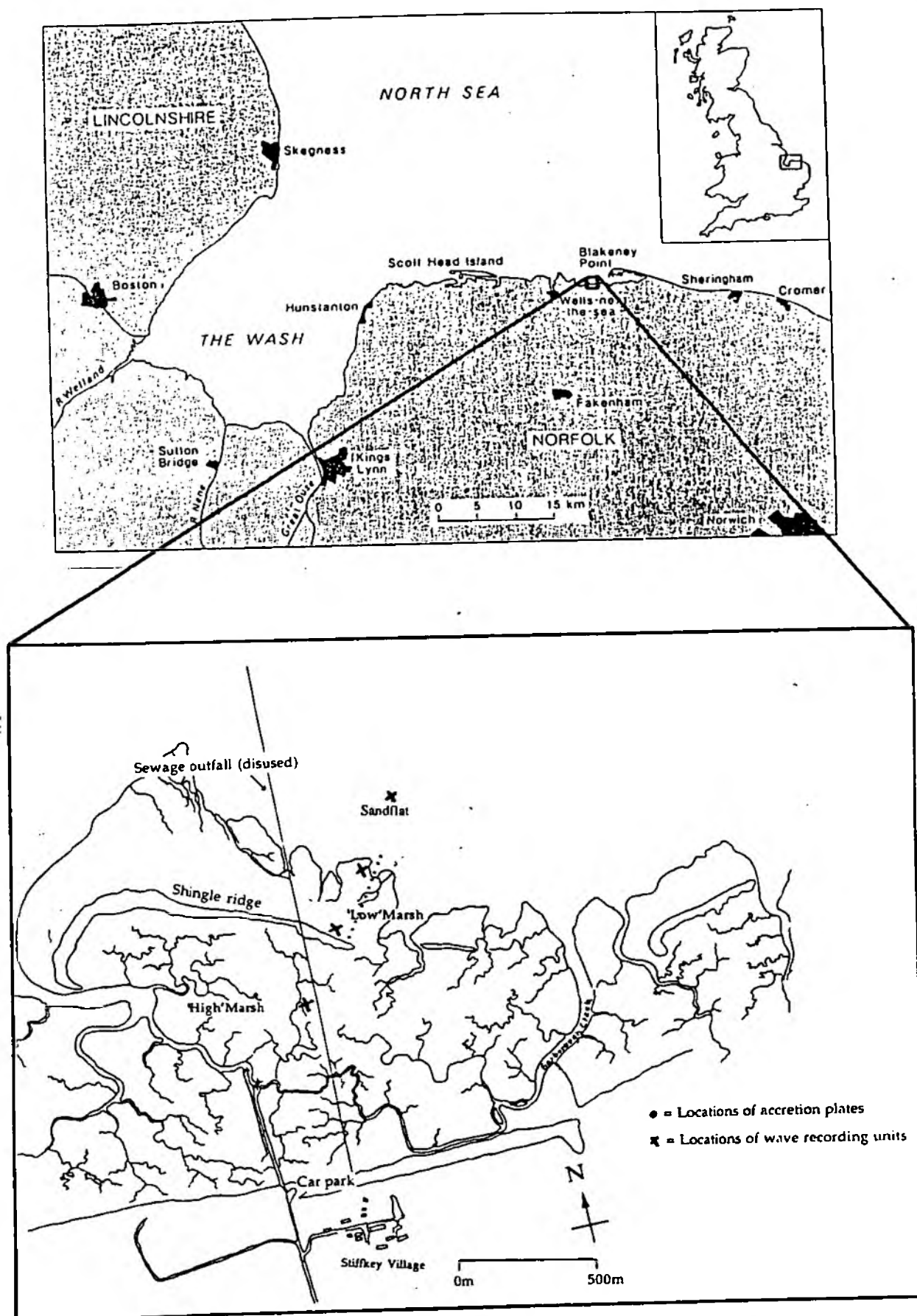


Fig. 27: Sketch of the Stiffkey marsh field site produced from air photographs.



Fig. 28: The 'low' marsh at Stiffkey, fronting the shingle ridge.

to property on this coastline. Information on the effect of salt marsh surfaces on wave energy under varying inundation heights is therefore very important in the context of future sea defence management of the north Norfolk coast. In addition, the north Norfolk coast is easily accessible from Cambridge, which greatly facilitates field work. A field visit to the coast in October 1993 established that the Stiffkey marshes between Wells-next-the-sea and Blakeney (see figure 26 and 27) provide a suitable field site (see Interim Report OI/569/1/A). These open coast marshes are exposed to the northeast (the direction of greatest fetch from the North Sea) and are easily accessible from Green Lane, Stiffkey (grid reference TF965439). Furthermore, the presence of a low shingle ridge (the Stiffkey Meals), aligned parallel to the coast provides an interesting setting for the comparison of wave dynamics on the completely exposed ('low') marsh fronting the ridge (see figure 28) and the slightly protected ('high') marsh behind the ridge (see figure 29). The Norfolk coast is a macrotidal environment with tidal range varying from 1.5 to 3.0 m (neaps) to 5.0 to 6.0 m (springs) (Pearson, 1986) (Davies (1964) defines macrotidal environments as those with tidal ranges exceeding 4 meters).

Little detailed knowledge is available on the evolution of the Stiffkey marshes. Most reports on the history of the marshes focus on low frequency/high magnitude events and their effect - such as for example the storm surge of 1953 (Steers and Grove, 1956) - or on short-term accretion budgets or tidal flows (Powell, 1979; Bayliss-Smith *et al.*, 1979). In 1980, however, Pethick published evidence from various sources suggesting the possible age of the north Norfolk





Fig. 29: The 'high' marsh at Stiffkey, between the mainland and the shingle ridge.

marshes. Using map and air-photo evidence, he infers that the outer marsh seaward of the Warham marshes (i.e. immediately behind the shingle ridge) originated sometime in the 1950s. According to the air-photo evidence of Pethick (1980), the sand/mudflats at Stiffkey (i.e. the area referred to as the 'low' marsh in this study) have been colonized by a sparse cover of *Salicornia* in the late 1970s. This suggests that both the marsh fronting the Stiffkey Meals and the marsh immediately landward of this shingle ridge are very young in comparison to most other Norfolk marshes (the marshes at Scolt Head Island for example date back as far as the 16th century and those at Blakeney Point are thought to have originated at the turn of the century (Pethick, 1980)). Pearson (1986) finds no evidence for the origin of the Stiffkey Meals, although four cores which were collected at Stiffkey suggest that the ridge is associated with a phase of transgression for which evidence is found at -1.0 m O.D. and that it has remained stable since its emplacement.

With respect to heights of the marsh surfaces at Stiffkey, contradicting values are found in the literature. Whereas Pethick (1980), for example, estimated the height of the high and low marsh at Stiffkey to be 2.47 m and 1.18 m respectively, Pearson (1986) gives the surface height at the four core location as 2.31 m (grid reference TF965439), 2.36 m (TF964442), 2.51 m (TF965445), and 2.79 m (just south of the Stiffkey Meals at grid reference TF965447). Preliminary levelling of the marsh surface at Stiffkey for this project (based on an NRA benchmark) resulted in estimates for the high and low marsh surface of around 2.78 m and 2.48 to 2.06 m O.D. respectively. These estimates are in close agreement with Pearson's, but

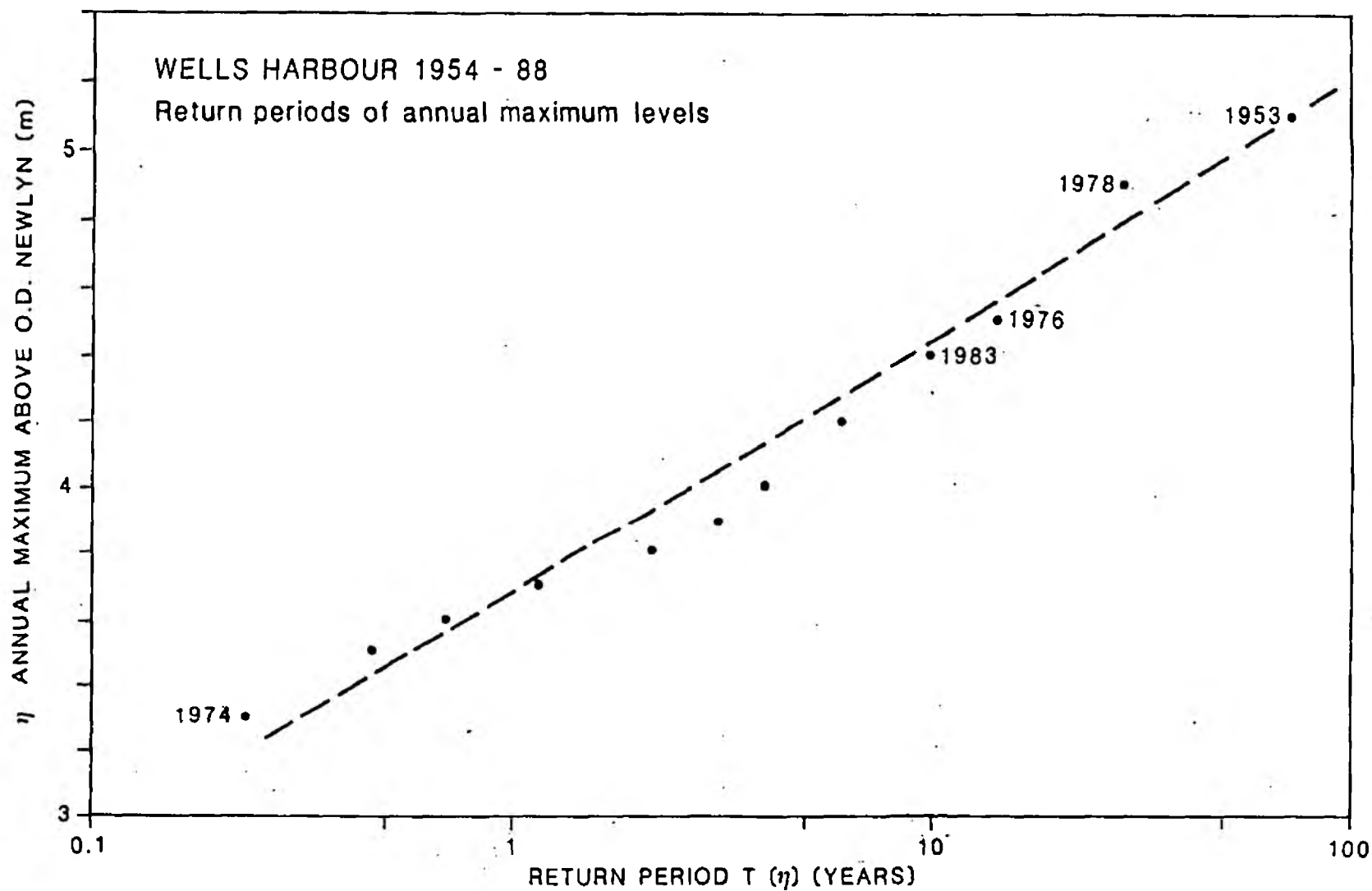


Fig. 30: Return periods of annual maximum tidal stage at Wells Harbour (source: T. Bayliss-Smith, unpublished)

much higher than Pethick's estimates. Based on the heights determined in this project, inundation depths of up to 3 m (4 m HAT + 1 m surge) are possible on the low marsh.

Some information on tide heights and their return periods is available from an analysis of tide gauge data for Wells Harbour (see figure 30). This shows, that water levels as high as 5 m O.D. have been observed at Wells (in 1953). A water level of this height would lead to an inundation depth of 2 to 3 meters at Stiffkey - a water depth large enough to allow for significant wave action.

No detailed information on wave heights at the north Norfolk coast is available, although Pearson (1986) estimates average wave heights for the Norfolk coast to be 0.46 m and mean wave period to be 6 seconds.

### **3.3. Data collection**

To achieve the objectives listed in 3.1, both contextual (mostly archival) and empirical field data will be collected, processed and compared. Figure 31 illustrates how the different data sources will be processed and combined to lead to a final model of wave attenuation over the salt marsh surface.

#### **i. Archival data**

For the forecasting and hindcasting of wave spectra measured at the coastal field site, contextual information is needed on offshore meteorological and wave data and coastal bathymetry (see Section 2.5. and 2.6.). The availability of meteorological and wave data for the North Sea from the National Rivers Authority (NRA) and the Meteorological Office is currently being investigated. Information on bathymetry and topographic variation in coastal waters will be obtained from the analysis of air photographs (of which several are available from the Aerial Photography Unit at the University of Cambridge) and bathymetric maps (possibly also available from the NRA). Data on future, present, and past sea-level rise will be taken from previous studies (see Section 2.2). Air photographs will also be used to assess the recent evolution of the Stiffkey marshes. This provides information which can then be compared to the field measurements of marsh surface accretion/erosion.

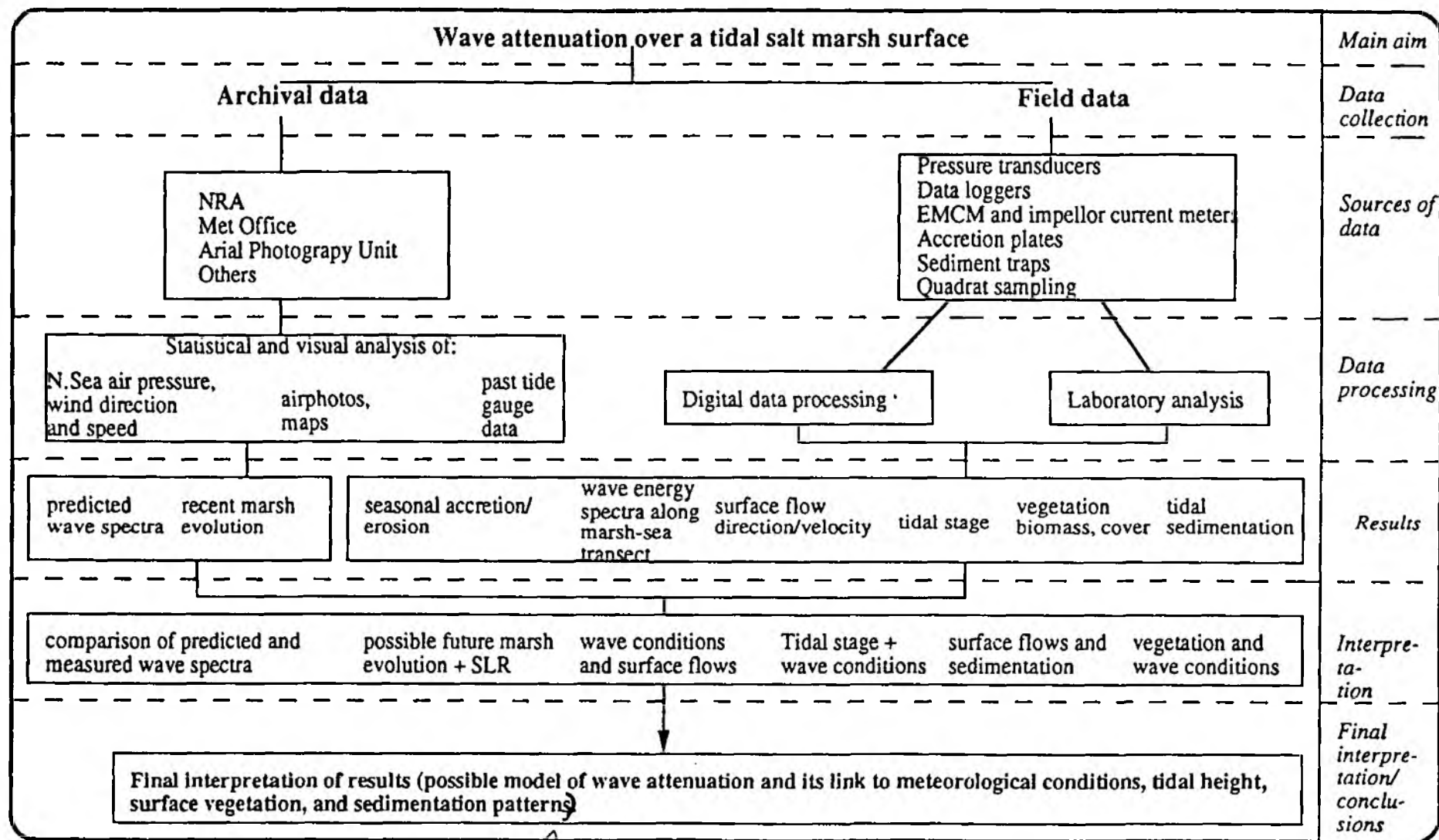


Fig. 31: The structure, data collection scheme, and data processing of the proposed project.

## ii. Field data (methods and technology)

**Waves and tides.** Planned fieldwork mainly focuses on the measurement of wave spectra at four locations along a marsh-sea transect. Three wave recording units will be located seaward of the shingle ridge. The fourth wave recording unit will be set up landward of the shingle ridge on the 'high' marsh. Each of the wave recording units consists of a pressure transducer wired into a (Campbell Scientific 21X) data logger which is placed on top of a 4 to 5 meter high dexion tower to protect the electronic logging equipment from salt-water inundation and wave splash. The alternative use of submergable logger enclosures (instead of dexion towers) was also investigated. This option, however, was not pursued any further as the cost of such enclosures (between £1,400 and £1,500) exceeds the budget of the project. After the determination of marsh surface heights in February 1994, the individual towers have been designed to protect the loggers in storm conditions during the highest astronomical tides (i.e. ca. 4 meters (HAT) + 1 meter (surge) + 1 meter (wave amplitude)) (see figure 32 and 33). Several guyropes will be used to secure the outermost towers during severe storm conditions and a dexion base to secure the outermost tower has been installed on the sandflat in July 1994. Water pressure records will be collected at all four stations at certain times during the tidal cycle. The length of each recorded time-series ('burst') is determined by the logging equipment and theoretical considerations. The main practical constraints on the collection of water pressure records are related to the limited storage capacity of the data loggers. Table 3 illustrates the total sampling time available before downloading for different sampling frequencies and different numbers of variables stored. Furthermore, the spectral analysis of the time series requires the removal of the trend in the data due to changing still water levels (SWL) in response to the tides. If the records are much longer than 10 minutes, this procedure becomes more difficult, as the trend due to the tidal change in SWL cannot be assumed to be linear (see Section 3.4). If the time series is very short, however, information on very low frequency waves may be lost. In addition, the individual time series ('bursts') have to be based on a sampling frequency high enough to detect high frequency waves so that a full spectrum is obtained. As a general rule, the 'Nyquist frequency' (i.e. twice the sampling frequency) is taken to be the lowest detectable wave frequency in the record.

It is suggested, that a sampling frequency of 2 to 5 Hz is used for the water pressure sampling. The logger programme execution time limits the execution interval to 0.2 seconds (i.e. 5 Hz) and the storage capacity of the loggers limits the time available for logging during one tidal cycle (before downloading) to 30 minutes (see table 3). These can be split into three 'bursts' of up to 10 minutes each, which will record a time series of water pressure during rising, turning,

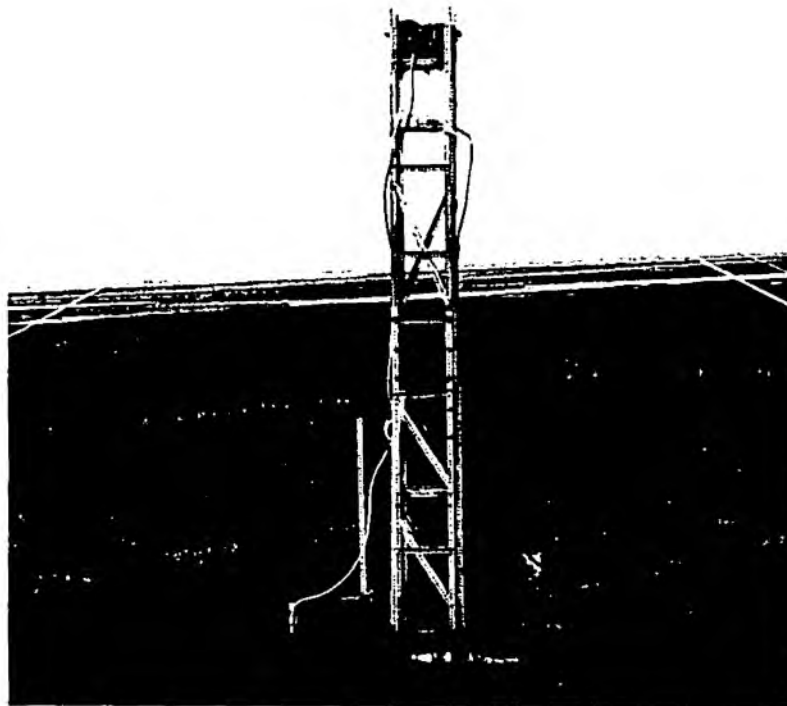


Fig. 32: One of the wave recording stations on the 'low' marsh during fieldwork in February 1994.

**21X (18000 final storage locations available)**

Seconds available				
Frequency (sec)	ID+Value	+1 Value (e.g. second)	+2 (e.g. sec+ min)	+3 (e.g. sec+ min+hour)
0.5	4500	3000	2250	1800
0.25	2250	1500	1125	900
0.2	1800	1200	900	720
0.125	1125	750	562.5	450
0.1	900	600	450	360
Minutes available				
0.5	75	50	37.5	30
0.25	37.5	25	18.75	15
0.2	30	20	15	12
0.125	18.75	12.5	9.375	7.5
0.1	15	10	7.5	6

Table 3: Time limits available for logging different numbers of variables at different frequencies (for 21X Campbell Scientific Logger).

and falling tidal stages respectively. Calibration of the logger readings against observed static water heights has already been carried out in the field (see figure 35, Appendix 1).

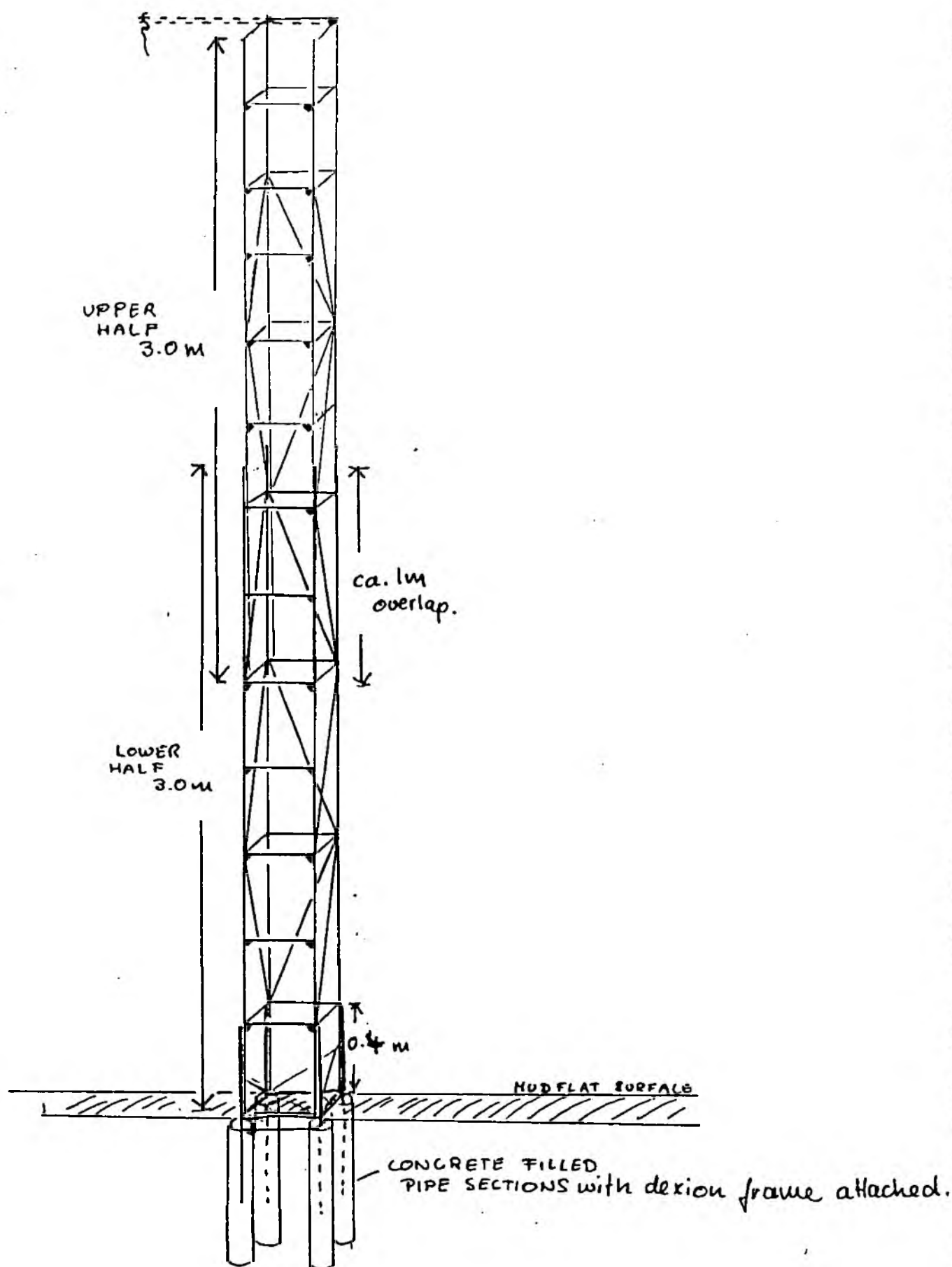
Further calibrations against observed wave heights recorded using video techniques are to be carried out in the field in September 1994. A video camera will be used to record water heights measured against a calibrated staff while the pressure transducer records water pressure simultaneously at the same location. Frame grabbing facilities at the Audio Visual Aids Unit, University of Cambridge, will then be used to compare visually observed wave heights to water heights calculated from the pressure record.

**Accretion/erosion.** As mentioned in Section 2.2, knowledge on present marsh surface accretion rates is needed for an assessment of future marsh elevation relative to mean sea level, future inundation depths and the future role of the marsh surface with respect to wave attenuation. Previous studies of marsh surface accretion have used a variety of materials as artificial marker horizons (for example sand (Steers (ed.), 1960; French and Spencer, 1993) or white clay (Bauman *et al.*, 1984)). The main disadvantage of previous artificial or natural marker horizons is that they form an irregular boundary with the marsh sediment. This makes the assessment of marsh sediment thickness above the marker horizon difficult and introduces measurement errors. Furthermore, the relocation of sand or clay layers can be difficult.

For these reasons, square (20 x 20 cm) aluminium plates will be used in this study as artificial marker horizons. The plates are perforated to ensure sufficient drainage and are inserted horizontally at a distance of ca 10 cm below the undisturbed marsh surface (see figure 34). They can be relocated for measurement and recovered using metal detectors sensitive to aluminium. Twenty such plates were buried at the Stiffkey marsh in February 1994 along a transect on the 'low' marsh and at several creek side and marsh surface locations on the 'high' marsh. Measurements of sediment depth above each plate will be made every two months using a metal pin. Additional accretion plates will be buried in September 1994 to increase spatial cover of the marsh before the main winter field season 1994/95.

In addition to the longer-term (ca two-monthly) accretion measurements at the accretion plate sites, information will be collected on sediment deposition patterns during individual tidal cycles for which wave records and tidal stage records are also available. This will be done using small (4.7 cm diameter) pre-weighed Whatman GF/C filter papers pinned to the marsh surface on upturned petridishes at low tide. These are collected after one tidal cycle and treated in the laboratory as described by French *et al.* (in press) to obtain the weight of the deposited sediment: they will be rinsed with 2 x 100 ml of distilled water in Millipore holders, left to dry at 30 to 40 °C for ca three hours, and reweighed. Such sediment traps will be pinned to the

Fig. 33: The basic design for the dexion towers used to protect the data loggers from tidal inundation and waves.





marsh surface in 9 to 10 clusters of 4 to 5 traps along a transect parallel to and in the immediate vicinity of the wave recording transect on the 'low' marsh. Sediment traps on the 'high' marsh will be distributed along smaller transects at right angles to individual creek sections, as the flooding of the 'high' marsh takes place through the creek network.

Repeated levelling of accretion plate and sediment trap sites will allow the assessment of spatial variations of long and short term deposition rates.

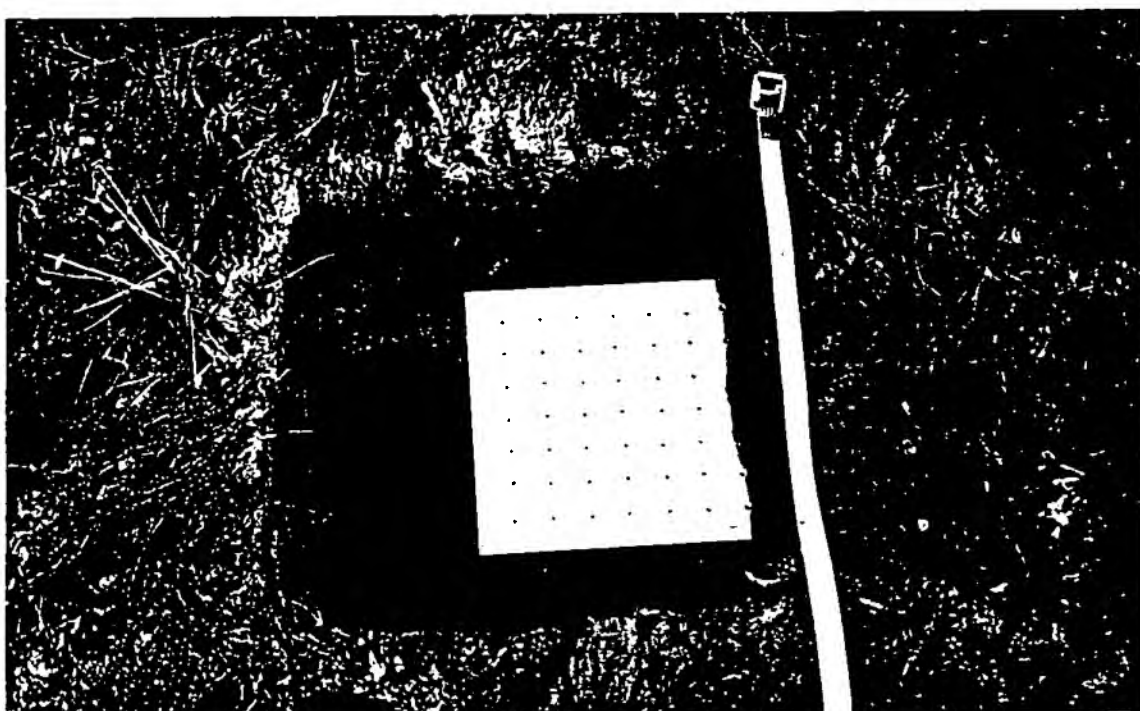


Fig. 34: Accretion plate (20x20 cm) before insertion underneath the marsh surface at Stiffkey 'low' marsh.

**Surface flow.** Information on marsh surface flow patterns during different wave conditions is useful for estimating direction and velocity of wave induced currents and the possible effect of different wave conditions on marsh surface accretion or erosion. Electromagnetic Current Meters (EMCMs) have been used successfully in studies of creek flows (French and Clifford, 1992). The technique is based on the fact that water flowing through an electromagnetic field generated by the instrument induces an electric potential which is proportional to the flow velocity. The instrument provides two-dimensional flow readings and information on short-term velocity pulses which may play a significant role in sediment movement. Two EMCMs and several additional impellor current meters will be used to take measurements of current

velocity and direction at different heights above the marsh surface during wave recording periods at incoming, turning, and outgoing tidal phases.

**Local meteorological data.** The possibility of installing a small automatic weather station at Stiffkey is currently being investigated. The most important information needed will be barometric pressure (to adjust the water pressure readings) and wind direction and speed. Meteorological records from existing local weather stations may also be available.

**Vegetation.** Vegetation development will significantly influence marsh surface roughness and therefore wave attenuation. Furthermore, varying exposure to wave action may be an important factor causing variation in vegetation zonation (Adam, 1981) which may then influence sedimentation patterns (Stumpf, 1983). Species composition, cover, and biomass of the marsh vegetation will be estimated using quadrat sampling techniques along transects parallel to the wave recording transect. Individual quadrats will be located along these transects at random distances. Qualitative presence/absence data will be collected for each quadrat and total vegetation cover is then estimated by lowering vertical pins from a frame and noting the species touched by the pin and the number of the points of contact. Biomass will be determined seasonally using standard quadrat harvesting methods.

**Surveying.** Information on general marsh topography and microtopographic variations (for example horizontal erosion at the marsh-sand flat edge) will be gained through detailed (repetitive) surveying. An extensive survey of the tidal flat fronting the outer marsh was carried out in July 1994 and will be used to establish a Digital Terrain Model for use in wave refraction calculation and the prediction of wave spectra.

### **3.4. Data processing and analysis**

Pressure records from all four wave recording stations will be downloaded from the loggers in the field within 24 hours of the last high tide. They will then be processed and analysed in Cambridge, using mathematical software with signal processing facilities.

The procedure for converting the maxima of the pressure records to wave height has been outlined in Section 2.3. It has, for example, been successfully used by Lugo-Fernández *et al.* (1994) for the calculation of significant wave heights and periods at Margarita Reef in the Caribbean Sea. As the pressure time series collected during the fieldtrips in December '93 and February '94 show a very complex signal and significant interference of high frequency noise (see figures 39 and 40, Appendix 2), the most dominant frequencies need to be determined

from the 'raw' pressure signal, before the respective amplitudes are converted to corresponding wave heights. The electronic noise of the instruments will be determined prior to field data collection in the laboratory, by analysing logger readings at different frequencies for various water depths. This electronic noise can then be removed from the data series collected in the field. The initial signal processing of the field pressure time series can be achieved by calculating the Fast Fourier Transform (FFT) of the series and plotting the energy density (given in  $\text{m}^2/\text{Hz}$ ) for each frequency (see figure 40, Appendix 2). One possible software package with a FFT facility is the 'Mathematica' software available on the PWF-Physics network at Cambridge or the 'Matlab' software available for PCs and Apple Macintoshes. 'Mathematica' has been used to process the preliminary data collected in the field (see Section 3.5).

The pressure maxima of individual frequencies can then be converted to wave heights according to equation (8):

$$\frac{H}{2} = \frac{N(r+rgz)}{rgK_z}$$

The processing of the wave data and the conversion of the various wave height parameters to wave energy will be based on linear wave theory and the methods outlined in Section 2.3. Lee and Wang (1984) suggest a method which may be used to filter high frequency noise and adjust the pressure records for the effect of current and non-linear processes which are of importance in shallow water. Most important in the context of this project (i.e. for the comparison of field spectra and predicted spectra and for the calculation of wave energy) is the determination of maximum and minimum wave heights, significant wave height ( $H_s$  or  $H_{1/3}$ ) and the mean wave height ( $H_m$ ). According to the Shore Protection Manual (CERC, 1984), these can be obtained from all wave heights present in the series through:

$$H_m = 0.886 H_{rms} \quad \text{and} \quad H_{1/3} = 1.416 H_{rms} = \sqrt{2} H_{rms}$$

where the 'root mean square wave height',  $H_{rms} = \sqrt{\frac{1}{N} \sum_{j=1}^N H_j^2}$  and  $H_j$  is the height of the successive waves in the record. Average wave energy per unit surface area for several sinusoidal waves of varying height can be calculated from:

$$(E)_A = gr/8 H_{rms}^2$$

In this way, wave energy will be calculated at each of the four stations. In order to establish a possible link between North Sea meteorological conditions (wind and pressure records) and the

wave spectra measured at the marsh, the methods for wave forecasting/hindcasting and for the calculation of shallow water refraction described in Section 2.5 and 2.6 will be used. The main focus will be on the methods outlined in the Shore Protection Manual (CERC, 1984). In its simplest form, this means that for the prediction of deep water waves:

$$\frac{gH_m}{U_A^2} = 1.6 \cdot 10^{-3} \sqrt{\frac{gF}{U_A^2}} \quad \frac{gt}{U_A} = 6.88 \cdot 10 \left(\frac{gF}{U_A^2}\right)^{2/3} \quad \frac{gt}{U_A} = 2.857 \cdot 10^{-1} \left(\frac{gF}{U_A^2}\right)^{1/3}$$

as modified from Hasselmann *et al.* (1973) by CERC (1984), where  $H_m$  = the spectral (significant) wave height,  $T_m$  = spectral period,  $t$  = duration,  $F$  = fetch distance,  $U_A$  = wind speed adjusted to account for the non-linear relationship between wind stress and wind speed ( $U_A = 0.7U^{1.23}$  ( $U$  in  $m\ s^{-1}$ )). Estimates of significant wave heights predicted from given wind speeds, fetch and duration can be obtained from diagrams in the Shore Protection Manual (CERC, 1984) similar to figure 14.

Shallow water prediction cannot solely be based on the above equations, as wave growth will be limited by bottom friction and percolation (see Section 2.6). A revised method which takes into account wave energy loss through bottom friction and percolation as calculated by Bretschneider and Reid (CERC, 1984, 355-365) will be used to estimate wave generation in the shallow coastal water fronting the Stiffkey marsh. Examples of a shallow water prediction curve given in the Shore Protection Manual is shown in figure 23.

Tidal stage data, data obtained from accretion plate readings, and data from the sediment trap will be processed using spreadsheets (such as 'Excel') and statistical software in Cambridge

### 3.5. Preliminary data

Two field trips to the Stiffkey marshes in December 1993 and February 1994 provided an opportunity for the calibration of three pressure transducers and the testing of the basic wave recording units. Calibration curves showing calculated hydrostatic pressures for still water levels in the main creek at Stiffkey and corresponding logger readings (in mV) are shown in figure 35, Appendix 1. Figure 36 and 37 (Appendix 2) show the time series for two 'bursts' (of 0.2 sec sampling interval), recorded simultaneously at the sea-facing and the land-facing side of the 'low' marsh on the 27th and 28th of February 1994 (figures 36 and 37, Appendix 2).

An additional pressure transducer was programmed to take 5-minute averages of tidal stage in order to provide information on the tidal trend contained in each of the 'burst' time series of the

other transducers. One such (unfortunately incomplete) tidal curve is shown in figure 38 (Appendix 2). With improved logger programmes and an improved experimental set up (i.e. new stilling well etc.), more detailed tidal information will be obtained during the main field season in the winter. After removal of the tidal trend in the time series, the data can be plotted as in figure 39 (Appendix 2).

The raw data plot of part of a five minute (0.5 sec sampling interval) 'burst' of December 1993 and the initial spectral (Fourier) analysis of this data (after subtraction of the tidal trend) (figure 40 (Appendix 2) showed the dominance of wave patterns with periods of 3 and 7 sec superimposed on much lower frequency water height fluctuations. Fourier spectra for the time series of figure 36 and 37 (see figure 41 and 42, Appenidx 2) show that this pattern changes significantly along the marsh transect. It is expected, that the pattern will also change in response to different meteorological conditions (the tides of the 27th and 28th of February were lower than predicted and weather conditions were extremely calm). The data also suggest that future measurements of water pressure variation would have to be at high frequencies (2 to 5 Hz) in order to detect waves of periods smaller than 1 second. As those waves are unlikely to contribute a significant amount to the total wave energy during severe weather conditions and high tides, however, lower sampling frequencies may be sufficient. Further field experiments with different sampling frequencies will be needed to clarify this point.

Weights of sediment collected at 7 sites on a marsh-sea transect on the 'low' marsh and 3 sites on the 'high' marsh during one tidal cycle on the 1st and the 2nd of March 1994 respectively are shown in table 4 (Appendix 3). The results indicate an increase in sediment deposition from the back of the 'low' marsh towards the tidal flat and from the marsh surface towards the creek banks of the 'high' marsh. It is suspected, that the increase in sediment weight towards the tidal flat is due to the movement of the sand on the surface during tidal inundation and does not reflect a general long-term trend of surface accretion. The increased sediment deposition near the creek sides of the 'high' marsh agrees well with the results of sedimentation studies on Scolt Head Island (French and Spencer, 1993). Further collection of sediment data, grain size analysis in the laboratory, accretion plate measurements, and air-photograph analysis will establish a more detailed picture of short-term and long-term sedimentation patterns on the Stiffkey marshes.

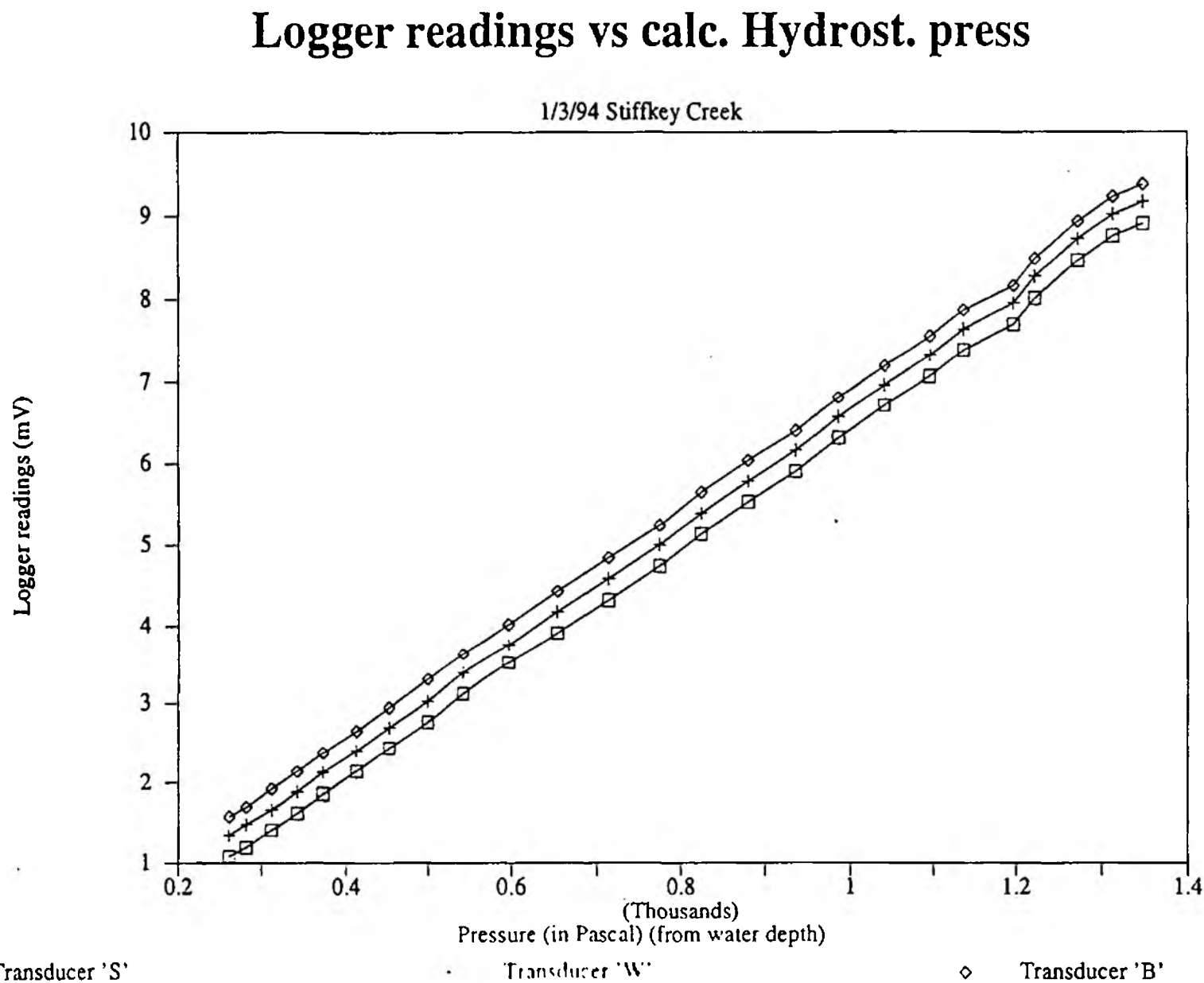


Fig. 35: Logger readings (in mV) compared with hydrostatic pressure (in Pa) calculated from observed water heights in Stone Meal Creek, Stiffkey.

27/2/94

## APPENDIX 2: Examples of water pressure time series

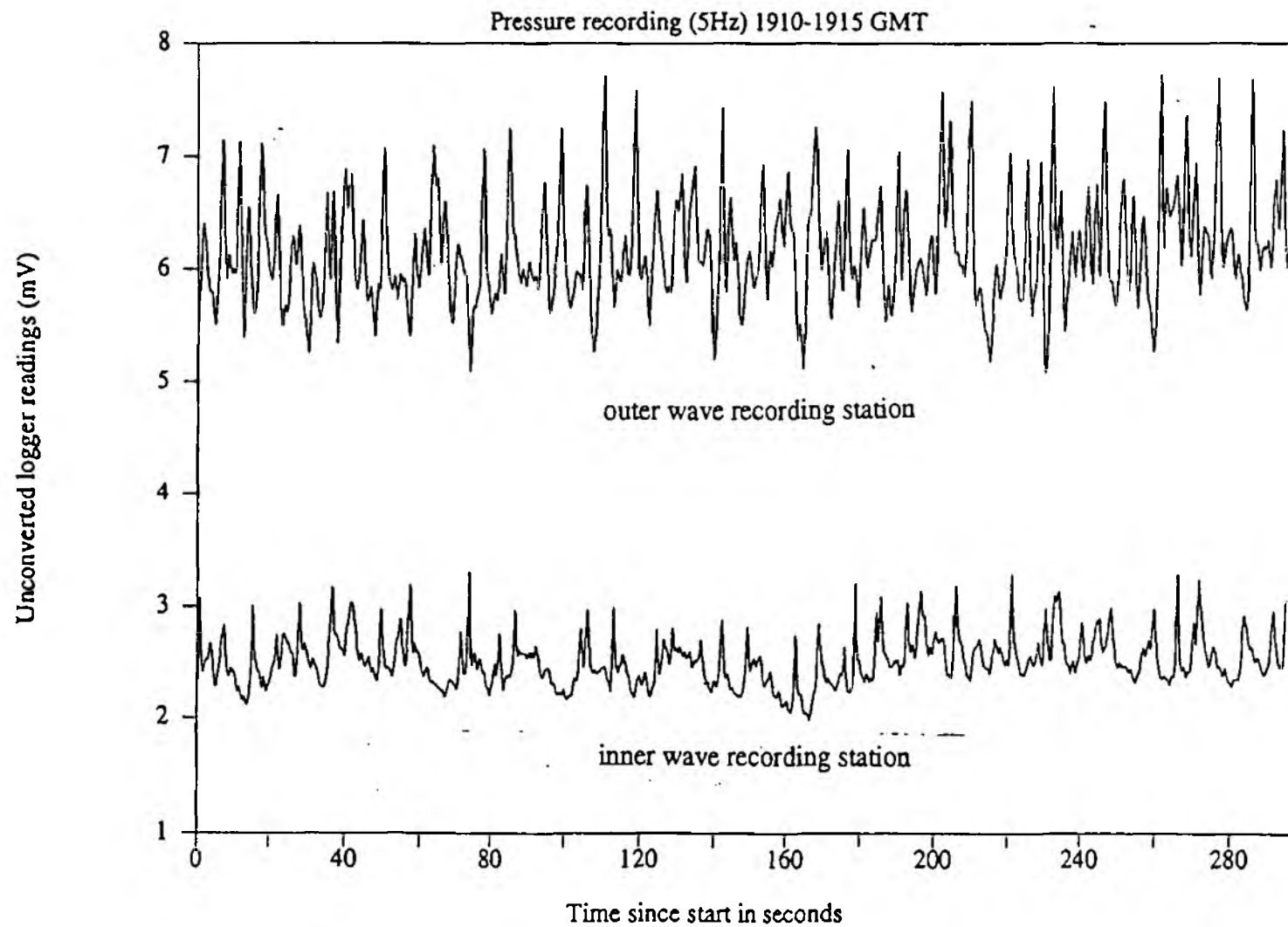


Fig. 36: Time series of water pressure for both locations (at the seaward and landward edge of the 'low' marsh) for a tide on the 27/2/94.

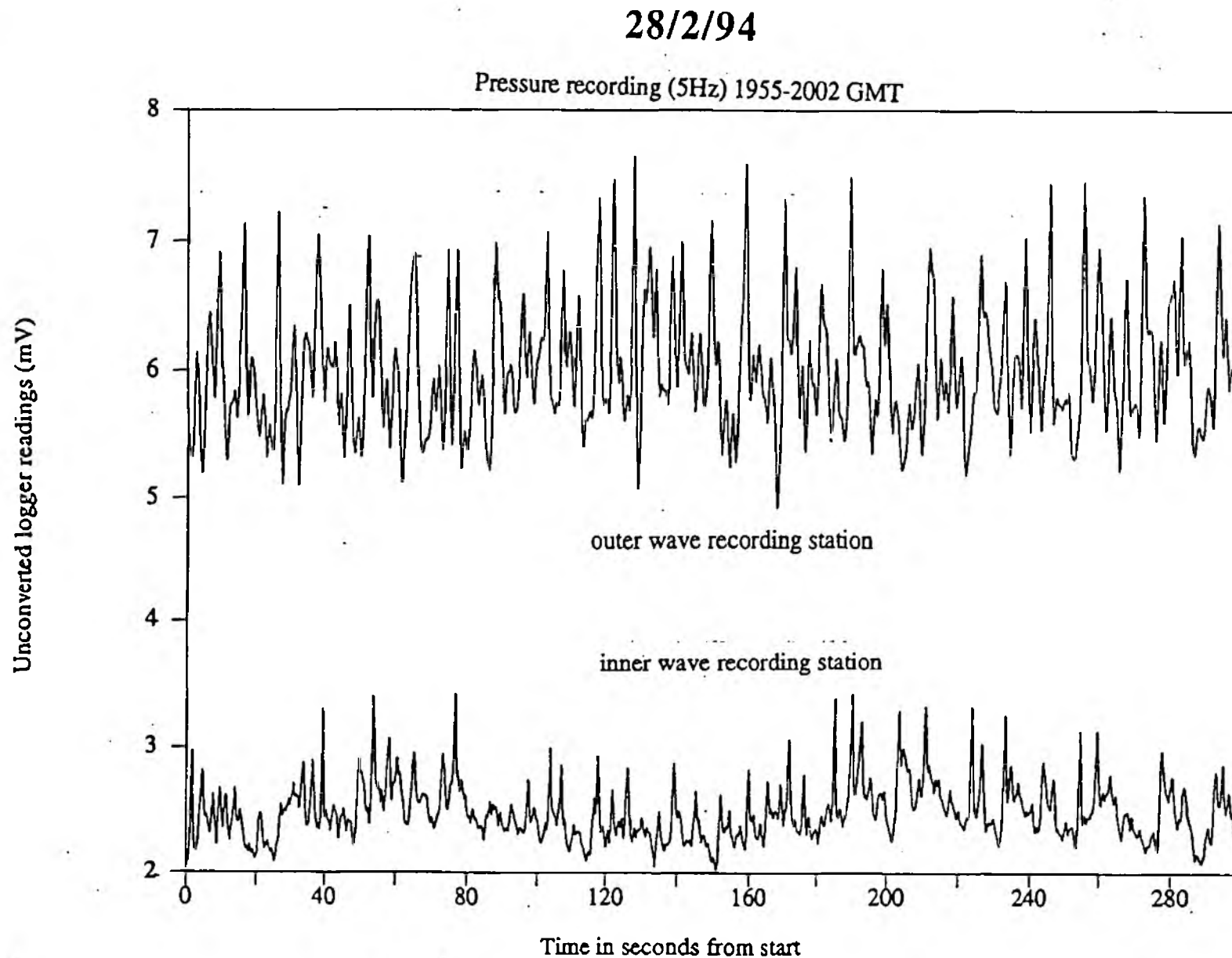


Fig. 37: Time series of water pressure for both locations (at the seaward and landward edge of the 'low' marsh) for a tide on the 28/2/94.



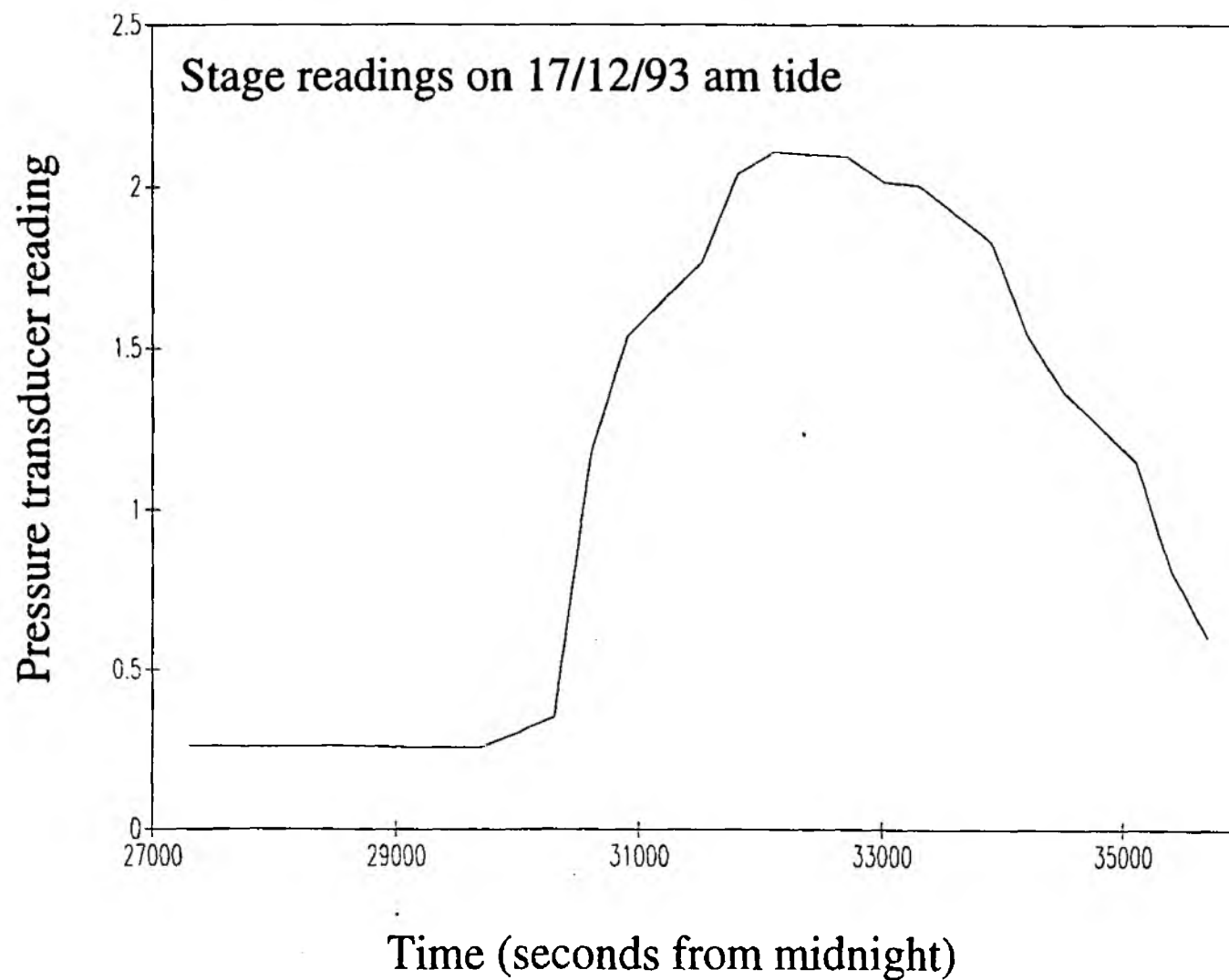


Fig. 38: Tidal stage recorded on Stiffkey 'low' marsh during the morning tide of the 17/12/93 (unfortunately, recording stopped before tidal stage had returned to zero).

Pressure residuals

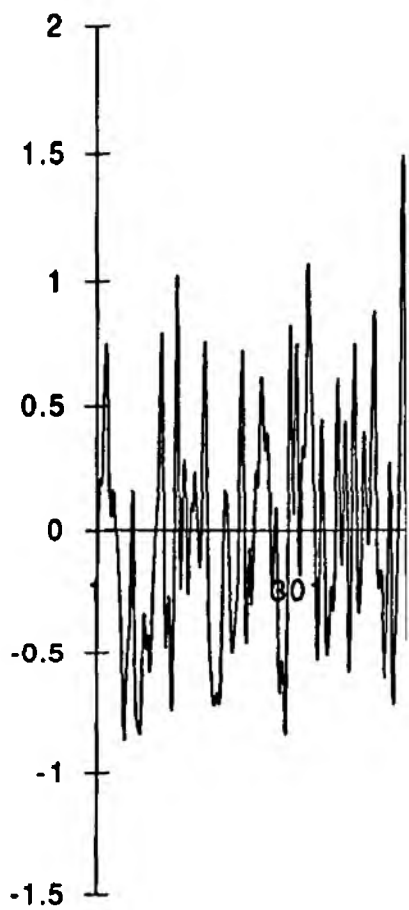
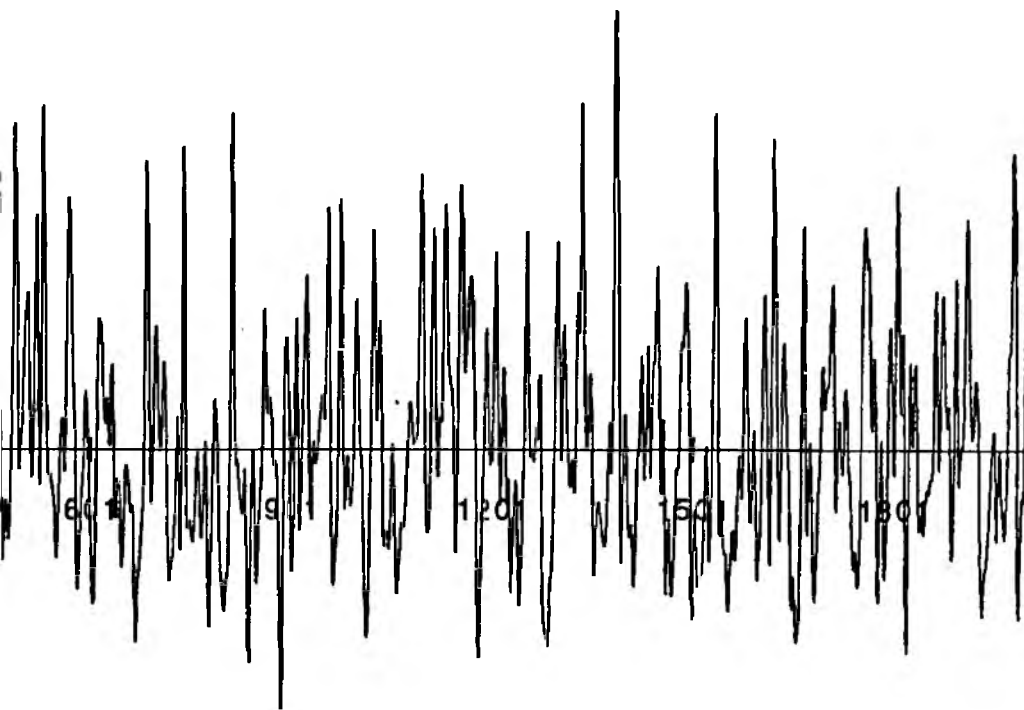


Fig. 39:

28//2/94 1915-1918 GMT (5Hz)



Time since start (in 0.2 sec intervals)

Time series residuals (after removal of the tidal trend in the series).

a. Five minute 'burst' at Stiffkey 17/12/93 am tide (0.5 sec sampling interval)

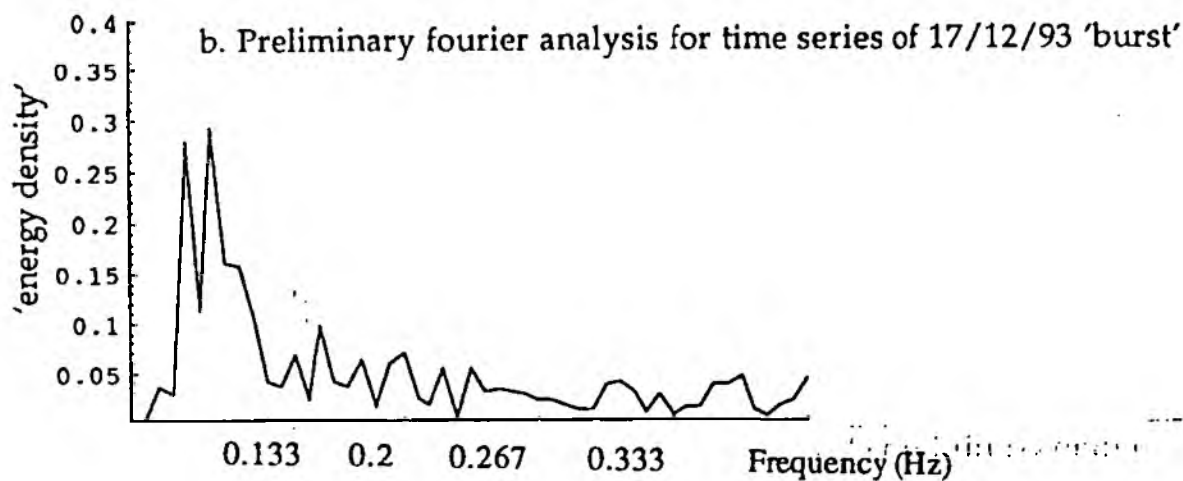
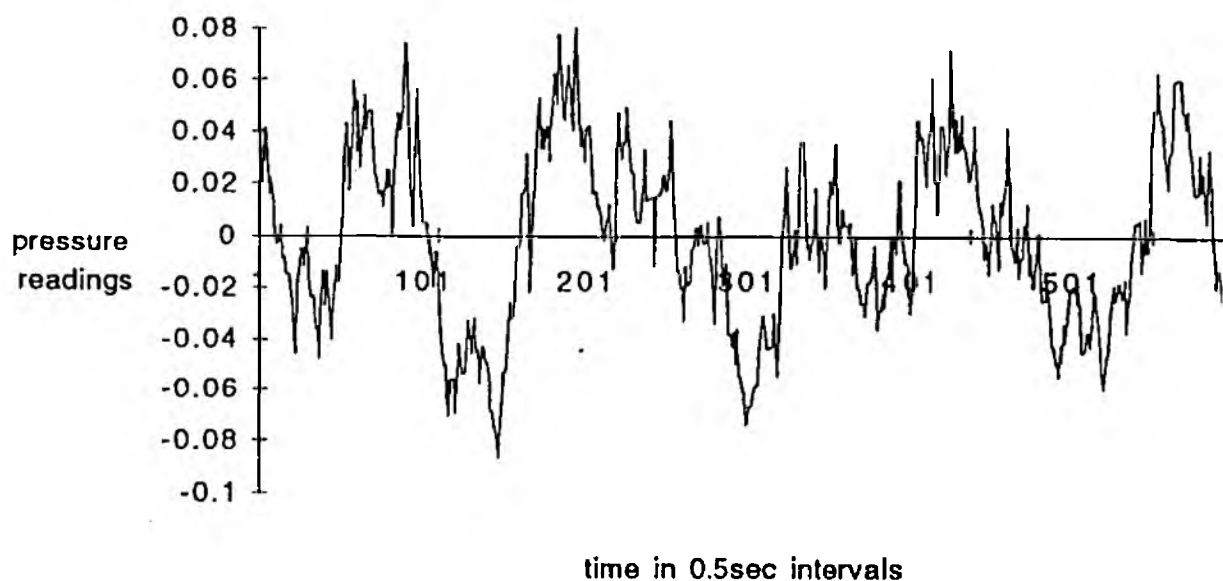
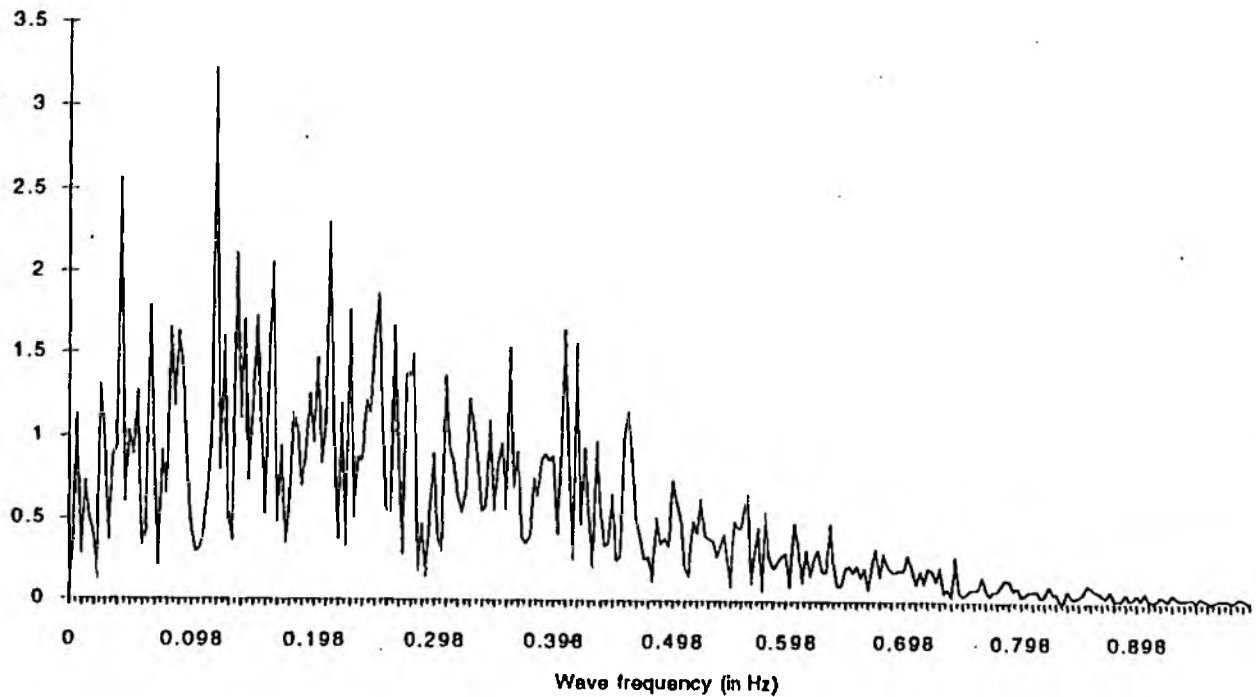


Fig. 40: Example of a water pressure time series residuals and the corresponding Fourier spectrum (produced using 'Mathematica' software). 'Pressure' given in unconverted logger readings (mV) (for conversion into water pressure (in Pascal) see figure 36).

FFT of 27/2/94 (1910-1915 GMT) MARSH EDGE



FFT of 27/2/94 (1910-1915 GMT) BACK OF MARSH

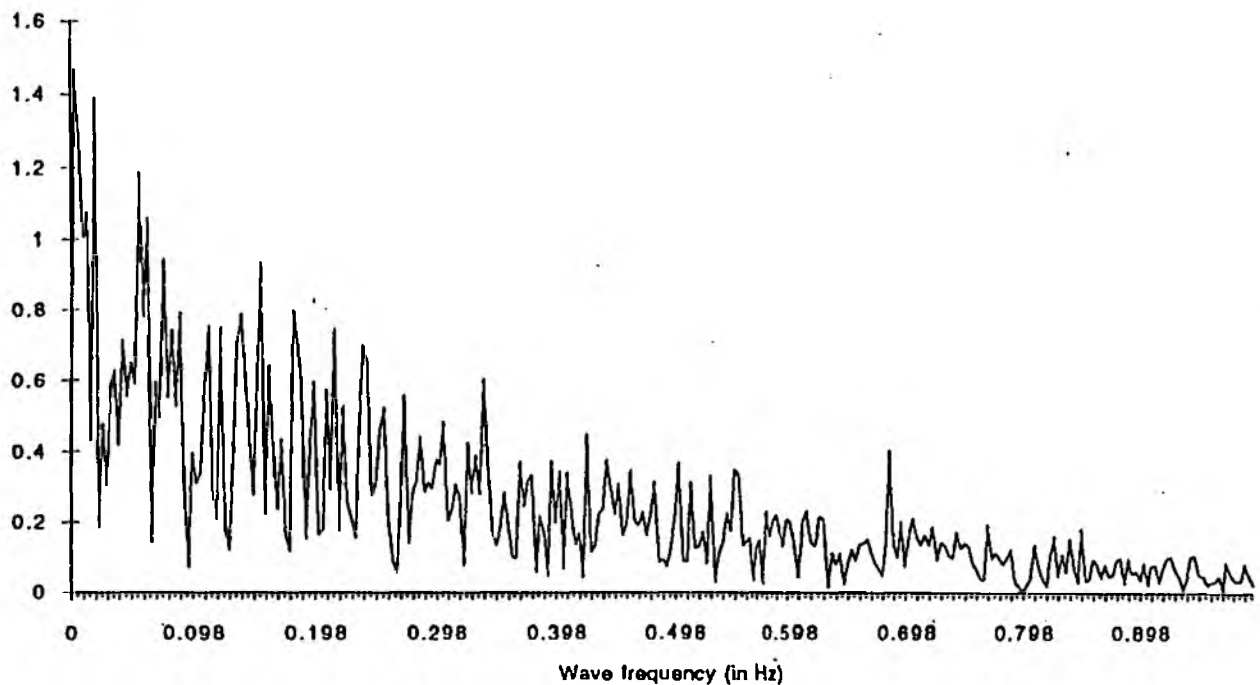
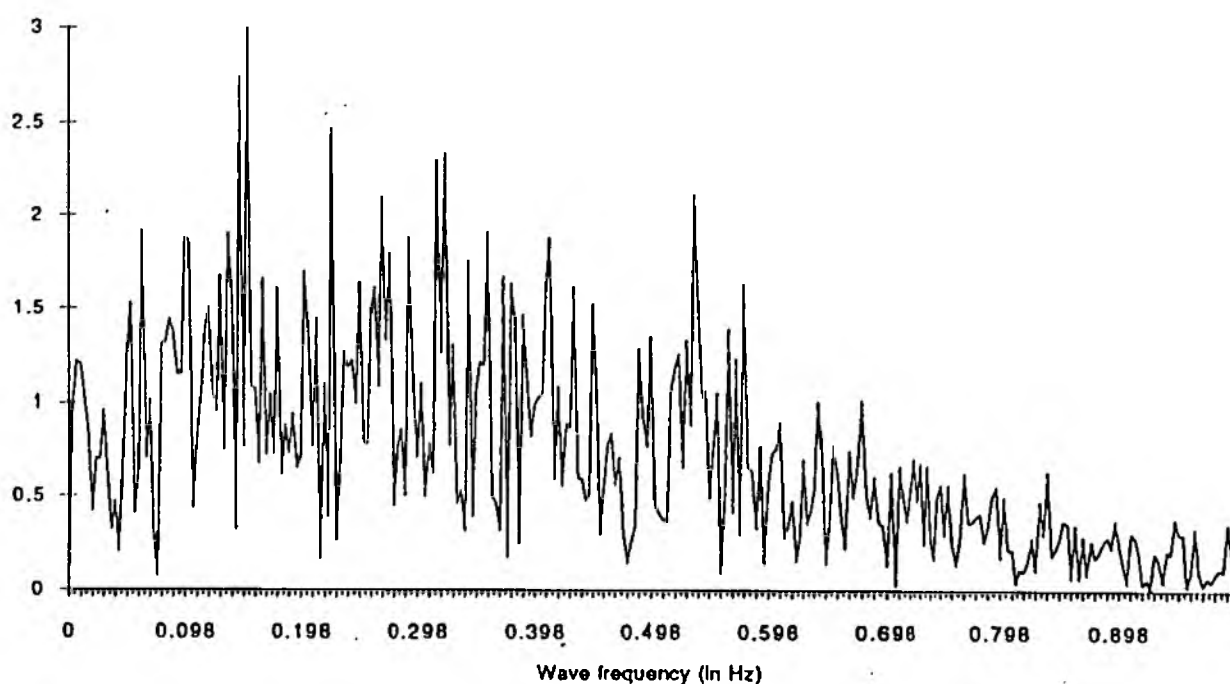


Fig. 41: Fourier spectra for the marsh edge station (a) and the station at the back (b) of the 'lower' marsh for a 5-minute 'burst' of pressure readings on the 27/2/94.

FFT of 28/2/94 (1955-2002 GMT) MARSH EDGE



FFT of 28/2/94 (1955-2002 GMT) BACK OF MARSH

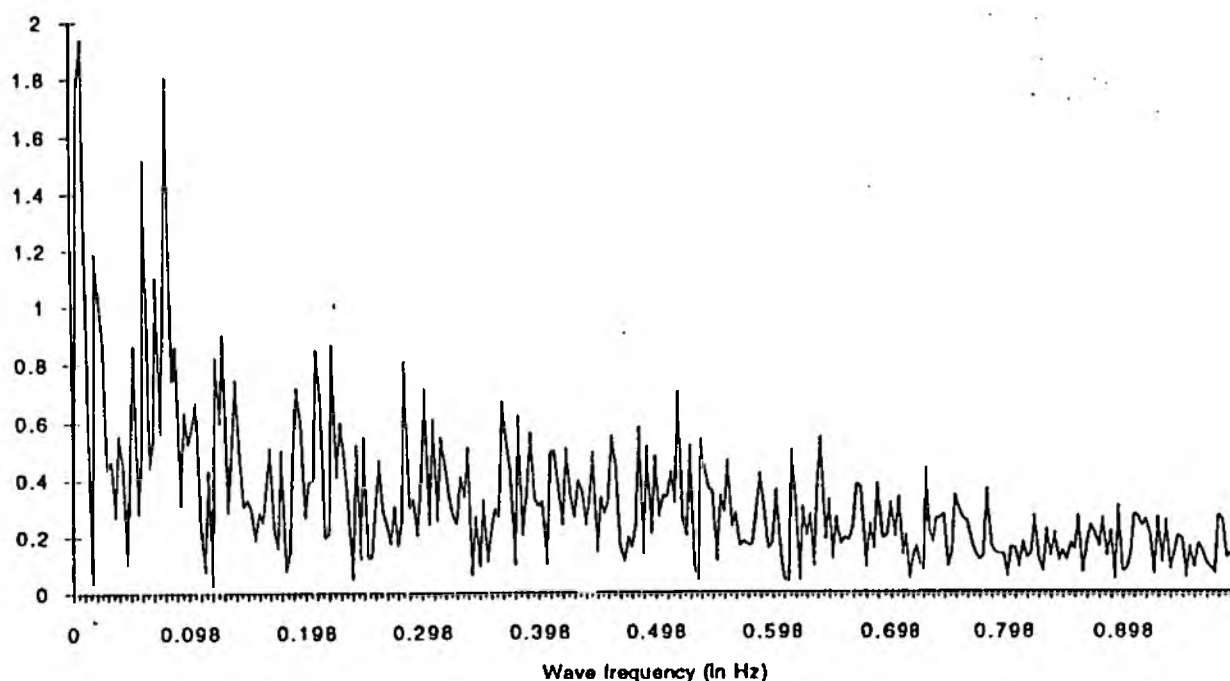


Fig. 42: Fourier spectra for the marsh edge station (a) and the station at the back (b) of the 'lower' marsh for a 7-minute 'burst' of pressure readings on the 28/2/94.

### APPENDIX 3: Sediment trap data

Mean sediment weights for one tidal cycle (in mg)		
	1/3/94	2/3/94
LM11	0.000	0.000
LM10	0.865	0.300
LM9	1.237	7.450
LM8	1.490	0.970
LM7	1.422	1.857
LM6	1.695	1.697
LM5	2.017	2.197
HM (surface)	0.967	0.000
HM (creek side A)	5.467	1.590
HM (creek side B)	7.240	---

Table 4: Sediment trap weights for individual tidal cycles. LM11-LM5 are sites on the 'low' marsh along a transect from the back of the marsh to the tidal flat. HM are sites on the 'high' marsh. (averages are taken from four sediment traps at each individual site).

## 5. REFERENCES

- Adam P 1981 The vegetation of British saltmarshes. *New Phytologist* 88, 143-19.
- Allen J R L 1990 Salt-marsh growth and stratification: a numerical model with special reference to the Severn Estuary, south-west Britain. *Marine Geology* 95, 77-96.
- Allen J R L 1991 Salt-marsh accretion and sea-level movement in the inner Severn Estuary, southwest Britain: the archaeological and historical contribution. *Journal of the Geological Society of London* 148, 485-494.
- Allen J R L and Pye K (eds.) 1992 *Saltmarshes. Morphodynamics, Conservation and Engineering Significance*. Cambridge University Press, Cambridge, pp.184.
- Anderson F E 1972 Resuspension of estuarine sediments by small amplitude waves. *Journal of Sedimentary Petrology* 42(3), 602-607.
- Anderson R S, Borns Jr H W, Smith D C and Race C 1992 Implications of rapid sediment accumulation in a small New England salt marsh. *Canadian Journal of Earth Science* 29, 2013-2017.
- Anglian Water 1983 *Sea Defences and Allied Coastal Matters*. Yare House, May 1983. Anglian Water, Norwich Division.
- Armstrong A C and W B Whalley 1985 An introduction to data logging. *British Geomorphological Research Group Technical Bulletin* 34.
- Bacon S and Carter D J J 1991 Wave climate changes in the north Atlantic and North Sea. *International Journal of Climatology* 11, 545-558.
- Barfoot P J and Tucker J J 1980 Geomorphological changes at Blakeney Point, Norfolk. *Transactions of the Norfolk and Norwich Naturalists' Society* 25(2), 49-60.
- Barkham J P, MacGuire F A S and Jones S J 1992 *Sea-Level Rise and the UK. A Report to Friends of the Earth*. Friends of the Earth Trust Limited.
- Barrett M G (ed.) 1992 Coastal Zone Planning and Management. *Proceedings of the conference 'Coastal Management '92: Integrating Coastal Zone Planning and Management in the next Century'*. Institution of Civil Engineers. Blackpool, 11-13 May 1992.
- Bauman R H, Day J W Jr and Miller C A 1984 Mississippi deltaic wetland survival: sedimentation versus coastal submergence. *Nature* 224, 1093-1095.
- Bayliss-Smith T P, Healey R, Lailey R, Spencer T and Stoddart D R 1979 Tidal flows in salt marsh creeks. *Estuarine and Coastal Marine Science* 9, 235-255.
- Bearman G (ed.) 1989 *Waves, Tides and Shallow-water Processes*. The Open University. Pergamon Press, Oxford, pp.187.
- Boorman L A, Goss-Custard J D and McGrorty S 1989 Climatic change, rising sea level and the British coast. *Institute of Terrestrial Ecology Research Publication* 1. Institute of Terrestrial Ecology, Natural Environment Research Council.



Brampton A H 1992 Engineering significance of British saltmarshes. Allen J R L and Pye K (eds.) *Saltmarshes. Morphodynamics, Conservation and Engineering Significance*. Cambridge University Press, Cambridge, 115-122.

Bretschneider C L 1966 Wave generation by wind, deep and shallow water. Ippen A T (ed.) *Estuary and Coastline Hydrodynamics. Engineering Society Monographs*. McGraw-Hill Book Company Inc., New York, Chapter 4, 133-196

Burd F 1989 The saltmarsh survey of Great Britain. An inventory of British salt marshes. *Research and Survey in Nature Conservation* 17. Nature Conservancy Council.

Camso H A and Pousa J L 1992 Length of wave records: a numerical model to simulate its influence upon frequency distribution of wave heights and periods. *Journal of Coastal Research* 8(2), 340/46.

Carter D J T and Draper L 1988 Has the north-east Atlantic become rougher? *Nature* 332, 494.

Carter R W G 1988 *Coastal Environments. An Introduction to the Physical, Ecological and Cultural Systems of Coastlines*. Academic Press Ltd., London.

Cartwright D E and Longuet-Higgins M S 1956 The statistical distribution of the maxima of a random function. *Proceedings of the Royal Society of London, Series A* 237(1209), 212-232.

Cartwright D E 1972 Secular changes in the ocean tides at Brest, 1711-1936. *Geophysical Journal of the Royal Astronomical Society* 30, 433-449.

Causton D R 1988 *An Introduction to Vegetation Analysis. Principles, Practice and Interpretation*. Unwin Hyman, London, pp.342.

Chapman V J 1974 *Salt marshes and salt deserts of the world*. 2nd edition. Cramer, Lehre, pp.392.

Clacton K M 1980 Coastal protection along the East Anglian coast, UK. *Zeitschrift fur Geomorphologie Supplementband* 34, 165-172.

Clayton K 1976 Coastal defence policy on the East Anglian coast. *Geographia Polonica* 34, 195-205.

Clayton K 1977 Salvation from the sea. East Anglian coastal erosion. *Geographical Magazine* 49(10), 622-625.

Clayton K M 1990 Sea-level rise and coastal defences in the UK. *Quarterly Journal of Engineering Geology* 23, 283-287.

Clymo R S 1967 Accretion rates in two of the salt marshes at Blakeney Point, Norfolk. *Transactions of the Norfolk and Norwich Naturalists' Society* 21(1), 17-18.

CERC (Coastal Engineering Research Center) 1984 *Shore Protection Manual*. 4th edition. , Department of the U S Army, U S Army Corps of Engineers (USACE), US Government Printing Office, Washington DC.

Cokelet E D 1977 Breaking waves. *Nature* 267, 769-774.

Cokelet E D 1977 Steep gravity waves in water of arbitrary depth. *Philosophical Transactions of the Royal Society of London, Series A* 286, 183-230.

Collins J I 1972 Prediction of shallow-water spectra. *Journal of Geophysical Research* 77(15), 2693-2706.

Dankers N, Binsbergen M, Zegers K, Laane R and van der Loeff M R 1984 Transportation of water, particulate and dissolved organic and inorganic matter between a salt marsh and the Ems-Dollard Estuary, The Netherlands. *Estuarine, Coastal and Shelf Science* 19, 143-165.

Davies J L 1964 A morphogenic approach to world shorelines. *Zeitschrift fur Geomorphologie* 8, 127-142.

DeJonge V N, Essink K and Boddeke R 1993 The Dutch wadden sea - a changed ecosystem. *Hydrobiologia* 265(1-3), 45-71.

DeLaune R D, Patrick W H Jr and Buresh R J 1978 Sedimentation rates determined by  $^{137}\text{Cs}$  dating in a rapidly accreting salt marsh. *Nature* 275, 532-533.

DeLaune R D, Smith C J and Patrick W H Jr 1983 Nitrogen losses from a Louisiana Gulf coast salt marsh. *Estuarine, Coastal and Shelf Science* 17, 133-141.

Denny M W 1988 *Biology and the Mechanics of the Wave-swept Environments*. Princeton University Press.

Dijkema K S (ed.), Beeftink W G, Doody J P, Gehu J M, Heydemann B and Rivas Martinez S 1984 *Saltmarshes in Europe*. Council of Europe. Nature and Environment Series 30, Strasbourg, pp.178.

Dijkema K S 1987 Geography of salt marshes in Europe. *Zeitschrift fur Geomorphologie* N F 31, 489-499.

Draper L 1957 Attenuation of sea waves with depth. *La Houille Blanche* 12(6), 926-931.

Ehlers J, Nagorny K, Schmidt P, Stieve B and Zietlow K 1993 Storm surge deposits in North Sea salt marshes dated by  $^{134}\text{Cs}$  and  $^{137}\text{Cs}$  determination. *Journal of Coastal Research* 9(3), 698-701.

Evans A W 1992 The applicaiton of geomorphology in coastal management studie. *Ocean and Coastal Management* 17, 47-55.

Evans G and Collins M B 1975 The transportation and deposition of suspended sediment over the intertidal flat of the Wash. Hails and Carr (eds.) 1975 *Dynamics of Nearshore Sedimentation*. John Wiley, New York. Chapter 11, 273-306.

Flather R A 1987 Estimates of tide and surge using a numerical model. *Estuarine, Coastal and Shelf Science* 24, 69-93.

Flemming C A 1989 The Anglian sea defence management study. Coastal Management Proceedings of the ICE Conference, Bournemouth, 153-164.

Fowler S L 1991 Conservation of the coastal and estuarine zones of the North Sea. *Ocean and Shoreline Management* 16, 349-358.

French J R 1993 Numerical simulation of vertical marsh growth and adjustment to accelerated sea-level rise, north Norfolk, UK. *Earth Surface Processes and Landforms* 18, 63-81.

French J R and Stoddart D R 1992 Hydrodynamics of salt marsh creek systems: implications for marsh morphological development and material exchange. *Earth Surface Processes and Landforms* 17, 235-252.

French J R, Spencer T and Stoddart D R 1990 Backbarrier salt marshes of the north Norfolk coast: geomorphic development and response to rising sea-levels. *University College London Discussion Papers in Conservation* 54. Ecology and Conservation Unit, University College London.

French J R and Clifford N J 1992 Characteristics and 'event-structure' of near-bed turbulence in a macrotidal saltmarsh channel. *Estuarine, Coastal and Shelf Science* 34, 49-69.

French J R and Spencer T 1993 Dynamics of sedimentation in a tide-dominated backbarrier salt marsh, Norfolk, UK. *Marine Geology* 110, 315-331.

French J R, Spencer T, Murray A L and Arnold N S (in press) Geostatistical analysis of sediment deposition in two small tidal wetlands, Norfolk, UK. *Journal of Coastal Research*.

French J R (in press) Tide dominated coastal wetlands and accelerated sea-level rise: a NW European perspective.

Frey R W and Basan P B 1985 Coastal salt marshes. Davis R A Jr (ed.) *Coastal Sedimentary Environments*. Springer-Verlag, New York.

Galvin C J 1968 Breaker type classification on three laboratory beaches. *Journal of Geophysical Research* 73(12), 3651-3659.

Gornitz V and Solow A 1991 Observations of long-term tide-gauge records for indications of accelerated sea-level rise. Schlesinger M E (ed.) Greenhouse-gas induced climatic change: a critical appraisal of simulations and observations. *Developments in Atmospheric Science* 19. Elsevier Science Publishers, Amsterdam, 347-367.

Gornitz V and Lebedeff S 1987 Global sea-level changes during the past century. Numedal D, Pilkey O H and J D Howard (eds.) Sea-Level Fluctuation and Coastal Evolution. *Society of Economic Paleontologists and Mineralogists Special Publication* 41, 3-16.

Goudie A S (ed.) 1990 *Geomorphological Techniques*. Unwin Hyman Ltd., London.

Gröger M and Plag H-P 1993 Estimations of a global sea level trend: limitations from the structure of the PMSL global sea level data set. *Global and Planetary Change* 8, 161-179.

Hamond R 1967 Variations in sea-temperature in and around Blakeney Harbour, Norfolk. *Transactions of the Norfolk and Norwich Naturalists' Society* 21(1), 7-15.

Hardy J R 1964 The movement of beach material and wave action near Blakeney Point, Norfolk. *Institute of British Geographer Transactions and Papers* 34, 53-69.

Hasselmann K, Barnett T P, Bouws E, Carlson H, Cartwright D E, Enke K, Ewing J A, Gienapp H, Hasselmann D E, Kruseman W, Meerburg A, Muller P, Olbers D J, Richter K, Sell W and Walden H 1973 Measurements of wind-wave growth and swell decay during the Joint North Sea Wave Project (JONSWAP). *Deutsche Hydrographische Zeitschrift. Supplementband A* 12, 1-96.

Healey R G, Pye K, Stoddart D R and Bayliss-Smith T P 1981 Velocity variations in salt marsh creeks, Norfolk, England. *Estuarine, Coastal and Shelf Science* 13, 535-545.

Heaps N S 1983 Storm surges 1967-1982. *Geophysical Journal of the Royal Astronomical Society* 74, 331-376.

Horikawa K 1978 *Coastal Engineering. An Introduction to Ocean Engineering*. University of Tokyo Press, Japan.

Huthnance J M 1991 Physical oceanography of the North Sea. *Ocean and Shoreline Management* 16, 199-231.

Jardine W G 1979 The western United Kingdom shore of the North Sea in the late Pleistocene and Holocene times. The Quaternary History of the North Sea. *Acta Universitatis Upsalienis. Symposia Universitatis Upsaliensis Annum Quingentesimum Celebrantis* 2, 159-174.

Jelgersma S 1979 Sea-level changes in the North Sea basin. The Quaternary History of the North Sea. *Acta Universitatis Upsalienis. Symposia Universitatis Upsaliensis Annum Quingentesimum Celebrantis* 2, 233-248.

Jenkins R D 1979 *Flood Periodicity and Perception in Kings Lynn, Norfolk*. Part II Dissertation. University of Cambridge.

Kinsman B 1965 *Wind Waves. Their Generation and Propagation on the Ocean Surface*. Prentice-Hall, Englewood Cliffs, New Jersey.

Kjerfve B, Miranda L B and Wolanski E 1991 Modelling water circulation in an estuary and intertidal salt marsh system. *Netherlands Journal of Sea Research* 28(3), 141-147.

Komar P D 1976 *Beach Processes and Sedimentation*. Prentice-Hall, INC., New Jersey.

Komar P D (ed.) 1983 *Handbook of Coastal Processes and Erosion*. CRC Press.

Lamb H H 1977 *Climate. Present, Past and Future*. Vol 2. *Climatic History and the Future*. Methuen & co. Ltd., London.

Lee D-Y and Wang H 1984 Measurement of surface waves from subsurface gage. *Proceedings of the Conference of Coastal Engineering 1984*, Chapter 19, 271-286.

Letzsch W S and Frey R W 1980 Deposition and erosion in a holocene salt marsh, Sapelo Island, Georgia. *Journal of Sedimentary Petrology* 50(2), 529-542.

Longuet-Higgins M S 1952 On the statistical distribution of the heights of sea waves. *Journal of Marine Research* 11(3), 245-266.

Longuet-Higgins M S 1975 Integral properties of periodic gravity waves of finite amplitude. *Proceedings of the Royal Society of London, Series A* 342, 157-174.

Lugo-Fernández A, Hernández-Ávila M L and Roberts H H 1994 Wave-energy distribution and hurricane effects on Margarita Reef, southwestern Puerto Rico. *Coral Reefs* 13, 21-32.

McCave I N 1970 Deposition of fine-grained suspended sediment from tidal currents. *Journal of Geophysical Research* 75(1), 4151-4159.

Mei C C and Liu P L-F 1993 Surface waves and coastal dynamics. *Annual Review of Fluid Mechanics* 25, 215-240.

Moreira M E S de A 1992 Recent saltmarsh changes and sedimentation rates in the Sado Estuary, Portugal. *Journal of Coastal Research* 8(3), 631-640.

Moskowitz L 1964 Estimates of the power spectrums for fully developed sea for wind speeds of 20 to 40 Knots. *Journal of Geophysical Research* 69(24), 5161-5179.

MuirWood A M and Fleming C A 1981 *Coastal Hydraulics*. 2nd edition. Macmillan Press Ltd., London and Basingstoke.

National Rivers Authority 1991a *The Future of Shoreline Management*. Conference Papers.

National Rivers Authority (no date (a)) *The 1953 East Coast Flood. The Battle to Prevent it Happening Again*. Public Relations Department, NRA Anglian Region, Peterborough.

National Rivers Authority 1991 *Happisburgh to Winterton Sea Defences*. Information Unit, NRA Anglian Region, Peterborough.

National Rivers Authority 1991b *Grey Tide Against Green Marsh - Sea Defences in East Anglia*. Synopsis of Proceedings of Conference held at Snape on 1st November 1991.

National Rivers Authority (no date(b)) *Sea Defence Survey*. NRA Bristol.

Neu H J A 1984 Interannual variations and longer-term changes in the sea state of the north Atlantic from 1970-1982. *Journal of Geophysical Research* 89(C4), 6397-6402.

Pearce F 1993 When the tide comes in... *New Scientist* 1854 (January 1993), 22-27.

Pearson I 1986 *Holocene Evolution of the North Norfolk Coast*. Ph.D Thesis, School of Environmental Sciences, University of East Anglia.

Peltier W R and Tushingham A M 1989 Global sea level rise and the greenhouse effect: might they be connected? *Science* 244, 806-810.

Pethick J S 1980 Saltmarsh initiation during the Holocene transgression: the example of the North Norfolk marshes, England. *Journal of Biogeography* 7, 1-9.

Pethick J S 1981 Long-term accretion rates on tidal salt marshes. *Journal of Sedimentary Petrology* 51(2), 571-577.

Pethick J 1984 *An Introduction to Coastal Geomorphology*. Edward Arnold (Publ.) Ltd., London.

Pethick J S 1992 Saltmarsh geomorphology. Allen J R L and K Pye (eds.) 1992 *Saltmarshes. Morphodynamics, Conservation and Engineering Significance*. Cambridge University Press, Cambridge.

Pethick J 1993 Shoreline adjustments and coastal management: physical and biological processes under accelerated sea-level rise. *Geographical Journal* 159(2), 162-168.

Pierson W J 1964 A proposed spectral form for fully developed wind sea based on the similarity theory of S.A. Kitaigorodskii. *Journal of Geophysical Research* 69(24), 5181-5190.

Pierson W J Jr and Moskowitz L 1964 A proposed form for fully developed wind seas based on the similarity theory of S.A. Kitaigorodskii. *Journal of Geophysical Research* 69(24), 5181-5190.

Pierson W J Jr, Neumann G and James R W 1955 *Practical Methods for Observing and Forecasting Ocean Waves by Means of Wave Spectra and Statistics*. College of Engineering,

New York University, Research Division, Department of Meteorology and Oceanography, Technical Report No. 1 Contract No. N189S-86743.

Pirazzoli P A 1989 Present and near-future global sea-level changes. *Palaeogeography, Palaeoclimatology, Palaeoecology* 75, 241-258.

Pirazzoli P A 1993 Global sea-level changes and their measurement. *Global and Planetary Change* 8, 135-148.

Powell S M 1979 *Contemporary sedimentation rates on the tidal salt marshes at Warham, Norfolk*. BA Dissertation, Part II, University of Cambridge.

Pugh D T 1987 *Tides, Surges and Mean Sea-Level*. John Wiley & Sons, Chichester.

Pye K 1981 Marshrock formed by iron sulphide and siderite cementation in saltmarsh sediments. *Nature* 294, 650-652.

Pye K 1984 SEM analysis of siderite cements in intertidal marsh sediments, Norfolk, England. *Marine Geology* 56, 1-12.

Reed D J, Stoddart D R and Bayliss-Smith T P 1985 Tidal flows and sediment budgets for a salt-marsh system, Essex, England. *Vegetatio* 62, 375-380.

Reed D J 1987 Temporal sampling and discharge asymmetry in salt marsh creeks. *Estuarine, Coastal and Shelf Science* 25, 459-466.

Reed D J 1988 Sediment dynamics and deposition in a retreating coastal salt marsh. *Estuarine, Coastal and Shelf Science* 26, 67-79.

Reed D J 1990 The impact of sea-level rise on coastal salt-marshes. *Progress in Physical Geography* 14, 465-481.

Reed D J and Cahoon D R 1992 The relationship between marsh surface topography, hydroperiod, and growth of *Spartina alterniflora* in a deteriorating Louisiana salt marsh. *Journal of Coastal Research* 8(1), 77-81.

Rye H 1976 Long term changes in the North Sea wave climate and their importance for the extreme wave predictions. *Marine Science Communications* 2(6), 419-448.

Sainty J E 1939 Past history sea flooding and the causes of the 1938 flood. *Transactions of the Norfolk and Norwich Naturalists' Society* 14, 334-345.

Schinke H 1992 Zum Auftreten von Zyklonen mit niedrigen Kerndrucken im atlantisch-europaischen Raum von 1930 bis 1991. *Wissenschaftliche Zeitschrift der Humboldt-Universität zu Berlin, Reihe Mathematik/Naturwissenschaft* 41(2), 17-28.

Schlesinger M E (ed.) 1991 Greenhouse-gas induced climatic change: a critical Appraisal of simulations and observations. *Developments in Atmospheric Science* 19. Elsevier Science Publishers, Amsterdam, 347-367.

Schmidt H and vonStorch H 1993 German Bight storms analysed. *Nature* 365, 791.

Shemdin O H, Hsiao S V, Carlson H E, Hassellmann K and Schulze K 1980 Mechanisms of wave transformation in finite-depth water. *Journal of Geophysical Research* 85(C9), 5012-5018.

Shennan I 1989 Holocene crustal movements and sea-level changes in Great Britain. *Journal of Quaternary Science* 4(1), 77-89.

Shepard F P and LaFond E C 1940 Sand movement along the Scripps Institution Pier. *American Journal of Science* 238, 272-285.

Shi Z 1993 Recent saltmarsh accretion and sea level fluctuations in the Dyfi Estuary, central Cardigan Bay, Wales, UK. *Geo-Marine Letters* 13, 182-188.

Smith C J, DeLaune R D and Patrick Jr W H 1983 Carbon dioxide emission and carbon accumulation in coastal wetlands. *Estuarine, Coastal and Shelf Science* 17, 21-29.

Spencer T and French J R 1993 Coastal flooding: transient and permanent. *Geography* 78, 179-182.

Steers J A 1938 The rate of sedimentation on salt marshes on Scolt Head Island, Norfolk. *Geological Magazine* 75, 26-39.

Steers J A 1946 Twelve years measurement of accretion on Norfolk salt marshes. *Geological Magazine* 85, 163-166.

Steers J A 1953 The east coast floods. January 31 - February 1 1953. *The Geographical Journal* 119, 280-298.

Steers J A 1956 Recent changes on the marshland coast of North Norfolk. *Transactions of the Norfolk and Norwich Naturalists' Society* 17, 206-213.

Steers J A and Grove A T 1956 Shoreline changes on the marshland coast of North Norfolk, 1951-53. *Transactions of the Norfolk and Norwich Naturalists' Society* 17, 322-326.

Steers J A (ed.) 1960 *Scolt Head Island*. Heffers & Sons Ltd., Cambridge.

Steers J A 1964 *The Coastline of England and Wales*. 2nd edition. Cambridge University Press.

Steers J A, Stoddart D R, Bayliss-Smith T P, Spencer T and Durbridge P M 1979 The storm surge of 11 January 1978 on the east coast of England. *Geographical Journal* 145, 192-205.

Stevenson J C, Ward L G and Kearney M S 1986 Vertical accretion in marshes with varying rates of sea level rise. Wolfe D A (ed.) *Estuarine Variability*. Academic Press, Orlando, 241-259.

Stoddart D R and Reed D J 1990 Sea-level rise as a global geomorphic issue. *Progress in Physical Geography* 14, 441-445.

Stumpf R P 1983 The process of sedimentation on the surface of a salt marsh. *Estuarine, Coastal and Shelf Science* 17, 495-508.

Suthons C T 1963 Frequency of occurrence of abnormally high sea levels on the east and south coasts of England. *Proceedings of the Institution of Civil Engineers* 25, 433-449.

Titus J G 1986 Greenhouse effect, sea level rise, and coastal zone management. *Coastal Zone Management Journal* 14(3), 147-171.

Tooley M and Shennan I (eds.) 1987 *Sea-level changes*. Institute of British Geographers Special Publication Series 20, Blackwell Ltd., Oxford.

Tooley M J 1992 Recent sea-level changes. Allen J R L and K Pye (eds.) 1992 *Saltmarshes. Morphodynamics, Conservation and Engineering Significance*. Cambridge University Press, Cambridge. Chapter 2.

Tricker R A R 1964 *Bores, Breakers, Waves and Wakes. An Introduction to the Study of Waves on Water*. Mills and Boon Ltd., London.

Tushingham 1989

VanMalde 1991

Wayne C J 1976 The effects of sea and marsh grass on wave energy. *Coastal Research Notes* 14(7), 6-8.

Wigley T M C and Raper S C B 1992 Implications for climate and sea level of revised IPCC emission scenarios. *Nature* 357, 293-300.

Wolaver T G and Zieman J 1984 The role of tall and medium *Spartina alterniflora* zones in the processing of nutrients in tidal water. *Estuarine, Coastal and Shelf Science* 19, 1-13.

Woldenberg M J 1972 Relationships between Horton's Laws an hydraulic geometry as applied to tidal networks. *Harvard Papers in Theoretical Geography* 45.

Wolfe D A (ed.) 1986 *Estuarine Variability*. Academic Press, Orlando, 241-259.

Woodell S R J and Dale A 1993 Biological flora of the British Isles. *Armeria maritima* (Mill.) Willd. (*Statice armeria* L.; *S. maritima* Mill.). *Journal of Ecology* 81, 573-588.

Woodworth P L 1990 A search for accelerations in recent records of European mean sea level. *International Journal of Climatology* 10, 129-143.

Woodworth P L, Shaw S M and Blackman D L 1991 Secular trends in mean tidal range around the British Isles and along the adjacent European coastline. *Geophysical Journal International* 104, 593-609.

Zedler J B 1977 Salt marsh community structure in the Tijuana Estuary, California. *Estuarine and Coastal Marine Science* 5, 39-53.

Zimmerman J F T 1981 Dynamics, diffusion and geomorphological significance of tidal residual eddies. *Nature* 290, 549-555.